CHARACTERIZING THE ROLE OF ACETYLCHOLINESTERASE IN MOUSE CARDIOMYOCYTE PROLIFERATION AND DIFFERENTIATION

by

Jessica Marie Robinson

Submitted in partial fulfillment of the requirements
for the degree of Master of Science

at

Dalhousie University
Halifax, Nova Scotia
October 2013

This thesis is dedicated to the memory of Fay Robinson and Nadine Holmes

I love you and miss you everyday

Table of Contents

List of Tables

List of Figures

Abstract

There is scarce information on the fate of cardiac progenitor cells (CPC) in the embryonic heart after chamber specification. Furthermore, the role of acetylcholinesterase (AChE) during heart development is unknown, despite record of its presence in the myocardium. Although three molecular variants of AChE (R, H and T) exist due to alternate splicing, temporal and spatial distribution of these splice variants during cardiac ontogeny is not well characterized. We hypothesized that the AChE "R" splice variant (AChE-R) is involved in directing lineage commitment of mouse ventricular CPCs to the conduction cell phenotype. Polymerase chain reaction (PCR) analysis revealed a progressive decrease in transcription of AChE-R in the ventricles with age, implying this enzyme variant may be more important during earlier stages of cardiac ontogeny. Further, immunofluorescent staining of embryonic heart sections revealed expression of AChE in ventricular tissue housing future fast conduction cells. Western blot analysis of detergent soluble and insoluble protein fractions indicated AChE protein is expressed in these fractions, where enzyme activity was measured to be the highest at developmental stages associated with a higher percentage of CPC populations. Lastly, exogenous addition of the AChE inhibitor galantamine to cultured embryonic heart cells revealed a significant reduction in the number of CPCs and a significant increase in the number of differentiated cells, when compared to the control population. Cell cycle activity monitored by radiolabeled thymidine was found to be significantly decreased in CPCs and increased in the mature cardiomyocyte population. It is possible that AChE may promote the breakdown of ACh and block the effects of ligand-binding via M_2 receptors present on the surface of CPCs. Taken together, our data suggest that AChE expressed in ventricular myocardial cells may regulate embryonic myocardial cell cycle dynamics and subsequent proliferation rates by directly modulating cholinergic signals. Our study has also provided a platform to suggest that AChE may play a role in the molecular mechanisms underlying functional diversification of myocardial cells into conduction system cells during ontogenesis.

List of Abbreviations and Symbols Used

AB/AM – antimyocotic-antibiotic

ACh – acetylcholine

AChE – acetylcholinesterase

AHF – anterior heart field

ANF – atrial natriuretic factor

ANOVA – analysis of variance

AP-1 – activator protein 1

ARP – acetylcholinesterase read-through peptide

AV – atrioventricular

AVB – atrioventricular bundle (bundle of His)

AVC – atrioventricular canal

AVN – atrioventricular node

B2M – beta-2-microglobulin

BSA – bovine serum albumin

cAMP – cyclic adenosine monophosphate

CCS – cardiac conduction system

ChAT – choline acetyltransferase

CREB – cAMP response element-binding protein

CRE – cAMP response elements

CPB – CREB-binding protein

CPC – cardiac progenitor cell

Cre – Cre- recombinase

Ct – threshold cycle

Cx40 – connexin 40

DAG – diacylglycerol

DMEM – Dulbecco modified Eagle's medium

DMF – N, N-Dimethyl Formamide

DNA – deoxyribonucleic acid

dRn – threshold fluorescence

E – embryonic day of gestation

ECG – electrocardiogram

EPDCs – epicardially derived cells

ET-1 – Endothelin-1

FBS – fetal bovine serum

G – globular

GAPDH – glyceraldehyde 3-phosphate dehydrogenase

GATA-3 – trans-acting T-cell-specific transcription factor GATA-binding protein 3

gDNA – genomic DNA

GFP – green fluorescent protein

GM-CSF – Granulocyte-macrophage colony-stimulating factor

GPI – Glycosylphosphatidylinositol

GRE – glucocorticoid responsive element

HNF-3 – hepatocyte nuclear factor 3

IL – Interleukin 1 family

IP – inositolphosphate

IP_3 – inositol 1,4,5-trisphosphate

IRES – internal ribosomal entry sequence

IVS – interventricular septum

LBB – left bundle branches

LMO-2 – LIM domain only 2

M – muscarinic receptor

MAPK – mitogen-activated protein kinase

mChR – muscarinic acetylcholine receptor

MF20 – anti-myosin heavy chain monoclonal

MK – megakaryocyte

mRNA – messenger ribonucleic acid

MW – molecular weight

NCCs – neural crest cells

NFκB – nuclear factor kappa-light-chain-enhancer of activated B cells

NMJ – neuromuscular junction

O.C.T. – Optimal Cutting Medium

OFT – outflow tract

PBS – phosphate buffered saline

PF – Purkinje fibers

PHF – primary heart field

PIP_2 – phosphatidylinositol 4,5-bisphosphate

PKA – protein kinase A

PKC – protein kinase C

PLC – phospholipase C

PLD – phospholipase D

qPCR – quantitative reverse transcription polymerase chain reaction

RACK1 – receptor for activated C kinase 1

RBB – right bundle branches

RNA – ribonucleic acid

RT – room temperature

RT-PCR – reverse transcription polymerase chain reaction

SA – sinoatrial

SAN – sinoatrial node

SCF – stem cell factor

SDS – sodium dodecyl sulfate

SDS-PAGE – sodium dodecyl sulfate polyacrylamide gel electrophoresis

SEM – standard error of the mean

SP-1 – Specificity Protein 1

Stat-5 – Signal Transducer and Activator of Transcription 5

TEMED - tetramethylethylenediamine

TNF-α – tumor necrosis factor alpha

TPO – thrombopoietin

VCS – ventricular conduction system

X-GAL – 5-bromo-4-chloro-3-indlyl-β-D-galactopyranoside

α – alpha

β – beta

ϒ – gamma

Δ – delta

ε – epsilon

θ – sigma

ϰ – kappa

λ – lambda

μ - mu

Acknowledgments

This thesis would not have been possible without the help of so many people in so many different ways. It has been the product of endless fortuitous encounters with wonderful people who have changed the course of my academic career in addition to loving family and friends. Above all, I would like to express my deepest gratitude to my supervisor Dr. Kishore Pasumarthi for not only providing me with the opportunity to learn and research in his lab, but for the insurmountable time and patience he has given me. Unfortunately, over the course of my master's degree, I have encountered several personal set backs; however, regardless of my on-going struggles Dr. Pasumarthi has continued to offer his guidance and support, never wavering from my side. He has been an outstanding mentor and my appreciation for all he has offered me goes beyond description.

I would like to further extend my appreciation to Adam Hotchkiss, Karim Wafa, Jessica MacLean, Sarita Chinni, Tiam Feridooni and Danielle Rioux for all the time they have spent teaching me lab procedures, contributing to my experiments, and assisting me in any other way possible. They have all become wonderful friends and shown me unconditional support, contributing immensely to my academic experience.

I would like to thank my committee for helping to guide me through my research and the entire Pharmacology department at Dalhousie University. As a whole, the faculty, staff and students have all assisted me in various ways, contributing to the progression and completion of my degree.

A special thank you is also necessary to Dr. Richard Harvey for providing the *Nkx2.5*-Cre/ROSA-*lacZ* mice and to Dr. Hermona Soreq for providing the ACHE-R specific antibodies.

I would like to thank my friends and family for their endless support during both personal and financial hardships. Jessica MacLean, Jeanne Egar and Jordan Warford have offered me continual positive encouragement and reassurance, useful suggestions, lent an ear whenever needed and really stepped up as true friends throughout my time at Dalhousie.

A person of note is Adam Cormier, who has been a pillar throughout this endeavor. He has supported me mentally, emotionally and financially through the highest and lowest of times. His love, friendship and support are most appreciated and will never be forgotten. My appreciation is also extended to Steve and Debbie Cormier, as they have welcomed me into their family and offered me unconditional love, encouragement and support during the entirety of this project.

I would like to especially thank my father and mother, who have been fundamental in the completion of this work, as they have assisted me both emotionally and financially during my weakest of moments. Lastly, thank you to my uncle Steve and aunty Sherry for making this adventure possible and to my sister and brothers: Candace, Evan, Layne, Travis and Andrew.

Thank you to all who have loved me and believed in me all this time, this achievement is as much mine as it is yours.

Chapter 1.0: Introduction

1.1 Summary of Cardiovascular Disease

Cardiovascular diseases such as hypertension, myocardial infarction and congestive heart failure, are some of the most serious challenges for modern medicine. Improvements in acute treatments have increased the number of patients who survive myocardial infarctions. However, infarcts remain a significant cause of mortality and morbidity, owing to the limited regenerative capacity of the mammalian heart, and contribute to progressive heart failure (Go et al 2013). For years, scientists have imagined using cell-based regenerative therapies to repair damaged cardiac tissue through transplantation. As of late, advances in surgical and pharmacological interventions, as well as the development of electrophysiological and mechanical devices, provide a wide variety of beneficial remedies for heart disease; though none offer a curable solution for the root cause of the disease. Although it is accepted that there is some capacity for cardiomyocyte DNA synthesis in the adult heart, the degree to which this occurs is questionable (Anversa & Kajstura 1998; Soonpaa & Field 1998). Despite data supporting at least some degree of myocardial renewal (Bergmann et al 2009; Soonpaa & Field 1997), the propensity for cumulative decreases in cardiomyocyte number during cardiovascular disease indicates that the rate at which renewal occurs naturally is insufficient to restore myocyte loss (Rubart et al 2003).

Developmental and molecular studies have identified cardiac progenitor cells (CPCs), which give rise to cardiomyocytes in the developing heart (Alvarez-Dolado et al 2003; Baba et al 2007; Makino et al 1999; Martin-Puig et al 2008; Wu et al 2008). Multipotent CPCs are found in the fetal and adult heart of many mammalian species (including humans) and form as intermediates during the differentiation of embryonic stem cells (Alvarez-Dolado et al 2003;

Baba et al 2007; Chiavegato et al 2007; De Coppi et al 2007; Gaustad et al 2004; Guan et al 2006; Jackson et al 2001; Makino et al 1999; Martin-Puig et al 2008; Okamoto et al 2007; Orlic et al 2001; Planat-Benard et al 2004; Rangappa et al 2003; Reinecke et al 2000; Rota et al 2007; Toma et al 2002; Ventura et al 2007; Winitsky et al 2005; Wu et al 2008). Despite similar biological properties, the molecular identities of these different CPC populations appear to be distinct. The increase in cardiac mass during embryogenesis can be highly contributed to the proliferation of immature cardiomyocytes found to possess contractile properties. The current body of evidence to support proliferative cardiomyocyte renewal is collectively consistent, yet does not oppose potential contributions from cardiomyogenic stem cells. Interestingly, studies employing an elegant conditional reporter transgene system observed stem-cell-based regeneration following injury to adult mice (Hsieh et al 2007). Considering these recent findings, the elucidation of the molecular underpinning of cell lineage commitment and morphogenesis could provide additional avenues of treatment and may accelerate clinical applications such as drug screening and cell therapy, in addition to shedding light on the pathogenic mechanisms underlying cardiac diseases.

Over the last decade, non-neuromuscular expression and activity of the acetylcholine hydrolyzing enzyme acetylcholinesterase (AChE, E.C. 3.1.1.7) has been discovered during gametes interaction (Angelini et al 2004; Falugi et al 2008; Piomboni et al 2001), embryonic development (Falugi & Aluigi 2012), and in temporal and spatial windows related to differentiation and cell migration (Falugi 1993; Fluck et al 1980). In fact, its presence in non-cholinergic cells such as specific neuronal populations (Bernard et al 1995; Hammond et al 1994; Landwehrmeyer et al 1993), cardiomyocytes (Lamers et al 1987; Nakamura et al 1994; Nyquist-Battie et al 1993) developing avian cartilage (Layer 1990) and multiple embryonic

and tumor tissues (Karpel et al 1994; Majumdar et al 1998; Massoulie et al 1993) including hematopoietic cells and megakaryocytes (Grisaru et al 1999a; Lapidot-Lifson et al 1992; Lev-Lehman et al 1997; Ott et al 1982; Patinkin et al 1994; Paulus et al 1981; Soreq et al 1994; Szelenyi et al 1982) and CPCs (McMullen et al 2009a) has led to the proposal that AChE may participate in additional cellular functions distinct from its well known catalytic activity. The transient, non-conventional functions of this enzyme are at least in part specific to three C-terminal variants of AChE, which are produced by alternative splicing of the single ACHE gene to yield "R", "H" and "T" forms. The rare, soluble, secreted AChE-R variant has been linked to hematopoiesis (Chan et al 1998; Grisaru et al 2001), erythropoiesis and megakaryopoiesis (Lev-Lehman et al 1994; Soreq et al 1994), myeloidopoiesis (Soreq et al 1994), glioblastoma proliferation (Brenner et al 2003; Perry et al 2004), astrocyte and astrocytoma cell proliferation (Guizzetti & Costa 2002; Gurwitz et al 1984), neurogenesis (Dori et al 2005) and neurite growth (Bataille et al 1998; Layer et al 1993; Sharma et al 2001; Sternfeld et al 1998).

Based on histochemical staining by McMullen et al 2009 and former evidence that AChE is secreted by ventricular cardiomyocytes (Nyquist-Battie et al 1993) we postulate that the presence of intracellular AChE, most likely the AChE-R variant, during cardiac development may be involved in the regulation of CPC proliferation and differentiation. Furthermore, we suggest AChE-R may play a more important role in the maturation of cardiomyocyte progenitors destined to possess electrical impulse conduction properties than those of contractile properties. Here we will outline the components of the cholinergic system, the history of AChE and its role in cellular proliferation and growth, describe the development

of the murine cardiac conduction system (CCS), and finally discuss plausible mechanisms that may direct AChE involvement in CCS formation.

1.2 Components and Signaling of the Cholinergic System

The vertebrate nervous system is divided into two major components: the central nervous system, consisting of the spinal cord and brain, and the peripheral nervous system, which can be subdivided into somatic and autonomic components. The somatic system is responsible for voluntary body movements and sensing external stimuli. The autonomic division exerts functional control over internal organs by way of efferent nerve fibers originating in the central system. It is composed of three subdivisions, (sympathetic, parasympathetic and enteric divisions) which exhibit opposing regulatory effects on various tissues; we will focus only on the sympathetic and parasympathetic systems for the purpose of this thesis. Parasympathetic activity in the heart is controlled by the vagus nerve, which originates in the medulla oblongata (Shoba & Tay 2000). In the mouse, nerve cells (sympathetic) are first seen in the dorsal mesocardium at embryonic day (E) 10.5, whereas the parasympathetic cells become abundant in the arterial and venous poles of the heart at E11.5 and E12.5 (Hildreth et al 2008; Shoba & Tay 2000) with a smaller number of sympathetic neurons present. Furthermore, at E12.5, the majority of cells in the vagal nerve and posterior cardiac plexus are also cholinergic parasympathetic neurons (Hildreth et al 2008). This demonstrates that the major neuronal input into the venous pole of the heart is parasympathetic. Innervation of the outflow tract also occurs around the same time in mice, with the first sympathetic and parasympathetic neural elements seen between the separating aorta and pulmonary trunk at E11.5 (Hildreth et al 2008).

Sympathetic innervation has been shown to occur more prominently at later stages (after E12.5) compared with parasympathetic innervation (Shoba & Tay 2000). The peripheral autonomic neurons play a crucial role in supporting the development of the normal heart, promoting growth and differentiation of the cardiomyocytes including the sensitivity of the neurotransmitters (Atkins & Marvin 1989; Deskin & Slotkin 1981). It has been shown that neonatal central catecholaminergic lesions, which do not affect the development of sympathetic nerves themselves, but cause a reduction in impulse activity in those neurons, result in altered cardiac growth (Deskin & Slotkin 1981). Neural input may also be important in the differentiation of myocardial cell membrane during normal cardiac ontogenesis (Atkins & Marvin 1989). Sympathetic maturation may also help terminate cardiomyocyte replication and initiate hypertrophic growth (Simpson et al 1991). Histological studies have demonstrated the presence of developing neurons and nerves (parasympathetic) in the rat heart from the 11th day of gestation onwards (Gomez 1958; Hildreth et al 2008; Shoba & Tay 2000). It has been shown in several species that the atria are innervated at the same time or prior to the ventricles, with preferential innervation of the nodal and perinodal areas with the progression of the innervation to the apex of the heart (Lipp & Rudolph 1972).

The adrenergic or sympathetic nervous system acts to increase heart rate by releasing epinephrine and norepinephrine. Conversely, the parasympathetic division, also known as the cholinergic nervous system, functions to decrease heart rate, via the sinoatrial (SA) node, by releasing the neurotransmitter acetylcholine (ACh). Additional cholinergic effects include the inhibition of the atrioventricular node (AV) and contractile force. ACh is released into the synaptic junction, where it binds to various G-protein coupled muscarinic receptors (M1-M5)(Sharma & Banerjee 1978). Among the five muscarinic acetylcholine receptor (mChR)

subtypes, M2-ChR is the predominant isoform present in the mammalian heart, where M1 and M3 expression is significantly less (Dhein et al 2001). This molecular divergence is mirrored in the coupling properties of these two classes: in principle, there is a subtype specific intracellular signaling with the 'odd' numbered M1-, M3- and M5-ChR preferentially coupling to $G_{s/q}$-protein and subsequently activating the phospholipase C–diacylglycerol–inositolphosphate (PLC–DAG–IP) system. In contrast, the 'even' numbered M2- and M4-ChR in principle couple to pertussis toxin-sensitive G-protein $G_{i/o}$ resulting in an inhibition of adenylyl cyclase (Caulfield & Birdsall 1998; Felder 1995). Moreover, M2-ChR can couple to certain K^+-channels and can influence Ca^{2+}-channels, I_f current, phospholipase A_2, phospholipase D (PLD) and tyrosine kinases (Caulfield 1993; Felder 1995). Despite record of molecular divergence, developmental alterations in muscarinic receptor expression in the heart have yet to be characterized, in addition to the possibility of selective expression by different cell types.

1.3 Getting to Know Acetylcholinesterase (AChE)

1.3.1 A look at splicing and structure

Acetylcholinesterase (acetylcholine acetyl hydrolase, AChE, EC 3.1.1.7) is a type of B carboxylesterase that rapidly hydrolyzes the neurotransmitter ACh at brain cholingeric synapses as well as at neuromuscular junctions (Taylor & Radic 1994). It has been found to exist in various molecular forms (asymmetrical and globular), depending on alternative splicing of its transcripts and association with structural proteins (Grisaru et al 1999b; Perrier et al 2005; Soreq & Seidman 2001). Alternative acceptor sites of 3' RNA splicing yield three different AChE variants (Figure 1.1). The AChE-R ('readthrough') variant results from the

absence of splicing after the last catalytic exon giving rise to a variant with unique soluble properties (Lev-Lehman et al 1997; Seidman et al 1995). The C-terminus of this splice variant lacks the cysteine residue necessary for disulfide intersubunit binding, therefore, it was initially believed that AChE-R could not be incorporated into the heavier AChE molecule, rather functioning as soluble monomers (Kaufer et al 1998). However, not all of the subunits in tetrameric AChE are disulfide-bonded (Flores-Flores et al 1996; Liao et al 1993), suggesting that the C-terminal cysteine may not be essential for assembly of the subunits into the heavier AChE complexes (Perrier et al 2003). Also, AChE-R was found to form intraneuronal heterotrimeric complexes with protein kinase CβII, and its scaffold protein RACK1 (Birikh et al 2003), suggesting that interprotein AChE-R complexes might exist. This homolog is expressed intracellulary in hematopoietic cells (Grisaru et al 2001; Lev-Lehman et al 1997), neuronal cells (Dori et al 2005; Perry et al 2004) and CPCs (McMullen et al 2009a).

The AChE-H ('hydrophobic') or 'erythrocytic' variant produces cell membrane-anchored glypiated dimers mostly found in blood cells; and the AChE-T ('tailed' or 'synaptic') variant constitutes the principle multimeric enzyme in brain and muscle. It appears that the polypeptide encoded by the T transcript, AChE-T ('tailed' or 'synaptic' form), is incorporated into the synapse, at least in vertebrate fast muscles and in the central nervous system (CNS). At the neuromuscular endplate, one to three catalytic subunit (AChE-T) tetramers are attached to a triple-helical collagen tail, which anchors them to the basal lamina within the synaptic cleft, whereas in the CNS, a single tetramer is attached to a 20 kDa membrane-spanning polypeptide. Because the AChE enzyme displays a rich polymorphism existing as a variety of molecular forms, it may be classified as either homomeric or

heteromeric (Figure 1.2) on the basis of its association with specialized structural subunits (Chan & Jasmin 1999; Massoulie et al 1998; Van Hoof et al 2010).

Homomeric forms include the globular (G)1 monomer and G2 dimer as well as a glycophospholipid-linked dimer. Conversely, heteromers consist of the asymmetric forms A4, A8, or A12 in which one, two, or three soluble G4 tetramers attach to a collagenic structural subunit, respectively; and amphiphilic tetramers G4-linked to a 20-kDa hydrophobic anchor. The functional significance of this polymorphism is to allow the placement of catalytically active subunits in distinct cell types and subcellular locations to perform site-specific functions. In mammals, for example, the asymmetric forms of AChE are expressed exclusively in differentiated muscle and neuronal cells, whereas glycophospholipid-linked dimers are found preferentially in tissues of hematopoietic origin. Such varied patterns of expression suggest that expression of AChE involves several levels of regulatory mechanisms ranging from tissue-specific transcriptional control to highly regulated post-translational events.

Figure 1.1. Splicing alternatives in mammalian AChE transcripts. The consensus AChE gene exons 2, 3, and 4 (box) encode the core, enzymatically active region of the AChE protein. AChE mRNA continues with 3′ alternative choices: pseudointron 4′, which initiates with an in-frame open reading frame creating a hydrophilic C-terminus with no adherence or assembly capacity, yielding monomeric (AChE-R) AChE; exclusion of the 4′ domain leads to exon 5, continuous with that of exon 4 yielding a GPI-linkable C-terminus allowing the production of AChE dimers adhering through their GPI domain to red blood cell membranes (AChE-H); or linkage of exons 4 and 6, yielding an amphipathic, cysteine-containing C-terminus that leads to the production of tetrameric complexes of the catalytic subunits that adhere to the synaptic membrane through intermediate structural subunits (AChE-T).

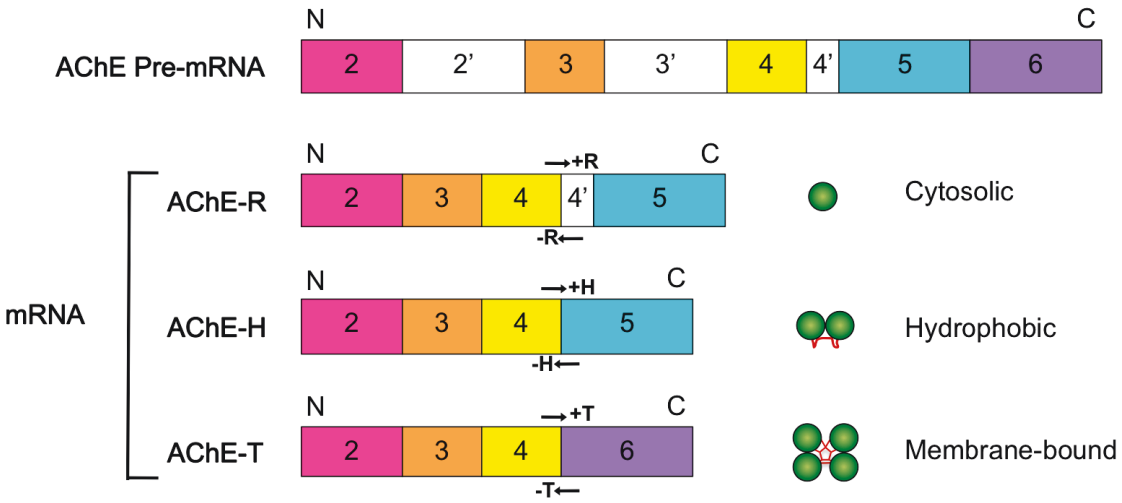
N
C
AChE Pre-mRNA
2
2'
3
3'
4
4'
5
6
mRNA
AChE-R
+R
-R
Cytosolic
AChE-H
+H
-H
Hydrophobic
AChE-T
+T
-T
Membrane-bound

Figure 1.2. A schematic representation of the catalytic subunits and detailed quaternary structures evolving from alternative splicing of AChE transcripts. Consistent to all forms of AChE is the invariant splicing of exons 2, 3 and 4 that collectively encode the catalytic core of the enzyme. The AChE gene includes three alternative 3′ end splices for AChE mRNA, giving rise to monomeric (AChE-R), dimeric (AChE-H) or tetrameric (AChE-T) forms. Multimers of tetramers of the AChE subunit translated from exon 6-spliced mRNA are tethered in place by collagen Q (ColQ), enabling anchorage to neuromuscular junctions (NMJs), and proline-rich membrane anchor (PRiMA) proteins responsible for the synaptic docking of AChE-T in the brain. Homomeric forms consist of monomer G1, dimer G2, tetramer G4 and a glycophospholipid (GPI)-linked dimer. Heteromeric forms consist of the hydrophobic-tailed G4 form and the asymmetric forms containing a collagenic structural subunit. AChE-R is a soluble monomer with a unique naturally unfolded C-terminal peptide. Because AChE-H and AChE-R are incapable of anchorage to the NMJ or to synaptic membranes through ColQ or PRiMA, only the AChE-T form of the enzyme is regarded as truly "synaptic" (Massoulie et al 1993; Silman & Sussman 2008; Taylor et al 1993). Adapted from (Pezzementi & Chatonnet 2010).

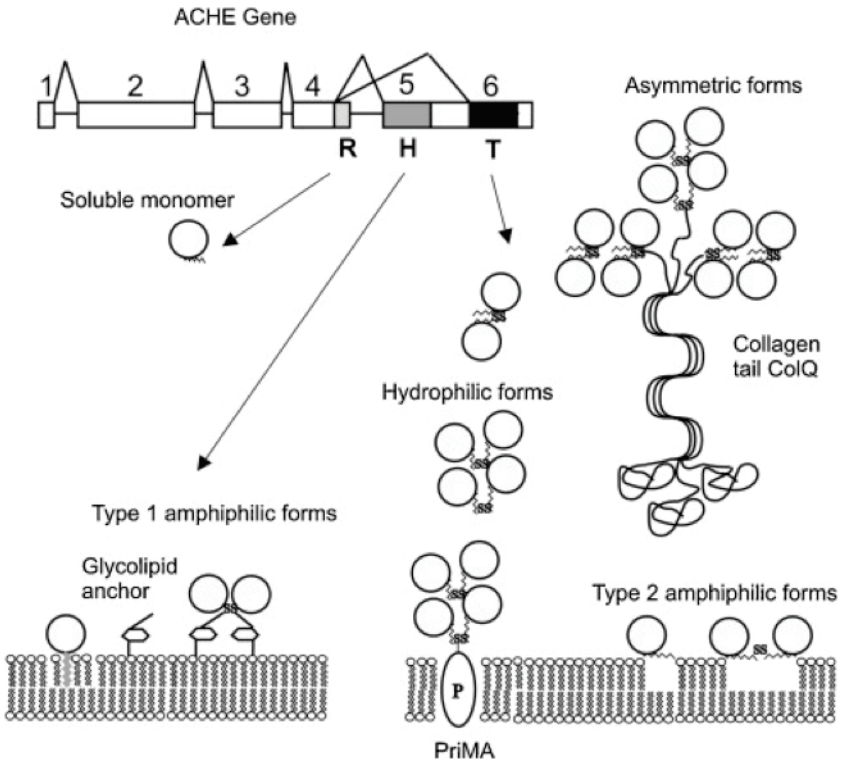
ACHE Gene
1
2
3
4
5
6
R
H
T
Asymmetric forms
Soluble monomer
Collagen
tail ColQ
Hydrophilic forms
Type 1 amphiphilic forms
Glycolipid
anchor
Type 2 amphiphilic forms
P
PriMA

1.3.2 Non-classical functions

Numerous reports suggest that AChE may have other roles apart from its 'classical' function in terminating impulse transmission at cholinergic synapses. In fact, its presence in non-cholinergic cells such as specific neuronal populations (Bernard et al 1995; Hammond et al 1994; Landwehrmeyer et al 1993), hematopoietic cells (Ott et al 1982; Paulus et al 1981; Szelenyi et al 1982) and cardiomyocytes (Lamers et al 1987; Nakamura et al 1994; Nyquist-Battie et al 1993) has led to the proposal that AChE may participate in additional cellular functions distinct from its well known catalytic activity. In fact, AChE is expressed transiently in early embryonic development, prior to synaptogenesis (Layer & Willbold 1995). Similarly in the adult, it is found in areas of the brain that lack cholinergic innervation (Greenfield & Vaux 2002).

The discovery of sequence homologies between AChE and cell adhesion molecules (neuroligins, neurotactins, gliotactin) suggested that AChE may function as a cell adhesion molecule (Pezzementi & Chatonnet 2010; Soreq & Seidman 2001). These proteins have adhesion properties and a heterophilic partner has been discovered in some instances (neurexin for neuroligins (Fabrichny et al 2007; Ko et al 2009), amalgam for neurotactins (Fremion et al 2000; Zeev-Ben-Mordehai et al 2009)). AChE, unlike neurotactin, lacks a transmembrane domain and it has been argued that soluble AChE-R might compete with its structural homologues for their binding partners, and thus conveys or interrupt morphogenic signals into neurons (Grifman et al 1998).

There is a considerable body of *in vitro* evidence indicating that AChE does indeed have non-classical functions promoting cell adhesion and neuritogenesis (Bigbee et al 2000; Johnson & Moore 2000; Karpel et al 1996; Koenigsberger et al 1997; Layer et al 1993; Small

et al 1995), synaptogenesis (Sternfeld et al 1998), amyloidosis (Inestrosa & Alarcon 1998; Inestrosa et al 1996), dopamine neuron activation (Holmes et al 1997), regulation of apoptosis (Yang et al 2002; Zhang et al 2002), nerve regeneration (Srivatsan & Peretz 1997) and hematopoiesis (Soreq et al 1994) and lymphocyte activation (Kawashima & Fujii 2000).

1.3.3 Structural importance

Several groups have provided evidence for the involvement of AChE in neurite growth (Bataille et al 1998; Layer et al 1993; Sharma et al 2001). Interestingly, in one case, neurite outgrowth was reported to be induced by a catalytically inactive form of AChE (Sternfeld et al 1998), suggesting a peripheral, anionic site may be responsible rather than the active site. The peripheral anionic site (PAS) of acetylcholinesterase lies at the entrance to the active site gorge (Sussman et al 1991). It is composed of five residues and associated with it are a number of surface loops (Bourne et al 1999), conferring a high degree of conformational flexibility on the area. The site is involved in the allosteric modulation of catalysis at the active centre (Radic et al 1991) and is the target of various anti-cholinesterases. It is also implicated in a number of non-classical functions, in particular, amyloid deposition (Inestrosa & Alarcon 1998; Inestrosa et al 1996), cell adhesion and neurite outgrowth (Hosea et al 1996; Johnson & Moore 1999; Munoz et al 1999; Radic et al 1991).

AChE has also been credited for accelerating the assembly of Aβ peptide into amyloid fibrils, most likely through interaction at this peripheral site (Bartolini et al 2003; Inestrosa et al 1996; Reyes et al 1997). With the exception of synpatogenesis and lymphocyte activation, which show mixed cholinergic and non-cholinergic aspects, these functions do not appear to be catalytic in nature and are therefore, presumed to be mediated by structural aspects of the AChE molecule. For example, converging lines of evidence indicate that the process of

terminal differentiation in specific lineages of hematopoietic cells is accompanied by large increases in the levels of AChE activity. Moreover, it has been suggested that AChE may participate directly in the regulation of bone marrow cell development by reducing the proliferative and expansive capacity of pluripotent stem cells committed to erythropoiesis, megakaryopoiesis, and macrophage production and by promoting apoptosis in their progenies (Lev-Lehman et al 1994; Soreq et al 1994).

Deutsch et al 2002 explored the involvement of AChE in cellular and molecular mechanisms that regulate blood cell proliferation and differentiation during fetal hematopoiesis or under hematopoietic stress. They found the AChE-R variant to be expressed in early hematopoietic ($CD34^+$) progenitor cells and may be linked to their response to stress. Furthermore, cytochemical staining of $CD34^+$ cells for AChE catalytic activity showed that the enzyme is active. A unique 26-residue COOH-terminal peptide ARP (acetylcholinesterase read-through peptide) of the "readthrough" form AChE (AChE-R), is produced when the *R* splice variant is secreted into the extracellular matrix (Deutsch et al 2002; Grisaru et al 2001; Kaufer et al 1998). The ARP peptide has been reported to modulate hematopoietic differentiation (Deutsch et al 2002; Grisaru et al 2001). Specifically, ARP was shown to act as a growth-promoting factor for hematopoietic progenitors (Deutsch et al 2002). It was found to contain clustered binding sites for hematopoietically active transcription factors in the AChE distal enhancer, proximal promoter, and its intron-1 enhancer domain. These include fully conserved motifs for cis-acting AP-1, NFκB, HNF-3, Stat-5, LMO-2, SP-1, and GATA-3, as well as the half palindromic glucocorticoid responsive element (GRE). It was also shown to facilitate the proliferation of early hematopoietic progenitors and to enhance the activity of stem cell factor (SCF), GM-CSF, and thrombopoietin (TPO). Grisaru et al 2001 found that

ARP, like cortisol, accumulates in the serum following acute stress and facilitates the cytokine-induced proliferation of human $CD34^+$ hematopoietic progenitors along the myeloid and MK lineages. ARP accumulation may involve stress- induced transcriptional activation (Ross et al 1990), modulation of alternative splicing (Lopez 1998; Xie & McCobb 1998), changes in the life- span of AChE-R mRNA (Chan et al 1998), enhanced proteolytic activity (Tarasenko et al 1992), or a combination of these processes. As this cleavable C-terminal peptide harbours strong growth stimulating activity for hematopoietic progenitors, the same may be true for cardiac progenitor cells. The stem cell survival and proliferative effects of ARP denote a previously unforeseen activity that is particular to the AChE-R protein yet distinct from the ACh hydrolysis and adhesion properties characteristic of the core domain common to all AChE isoforms. Thus, the significance of ARP may extend beyond the hematopoietic system. Currently, ARP presents as a potential cue that may be involved in the induction of such growth and expansion capacities of pluripotent stem cells from multi-tissue origins. If so, the unique properties of this peptide might also contribute developmental or stress induced cardiac progenitor cell changes.

1.3.4 Mechanism of action

Other functions of AChE might involve the hydrolysis of ACh in a non-synaptic context. ACh is normally present in cholinergic systems and acts mainly via muscarinic (M_2) G_i protein coupled receptors in ventricular cardiomyoctyes (Pazos et al 1986; Zhou et al 1988). These muscarinic receptors negatively couple to adenylate cyclase, the enzyme that synthesizes cyclic AMP (cAMP) from ATP (Zhou et al 1988). In the presence of ACh, G_i is active and inhibits cAMP formation; however, introduction of AChE reduces ACh levels and cAMP production is resumed (Dvir et al 2010). Following cAMP production, cAMP activated

protein kinase A (PKA), a cAMP-dependent protein kinase that is important in regulating numerous cellular functions including cell cycle activity and cyclin levels, is activated (Shah & Catt 2004). Once activated, PKA phosphorylates the transcription factor CREB, which is coactivated by association with CREB-binding protein (CPB). The newly formed dimer binds to certain DNA sequences called cAMP response elements (CRE) and, thereby, increases or decreases the transcription of downstream genes involved in cell proliferation and differentiation. Considering ACh is normally present, its inhibitory effects on this cAMP signaling pathway are prevented by the hydrolytic activity of AChE, which acts to degrade ACh ligand (Figure 1.3.1). The splice variant AChE-R form has previously been shown to regulate the proliferation and differentiation of neural progenitor cells and hematopoietic stem cells (Dori et al 2005; Dori & Soreq 2006; Pick et al 2004). Furthermore, it was demonstrated that AChE-R induced proliferation of glioblastoma cells can be blocked by overexpression of CREB, or antisense destruction of AChE-R mRNA, protein kinase C (PKC; Figure 1.4) or PKA inhibitors (Perry et al 2004). Proliferation was not, however, suppressed when over-expressed CREB was combined with PKC inhibition suggesting that CREB's functional repressive activity of this process involves a PKC-mediated pathway. Conversely, these results imply that impaired CREB regulation permits AChE-R induced, PKA-mediated proliferation. Considering histochemical staining done by McMullen et al 2009 suggested intracellular AChE-R form is present in CPCs, and AChE has formerly been shown to be secreted from ventricular cardiomyocytes (Nyquist-Battie et al 1993), these findings suggest it may influence embryonic myocardial cell cycle dynamics via cholinergic dependent or independent pathways. Furthermore, AChE may regulate proliferation of CPCs and mature cells in a differential manner.

Although there is little known about the fate of CPCs in the embryonic heart following chamber specification, it has been previously shown that E11.5 mouse ventricular myocardium give rise to functional cardiomyocytes and conduction system cells (McMullen et al 2009a). Previous studies have shown that the majority of E11.5 CPCs or their derivatives positive for lineage specific markers such as atrial natriuretic factor (ANF) are not capable of developing Ca^{2+} transients. E11.5 ANF+ ventricular myocardial cells were also positive for the enzyme AChE (McMullen et al 2009a). Interestingly, Ca^{2+} transients could be invoked in ANF+/AChE+ cells only after inhibition of muscarinic receptors or G_i signaling pathway.

This finding suggests that the G_i inhibitory pathway may delay functional specification in a subset of developing ventricular cells. Additionally, it implies AChE may play a role in the molecular mechanisms underlying CPC differentiation with respect to cardiac muscle cells versus conduction system cells which exhibit different characteristics involved in Ca^{2+} handling. Based on this assumption, it is expected that blocking the action of AChE will result in higher levels of free ACh M_2-ligand and thereby increased stimulation of this G_i pathway (Figure 1.3.2). Furthermore, impeding G_i activity with an M_2-receptor blocker should permit production of cAMP (Figure 1.3.3). Additionally, co-introduction of an AChE inhibitor with an M_2-receptor blocker should restore cAMP levels back to normal. Through downregulation of cholinergic axis by AChE, levels of cAMP may rise thereby activating the transcription factor CREB in mature cardiomyoctyes but not in CPCs, or vice versa depending on relative levels of muscarinic receptor expression (Figure 1.3.1).

Figure 1.3. An illustration of the M_2 muscarinic receptor-signaling pathway mediated by G_i-protein signaling. 1.) The possible effects of AChE regulation on cardiac progenitor cells (CPCs) through activation of adenylate cyclase leading to cAMP induced transcription **2.)** The affect of AChE inhibition on this intracellular signaling pathway by enabling ACh binding thereby inhibiting adenylate cyclase activity and **3.)** The affect of blocking the G_i receptor with a muscarinic antagonist to restore active adenylate cyclase levels.

*CPB = CREB-binding protein; CRE = cAMP response elements; protein kinase A (PKA), AC = adenylyl cyclase; PKA = protein kinase A;

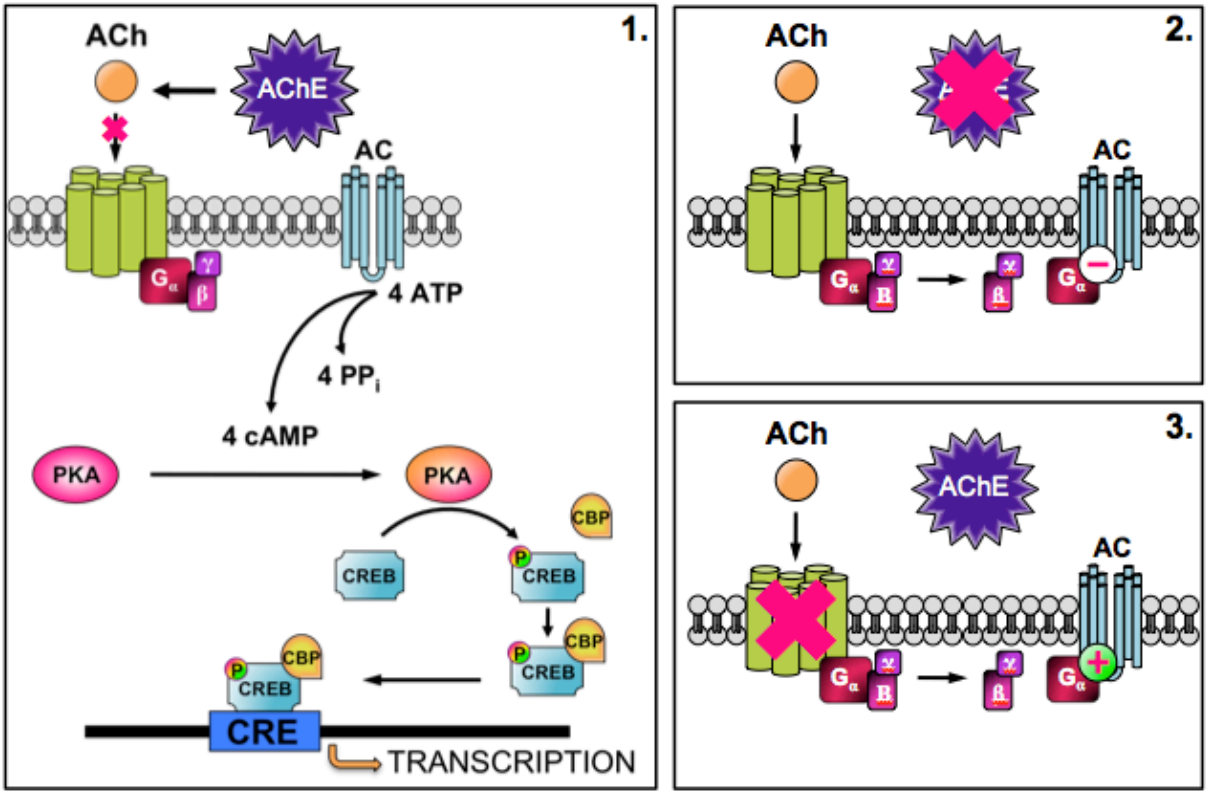
1.
ACh
AChE
AC
4 ATP
4 PPi
4 cAMP
PKA
PKA
CBP
CREB
CREB
CBP
CREB
CBP
CREB
CRE
TRANSCRIPTION
2.
ACh
AC
3.
ACh
AChE
AC

Figure 1.4. A model representing the possible effect of muscarinic M_1 receptor stimulation in cardiac cells. The phospholipase C (PLC) pathway of intracellular signaling is mediated by G_q-proteins, which are activated when ACh ligand binds to the cell-surface M_1 receptor. G-protein-mediated activation of PLC stimulates the breakdown of phosphatidylinositol 4,5-bisphosphate (PIP_2) to form inositol 1,4,5-trisphosphate (IP_3) and diacylglycerol (DAG). IP_3 releases Ca^{2+} from intracellular stores and DAG activates protein kinase C (PKC), which together modify the activity of cellular proteins and possibly induce cell cycle activity, cell division and differentiation in myocardial cells.

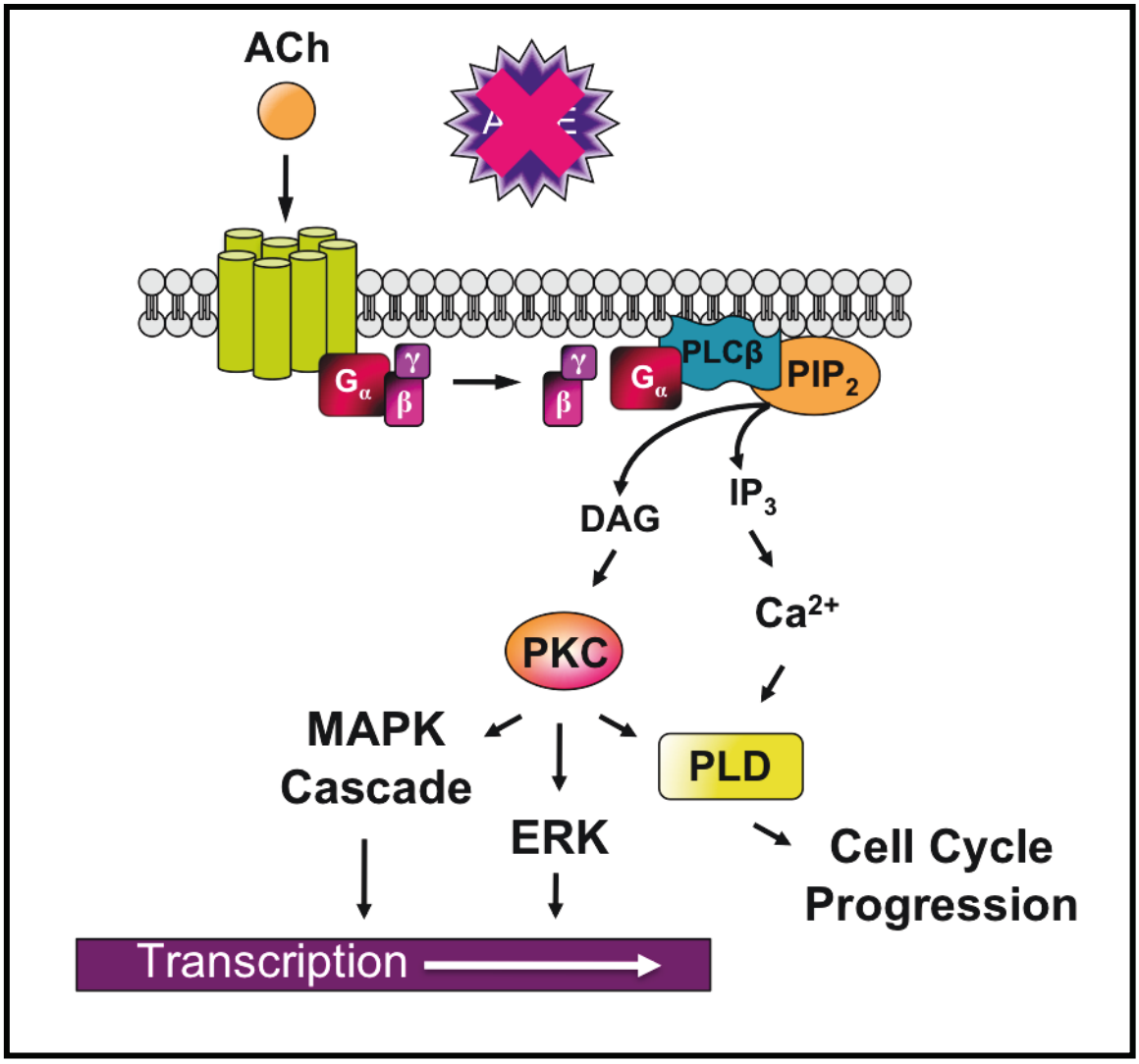
ACh
Gα
γ
β
PLCβ
PIP2
DAG
IP3
Ca2+
PKC
MAPK
Cascade
ERK
PLD
Cell Cycle
Progression
Transcription

1.4 Understanding the Murine Cardiac Conduction System

1.4.1 A brief history of cardiac conduction system discovery, anatomy and function

The atrioventricular cardiac conduction system (CCS) is the electrical wiring responsible for the coordination of cardiac contraction. The electrical activity is generated by pacemaker cells localized in the sinoatrial node (SAN) in the dorsal region of the right atrium (Anderson & Ho 2003). From the SAN, electrical activity spreads rapidly to both atria, provoking simultaneous atrial contraction. The atria and ventricles are electrically isolated by the annulus fibrosus (or cardiac skeleton), which is a structure composed of non-myocardial, dense connective tissue that establishes electrically impermeable boundaries to autonomic influence (Anderson & Ho 2003). As electrical impulses cannot pass directly through the cardiac skeleton, they are re-directed through an electrical conduit within the inert collagen framework, termed the atrioventricular (AV) conduction system. Electrical activity from the atria converges on the atrioventricular node (AVN), where its conduction velocity is reduced to delay the spread of electrical activity and allow atrial contraction before ventricular activation. The electrical activity is then rapidly propagated to the ventricular apex through a specialized fast conducting system or ventricular conduction system (VCS), which includes the atrioventricular bundle (AVB, also known as the bundle of His), the right and left bundle branches (RBB, LBB) on either side of the inter-ventricular septum, and a complex network of Purkinje fibers (PF) ramifying over the subendocardial ventricular surface (Anderson & Ho 2003). The VCS plays a critical role in coordinating the heartbeat by rapidly conducting the electrical impulse to the ventricular apex in order to activate contraction from the apex and maximize efficiency of expulsion of blood from the base of the heart into the network of arteries, arterioles and capillaries reaching throughout the body.

It was as early as the second century when Cladius Galen first noted a denervated, excised heart continued to contract, indicating that a heartbeat is triggered by inherent muscular excitation (Viragh & Challice 1982). The first anatomical description of the human VCS was made by Sunao Tawara at the beginning of the 20th century (Suma 2001), where he noticed that conductive cells can be distinguished from the working myocardium by the presence of a poor contractile apparatus with fewer sarcomeres, enriched glycogen content and reduced numbers of T tubules (Viragh & Challice 1977). The function of conductive cells has been resolved by electrophysiological experiments demonstrating specific electrical properties, including rapid conduction (Anumonwo et al 2001); however, it is the global anatomy of the VCS that orchestrates coordination of heartbeats, and disturbances in its anatomy can result in arrhythmias (Haissaguerre et al 2002). The availability of genetically modified mouse models has provided a sturdy platform for the investigation into the origin and development of the VCS.

Visualization of the anatomy of the entire murine VCS was achieved using a transgenic mouse line in which a green fluorescent protein (GFP) reporter gene was inserted at the *Cx40* locus, which normally drives connexin 40 (*Cx40*) expression throughout the VCS (Miquerol et al 2004). *Cx40* defines the adult VCS both by its pattern of expression and by its role in conduction, as it forms gap junction channels with a high conductance and is expressed in all compartments of the fast conduction system; it is not present in the working myocardium or slow-conducting compartments such as the SAN and AVN (Gros et al 2004) and so can be used as a definitive marker of the mature VCS. $Cx40^{GFP}$ expression delineates the adult ventricular conduction system, revealing a network extremely similar to the drawings of Sunao Tawara for the human heart (Suma 2001) and consistent with classical histological

images of the mouse VCS (Lev & Thaemert 1973), supporting the reliability of this method.

1.4.2 Development of central and peripheral components of the cardiac conduction system

The first peristaltic contractions of the mouse heart appear by E8.5 and are rapidly replaced as the cardiac tube loops by sequential contraction of the atria and ventricles detected by a regular ECG (Christoffels & Moorman 2009; Moorman & Christoffels 2003b). There has been no evidence to indicate the presence of specialized conductive cells at these early stages (Viragh & Challice 1977), however, sequential contraction of the primary heart tube is thought to be ensured by alternating regions of fast-conducting (future atria and ventricles) and slow-conducting myocytes [atrioventricular canal (AVC), and outflow tract (OFT)] (de Jong et al 1992; Gourdie et al 2003; Moorman & Christoffels 2003a). By E9–E10, the primordium of the AV conduction pathway appears in the inner dorsal wall of the AVC and becomes increasingly compact as development proceeds to form the AVN (Viragh & Challice 1977). At the same time, a group of cells differentiate along the ridge of the IVS, extending from the primordium of the AVN to the middle portion of the rim of the interventricular foramen, where it divides into right and left branches (Viragh & Challice 1977). This has been visualized using a number of transgenic reporter gene mouse models, such as the *Mink-LacZ* or *CCS-LacZ* systems (Christoffels & Moorman 2009; Jongbloed et al 2008; Jongbloed et al 2005; Kupershmidt et al 1999; Myers & Fishman 2004; Rentschler et al 2001). The peripheral conduction system comprising of Purkinje fibers is not yet delineated at this stage of development (Hoogaars et al 2004). At E9.5, *Cx40*-positive trabeculae form at the subendocardial surface of both ventricles and are thought to play the role of a fast-conducting network in the embryonic heart (Moorman & Christoffels 2003b; Viragh & Challice 1982). Optical mapping of embryonic hearts has shown that ventricular activation switches from an

apex to base pattern at E10.5, to biventricular activation points by E12.5 (Rentschler et al 2001). A functional embryonic route equivalent to the His–Purkinje network is thus present prior to completion of ventricular septation.

1.4.3 Analysis of CCS development using lineage restricted reporter gene mouse models

Christoffels and Moorman have recently published a recapitulative table of the expression pattern of known markers of conduction system development (Christoffels & Moorman 2009). Many of these molecular markers are not selective for the definitive conduction system and are also expressed in surrounding tissues that share a common developmental pathway. *Tbx3*, for example, is expressed in the AVC and in AVC-derived cells, such as the central conduction system, and broad expression of the *CCS-LacZ* transgene is observed in the IVS and valves (Hoogaars et al 2004; Jongbloed et al 2005). *Cx40*, a definitive marker of the mature VCS, is expressed in ventricular myocardium but not in the AVN and AVB before E14.5 (Gros et al 2004). In contrast, the *CCS-LacZ* transgene is present in the AVC and IVS at E10.5, thus differing in expression from the $Cx40^{GFP}$ allele in early development, despite a subsequently convergent expression pattern throughout the definitive VCS. These results reveal the complexity underlying the development of the VCS and suggest that the central and peripheral components of the conduction system develop independently prior to integration in a single conductive pathway. More recently, a new marker of the VCS, contactin 2 (*cntn-2*), encoding a cell adhesion molecule critical for neuronal patterning and ion channel clustering, has been identified by transcriptome analysis of Purkinje fibers purified from *CCS-LacZ* mice (Pallante et al 2010). Immunohistochemistry and electrophysiological recordings showed that GFP+ fibers have a conductive phenotype, however, the expression pattern of contactin 2 during embryonic development remains to be described.

More recently, an inducible *Cre* allele expressed under transcriptional control of *Cx40* regulatory sequences has been generated (Beyer et al 2011). *Cx40*^{Cre} mice allow precise temporal control of Cre recombination in the *Cx40* expression domain, where *Cx40* expression initiates at the onset of trabeculation and persists in trabeculae throughout cardiac development (Delorme et al 1997). Recombination at E10.5 demonstrates that *Cx40* is expressed in cells giving rise to both conductive and working myocytes in each ventricle. In contrast, recombination at E16.5 reveals that *Cx40*-expressing cells at this stage contribute only to the VCS, including the AVB, right and left bundle branches, and PF network (Miquerol et al 2010). These data illustrate the lineage relationship between *Cx40*-positive embryonic trabeculae and the peripheral PF network. Laugwitz et al 2007 also elucidated the critical stage between E10.5 to E18.5, where a subset of isl1^{+} undifferentiated precursor cells remain embedded in the embryonic mouse heart after its formation and their number decreases progressively during this time. After birth, relatively few isl1^{+} cardioblasts are even detectable. Lineage analysis studies should, therefore, consider E11.5, E14.5 and E16.5 as stages of critical importance for developmental studies aimed at elucidating the pathway guiding ventricular conduction lineage cell commitment.

1.4.4 Role of a transcriptional gene network and secreted factors in the regulation of CCS development

A long-standing debate in the cardiac field concerns the origin of conductive cells. This debate reflected observations that conductive cells express certain neuronal genes and the heterogeneity of cardiac cell populations potentially contributing to the VCS, i.e. cardiomyocytes, neural crest cells (NCCs) and epicardially derived cells (EPDCs) (Vincent & Buckingham 2010). Retroviral and retrospective clonal analyses have clearly demonstrated the participation of common myogenic progenitors in the formation of ventricular myocytes as

well as VCS cells (Aanhaanen et al 2009; Cheng et al 1999; Gourdie et al 2003; Gourdie et al 1995; Kitajima et al 2006; Meilhac et al 2003; Miquerol et al 2010; Nakamura et al 2006). Most recently, the different components of the CCS system are thought to form locally from non-migrating myocardial precursor cells present at a particular location within the developing heart (Cheng et al 1999; Christoffels & Moorman 2009; Pennisi et al 2002). Thus, the developmental path taken by a given myocyte depends on its position in the developing heart. The formation of a distinct conduction system component from its precursor can be modeled as a simple decision process, in which a precursor cell will turn into either a conduction cell or a working cardiomyocyte. Molecular genetic studies have revealed the functional requirement of a network of transcription factors for the formation of the sinus and atrioventricular nodes and the rapidly conducting ventricular pathways. These include broadly expressed factors of the core cardiac transcriptional network, such as Tbx5 and Nkx2.5, and the transcriptional repressors Tbx2, Tbx3, and Id2, which are expressed specifically in the precursors of these conduction system components (Bakker et al 2008; Hoogaars et al 2004; Moskowitz et al 2007). These repressors maintain the phenotype typical for the conduction system, and in their absence, the precursors differentiate into working myocardium, which seems to be the default developmental path (Bakker et al 2008; Christoffels et al 2004; Christoffels & Moorman 2009; Hoogaars et al 2004; Moskowitz et al 2007). As previous literature has shown, AChE is involved in proliferation and differentiation of several cell types, and as it is present in CPCs associated with a conduction cell phenotype, it is plausible that such activity is extended to CCS cell formation.

The development of the VCS also depends on extrinsic parameters, which in turn induce the transcriptional pathways directly involved in the differentiation and maturation of

conductive cells. As previously described, the heart is comprised of diverse cell populations: cardiomyocytes, endothelial cells, smooth muscle cells, and fibroblasts all of which originate from different progenitor populations. While neural crest cells and epicardium derived cells may not contribute directly to the VCS, these cells may be play a role in, and are required for normal VCS development (Eralp et al 2006; Gurjarpadhye et al 2007; Nakamura et al 2006; Poelmann et al 2004; St Amand et al 2006). Cross-talk between endothelial and myocardial cells also play a major role during cardiac development. Endothelin-1 (ET-1) and neuregulin are two factors secreted by endothelial cells that play important roles in the development of ventricular trabeculae and have been shown to direct the differentiation of embryonic murine cardiomyocytes into conductive cardiomyocytes (Patel & Kos 2005).

Similarly, (Re & Cook 2008) describe AChE as an intracrine factor. A large number of peptide growth factors, hormones, enzymes, DNA binding proteins, and other moieties have been shown to act as extracellular signaling agents, while at the same time apparently having the capability to act in cellular interiors. These considerations, in turn, let us propose a role for intracellular, finite-gain, positive feedback loops in some forms of cellular differentiation. That is, cells supporting such intracellular paracrine loops could potentially secrete paracrine factors to affect nearby target cells and result in an active form of cellular differentiation; that is, a change in state that persists long after the initial intracrine secretion has ceased. The C-terminal peptide of AChE-R, ARP, the "readthrough" form of acetylcholinesterase (AChE-R), a translational product generated by alternative splicing, is secreted by myeloid hematological progenitor cells, whereupon a unique COOH-terminal fragment [AChE-R peptide (ARP)] is cleaved from the protein in the extracellular space (Deutsch et al 2002; Grisaru et al 2001). This C-terminal peptide of AChE-R, which lacks enzymatic activity, subsequently acts on

target stem cells; ARP is found in circulating blood cells, bone marrow cells, and fetal human $CD34^+$ cells, and promotes proliferation following upregulation of its own synthesis via a positive feedback loop (Deutsch et al 2002; Grisaru et al 2001). This is further confirmed as administration of antisense to AChE-R prevents the proliferation (Perry et al 2004). AChE, therefore, has been considered a paracrine-AChE gene product that, depending on splicing, can function as extracellular signaling molecules or as moieties active in the intracellular space (Birikh et al 2003; Deutsch et al 2002; Dori & Soreq 2006; Nijholt et al 2004; Perry et al 2007). With this as a consideration, it is possible that AChE-R, or its cleaved peptide ARP, may be expressed in and secreted by immature cardiomyocytes, thereby functioning as an extrinsic agent acting on ventricular trabeculae to direct the differentiation of embryonic murine CPCs into a conductive phenotype (Figure 1.5). Currently, it is not feasible to examine whether ARP peptide is directly involved in conduction system formation due to lack of commercially available antibodies for this peptide.

Figure 1.5. A schematic representing the potential for ARP to mediate cardiac conduction cell commitment. The C-terminal peptide of AChE-R, ARP, is cleaved from the translated AChE-R protein in the extracellular space. This COOH-terminal fragment may interact with the gene promoters of transcriptional repressors Tbx2, Tbx3 and Id2 (alternatively it could also promote gene transcription of cardiac factors Tbx5 and Nkx2.5 in a similar manner). Gene expression of these repressors maintains the cellular phenotype typical for the conduction system.

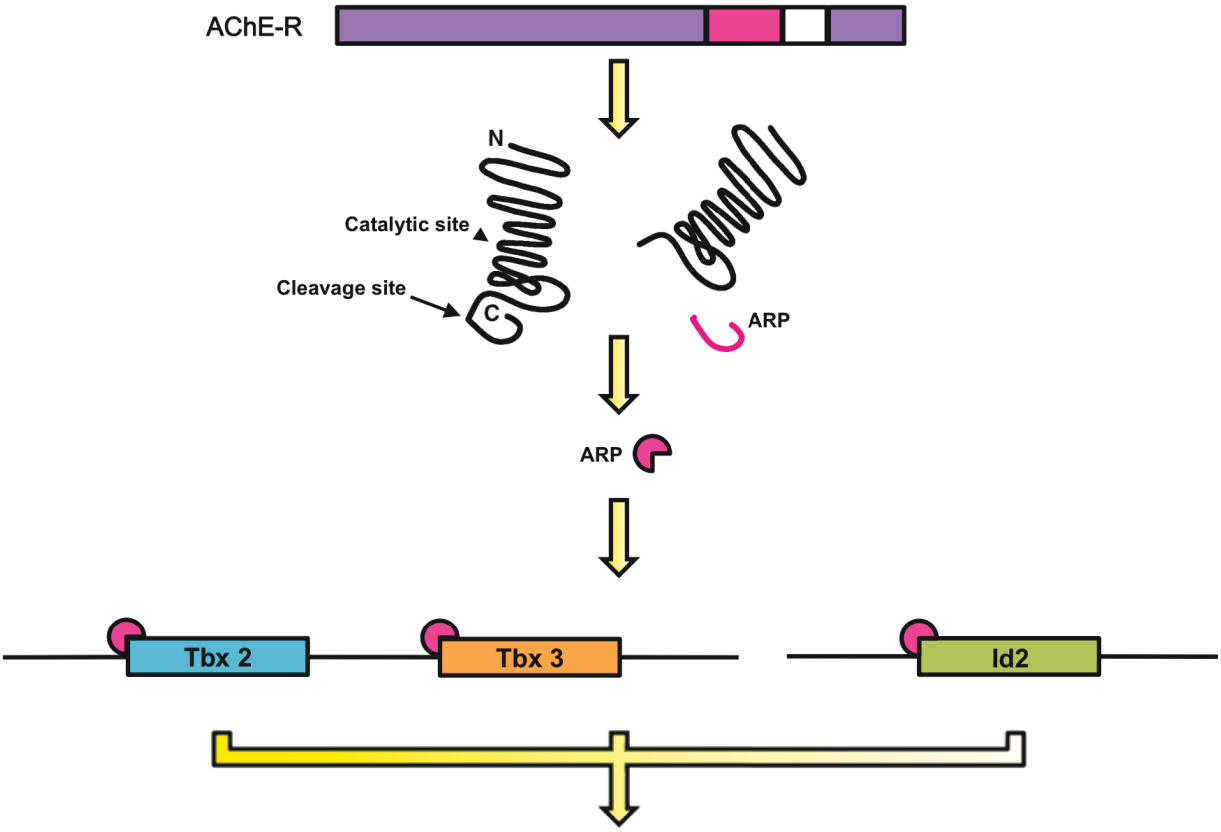

CARDIAC CONDUCTION CELL COMMITMENT

1.5 Rationale

In summary, the VCS is responsible for the synchronization of the heartbeat, and physiologists have extensively studied the automatic and rhythmic activity of these specialized cardiomyocytes. Despite important discrepancies between human and mouse cardiac physiology, mouse VCS anatomy is close to that of the human heart, making the mouse an attractive model for developmental biologists. Defects in the establishment of this circuit can result in the development of ectopic pacemakers in the myocardium, interfering with the natural rhythm and pattern of ventricular contraction and inducing the occurrence of cardiac arrhythmias. Understanding the pathway that guides conduction circuit formation and identifying important factors involved in cardiac progenitor cell commitment will provide insight into the origin of ectopic pacemaker development. Murine genetics, including the use of VCS reporter lines, lineage tracing and retrospective clonal analysis, has established the myogenic origin of the VCS and elucidated important signaling factors and genes involved in regulating its establishment, as well as determined several properties of conductive progenitor cells. Furthermore, it has also identified a crucial time period where developing mouse ventricles are composed of a mixed cell population made up of CPCs and lineage-committed cardiomyocytes. Considering this, manipulation and observation of cells should be carried out between E11.5 to E14.5 to address specific questions regarding cellular divergence. As such, convergent genetic and physiological studies in different model systems will further define the relationship between structure and function in the VCS and cardiac rhythm and contribute to new therapeutic approaches for myocardial damage and disease. The goal of the present study was to examine the existence and effects of AChE expression on cardiomyocyte cells during differentiation. We initiated our studies using CPCs as they differentiate into two main types

of cardiac cells: muscle cells and conduction cells. Using fluorescent labeling techniques, we are able to identify each cell type, offering the ability to investigate potential differential affects as a result of AChE inhibition.

We hypothesized that the presence of intracellular AChE (likely the soluble AChE-R form) during cardiac development may be involved in directing lineage commitment of mouse ventricular CPCs to the conduction cell phenotype. In order to investigate this hypothesis, we have formulated the following specific aims:

1. Is AChE mRNA expression developmentally modulated in ventricular cells?
2. Is AChE enzyme activity developmentally modulated at the subcellular compartmental level?
3. Does the AChE spatial expression pattern in myocardium correlate well with the regions of fast conduction system formation?
4. Does AChE inhibition affect CPC proliferation and differentiation?

Chapter 2.0: Materials and Methods

2.1 Experimental Animals and Aging

Experiments were conducted using myocardial cells isolated from the heart tissue of three strains of mouse embryos collected after five developmental stages. The ROSA- *Lac Z* mouse strain was obtained from the Jackson Laboratory (Bar Harbor, ME), the *Nkx2.5*-Cre mouse was obtained from Dr. Richard Harvey's laboratory (Victor Chang Cardiac Research Inst, Australia) and were cross bred to obtain a double transgenic strain specifically used for cell culturing of embryonic ventricular cells at 11.5 days gestation. The CD-1 mouse strain (non-transgenic) was obtained from Charles Rivers, Canada and was used for mRNA and protein extraction at five developmental stages (embryonic day 11.5, 14.5. 16.5, and post natal day 2 and 2 months). The breeding colonies were maintained in-house and female mice were mated with males under a 12 hr light/dark cycle. Embryonic day (E) 0.5 post coitus (p.c.) was recorded as 12:00 pm following discovery of a copulation plug. All transgenic mouse crosses were performed using homozygous ROSA- *Lac Z* and homozygous *Nkx2.5*-Cre mice, eliminating the need for genotyping. Double transgenic embryos were confirmed using β-galactosidase staining of atrial tissue. In order to obtain cardiomyocytes, pregnant females considered to be 11.5 days post gestation (11 days following the 0.5 p.c. copulation plug denoted E11.5) were sacrificed, embryos were isolated from uterine horns and cardiac tissue was removed under a stereomicroscope. Atrial appendages were carefully disposed of and only myocardial cells residing in the ventricular tissue were used for culturing. The identical method was used for obtaining ventricular tissue of CD-1 embryos at embryonic days 11.5, 14.5 and 16.5 as described above. The two stages post gestation (neonatal day-2 and adult) were sacrificed, their hearts removed, and ventricular tissue was removed from the apex of the

heart for processing. All of these procedures were performed according to the guidelines set by the Canadian Council on Animal Care and were approved by the Dalhousie University Committee on Laboratory Animal Care.

2.2 Total RNA Isolation

Total RNA was isolated using either: the RNeasy mini-kit PLUS according to manufacturer's instructions (Qiagen, Mississauga, Ontario), or the TRIzol (Invitrogen) method.

RNeasy mini-kit PLUS Method

In brief, samples were collected from ventricular tissue of CD-1 mice at five developmental stages and lysed in a guanidine-isothiocyanate denaturing buffer and passed through a gDNA eliminator column (embryonic day 11.5 and 14.5 were briefly vortexed and embryonic day 16.5, post natal 2 and 2-month old adult tissues were homogenized using a rotor (Tissue Tearor™; Biospec Products, Inc.) before passing through the eliminator column). In conjunction with a high salt buffer, the gDNA column measures the total elimination of gDNA. Total RNA concentrations were determined using the 260 nm absorbance value obtained by a spectrophotometer (SmartSpec™ Plus, Bio Rad, Mississauga, Ontario). The quality of the RNA was determined by taking the ratio of the absorbance measured at 260 nm to the absorbance measured at 280 nm. A ratio of 1.8 to 2.0 indicates a high level of RNA purity, devoid of DNA contamination. RNA samples with values deviating from these ratios were rejected for further analysis.

TRIzol Method

Ventricles were carefully dissected from five embryonic and post-natal stages of CD-1 mice, homogenized in 1 mL of TRIzol (Invitrogen) and incubated at room temperature (RT) for five minutes. 200 μl of chloroform was added, the samples were shaken for approximately 15 seconds and incubated at RT for three minutes. The aqueous phase was transferred into a separate tube and the RNA was precipitated using 0.5 mL isopropyl alcohol. The sample was then incubated at RT for 10 min and subjected to centrifugation (4°C; 12 000g; 10 min). The supernatant was removed and the remaining RNA pellet was washed with 1 mL of 75% ethanol (in DEPC treated H_2O). The sampled was vortexed and the pellet was briefly air-dried for 5-10 min. RNA was dissolved in RNAase free water, mixed by pipetting, and incubated at 55-60°C for 10 min. RNA concentrations were determined by absorbance at 260 nm.

2.3 Reverse Transcription and Quantitative Real Time Polymerase Chain Reaction

Total RNA extracted from CD-1 mouse hearts at five developmental stages and was reverse transcribed to cDNA using SuperScript II reverse transcriptase (RT) and random primers (Invitrogen, Burlington, Ontario). The reaction mixture consisted of 3 μg of either TRIzol or RNeasy purified RNA, 1 μl of random primers (0.5 µg/µl), and 1 µl dNTP mix (10mM each) – the final volume of the reaction mixture was adjusted to 12 µl using sterile water. The samples were then heated to 65°C for five minutes, briefly subjected to centrifugation (4000 RPM) and chilled on ice for another five minutes. Following cooling, 4 μl of 5x SuperScript First-Strong buffer, 2 μl of 0.1M DTT, and 1 μl RNaseOUT (40 units/µl) was added to the samples and mixed at RT for two minutes. 1 μl (200 units) SuperScript II RT

was added, mixed gently using a pipet, incubated (25°C for 10 min; 42°C for 50 min; 70°C for 15 min) and stored at -80°C. All RT reagents were purchased from Invitrogen (Burlington, Ontario). For each RNA reaction, a no-template control reaction was prepared, where RNA was omitted and sterile water was used as a replacement.

The cDNA, obtained from RNeasy purified RNA, was amplified by Quantitative Real-Time Polymerase Chain Reaction (QPCR) using the following primers: mb2m, mRpl13a, mTbp, β-actin, GAPDH-1, GAPDH-2 (Table 2.1), GAPDH-2 (Denoted GAPDH), AChE-R, AChE-H and AChE-T (Table 2.2). The AChE-R, H and T primers were generated using the NCBI primer-blast software, (http://www.ncbi.nlm.nih.gov/tools/primer-blast/index.Cgi?LINK_LOC=BlastNews). The mb2m, mRpl13a, mTbp, β-actin, GAPDH-1 and GAPDH-2 primers were generated from http://mouseprimerdepot.nci.nih.gov/ and purchased from Invitrogen (Burlington Ontario). Where possible, primers were designed to be exon spanning as to eliminate gDNA amplification. In addition, gDNA was further eliminated using gDNA removal columns provided by the RNeasy mini-kit PLUS during total RNA isolation. The reaction mixture consisted of 2 µl of cDNA product, 0.25 µl of the forward and reverse primers (2.5 µM), 2.0 µl of MBI EVOlution EvaGreen ® qPCR master mix (MBI Hotstart DNA Polymerase, 5 x qPCR buffer, $MgCl_2$ (1 x PCR solution – 2.5 mM $MgCl_2$), dNTPs (including dTTP to improve reaction sensitivity and efficiency compared to dUTP), EvaGreen® dye) and 5.5 µl RNase/DNase free dH_2O. QPCR conditions were set on the Eco™ Real-Time PCR System (Illumina, Inc., San Diego, California) according to Tables 2.1 and 2.2. The melting point curve was used to verify the amplification of one gene per primer pair (Figures 2.1 and Figure 3.2). After evaluation, it was determined that GAPDH-2, denoted as GAPDH for the entirety of this manuscript, was the most appropriate internal control as any

variability over the five developmental stages was considered insignificant. Gene expression was normalized to the control housekeeping gene GAPDH using the $\Delta\Delta C_T$ method (Livak & Schmittgen 2001). In brief, the threshold fluorescence (dRn) was set at 0.1 and the threshold cycle (Ct) values for the amplified genes were collected. The Ct value of an amplified gene refers to the cycle number at which the amplified gene intersects the dRn threshold. Using the Ct values, a series of calculations were executed to determine experimental gene expression relative to control gene expression. First, the ΔCt value for each experimental gene was determined by subtracting the control gene Ct value from the experimental gene Ct value, and the average ΔCt value was calculated. The average ΔCt value was then subtracted from the ΔCt values calculated for each experimental gene yielding the ΔΔCt. The $2^{-\Delta\Delta Ct}$ was calculated using the ΔΔCt values, and the average of the $2^{\Delta\Delta Ct}$ was determined. Finally, the corrected $2^{-\Delta\Delta Ct}$ value was determined for each gene by dividing the $2^{\Delta\Delta Ct}$ values by the $2^{\Delta\Delta Ct}$ average.

Table 2.1. Quantitative Real-Time PCR mouse primer sequences and expected amplicon band sizes. This table provides an overview of each gene that was evaluated for the consideration as an internal housekeeping control gene during real-time polymerase chain reaction analysis of the AChE splice variants throughout development. It was found that GAPDH-2 would be the most appropriate choice, as any fluctuation in mRNA expression at each developmental stage was found to be insignificant.

Gene	Sequence 5'-3'	Amplification Cycles	Efficiency (%)
mb2m	F:CTGACCGGCCTGTATGCTAT R:TTTCCCGTTCTTCAGCATTT	94°C for 15 s, 60°C for 30 s, 72°C for 10 s, 40 cycles	96.38
mRpl13a	F:CCCTCCACCCTATGACAAGA R:GGCTGTCACTGCCTGGTACT		99.40
mTpb	F:ACATCTCAGCAACCCACACA R:CTGGTGTGGCAGGAGTGATA		56.20
β-actin	F:ATGGAGGGGAATACAGCCC R:TTCTTTFCAGCTCCCTCGTT		73.23
GAPDH-1	F:CGTCCCGTAGACAAAATGGT R:TCAATGAAGGGGTCGTTGAT		75.96
GAPDH-2	F:TTGAGGTCAATGAAGGGGTC R:TCGTCCCGTAGACAAAATGG		98.76

*F = forward primer; R = reverse primer

Table 2.2. Reverse Transcription Polymerase Chain Reaction analysis of mRNA from three AChE isoforms (R, H and T) in ventricular cardiac cells extracted from five developmental stages of CD-1 mice. The enzyme glyceraldehyde-3-phosphate dehydrogenase (GAPDH) was used as an internal control. Developmental stages for E14.5 and E16.5 were determined as described for E11.5 (Section 2.1). The neonatal stage refers to the first two-days post parturition, and the adult samples are from 8-11 week old mice. It is useful to mention that the R and H mRNA sequences are identical with the exception of an intron; therefore, primers cannot distinguish these two isoforms. Instead, the primers were designed to span this intron in order to separate these variants via band sizes.

AChE Variant	Sequence 5'-3'	Product Length	Amplification Cycles	QPCR Efficiency
AChE-R	F: CAGGGGACCCCAATGACCCTCG R: CCCACTCCATGCGCCTACCGGT	192 bp	95°C for 15 s, 60°C for 1 min, 95°C for 15 s, 40 cycles	95.8%
AChE-H*	F: CCGCGCAGCAATATGTGAGCCT R: GCAGGTGCAAGGAGCCTCCGT	253 bp (H) 137 bp (R)	95°C for 15 s, 60°C for 1 min, 95°C for 15 s, 40 cycles	…
AChE-T	F: TAGAGGTGCGGCGGGGACTG R: TGAGCAGCGCTCCTGCTTGC	168 bp	95°C for 15 s, 62°C for 1 min, 95°C for 15 s, 40 cycles	96.3%
GAPDH	F: TTTCCCGTTCTTCAGCATTT R: CTGACCGGCCTGTATGCTAT	150 bp	95°C for 15 s, 60°C for 1 min, 95°C for 15 s, 40 cycles	92.4%

*F = forward primer; R = reverse primer

*This transcript does not contain any additional introns or exons that might distinguish it from the R transcript (see Figure 1.1), and as such, this primer pair could not be included in our QPCR analysis. Rather, RT-PCR was used to confirm the presence of AChE-H mRNA where amplification products were resolved strictly via band sizes.

Figure 2.1. GAPDH gene expression does not fluctuate with age and is therefore a useful internal control. Melting curves completed for QPCR primers indicate the presence of only one amplified product for each primer as depicted by a single peak per primer pair.

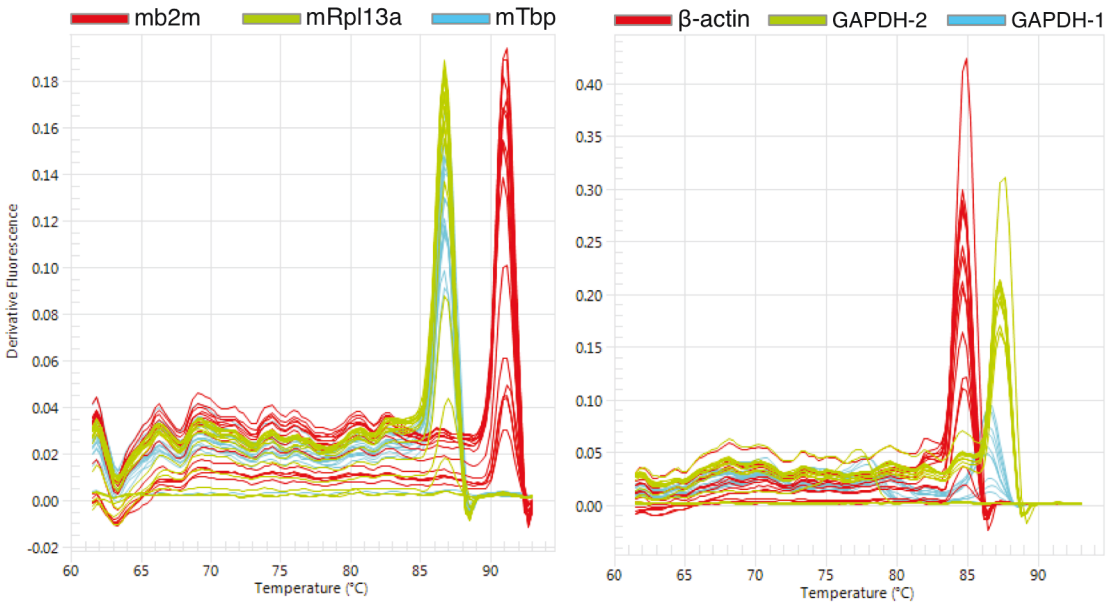
mb2m
mRpl13a
mTbp
Derivative Fluorescence
0.18
0.16
0.14
0.12
0.10
0.08
0.06
0.04
0.02
0.00
-0.02
60
65
70
75
80
85
90
Temperature (°C)
β-actin
GAPDH-2
GAPDH-1
0.40
0.35
0.30
0.25
0.20
0.15
0.10
0.05
0.00
60
65
70
75
80
85
90
Temperature (°C)

PCR was also performed using primers for M_1 and M_2 muscarinic receptors. cDNA was removed for -80°C storage and samples were made using: 5 μl 10x Taq Buffer, 4 μl dNTP (2.5 mM), 4 μl $MgCl_2$ (25 mM), 0.25 μl *Taq* DNA Polymerase, 1 μl Primer I (M1F/M2F), 1 μl Primer II (M1R/M2R), 1 μl DNA (RT) and 33.75 μl PCR H_2O. For the mAChR M_1 and M_2 subtypes, the amplification protocol entailed 40 cycles of denaturation at 95 °C for 30 s, annealing at 50 °C for 30 s and extension at 72 °C for 45 s. As an internal control for the efficiency of cDNA amplification, we also amplified glyceraldehyde-3- phosphate dehydrogenase (GAPDH) mRNA using the primers shown in Table 2.2. Amplification for GAPDH entailed 40 cycles of 95 °C for 15 sec, 60 °C for 1 min and 95 °C for 15 sec, followed by a 15-min final extension at 72 °C.

The PCR products present in 10 μl of the reaction mixture were then separated according to size on 1.5% agarose gels and visualized by ethidium bromide staining. The resultant fluorescent bands were digitized using a Kodak EDAS 290 Dual Intensity UV Transilluminator.

The forward and reverse oligonucleotide primers used for RT-PCR analysis in the present study were custom synthesized at Invitrogen, Canada. All other reagents used were of reagent grade and purchased from commercial sources (e.g. Sigma).

2.4 Protein Extraction and Western Blotting

Ventricular tissue was carefully dissected from female CD-1 mice (non-transgenic) at five developmental stages (embryonic day 11.5, 14.5 and 16.5 and post-natal stages at 2 days and 2 months after birth) and placed in tumour lysis buffer (1% NP40/Igpal, 5mM EDTA, 50mM Tris HCl pH 8.0, 10mM phenylmethylsulphonyl fluoride (PMSF) and 1mM Aprotinin). The tissue was then homogenized using a rotor (Tissue Tearor™; Biospec

Products, Inc.) and subjected to sonication (Sonic Dismembrator, model 100; Thermo Fisher Scientific, Nepean, Ontario: Setting 3.5, duration: 10 seconds x 3). Cell lysates were incubated at 4°C for fifteen minutes. Detergent soluble (cytosol) and detergent insoluble (whole membrane) fractions were collected by high-speed centrifugation (13, 300 rpm x 15 minutes) at 4°C. Aliquots were taken to determine protein concentration by Bradford assay (Thermo Fisher Scientific, Napean, Ontario) followed by protein sample denaturation in Lamelli buffer [62.5mM Tris-Cl pH 6.8, β-Mercaptoethanol, 25% glycerol, 2% sodium dodecyl sulfate (SDS), 0.02% bromophenol blue, and double distilled water (ddH_2O)] at 95°C for 15 minutes. Protein samples were either stored at -80°C for further use, or resolved in a 7.5% SDS-polyacrylamide gel (25% 1.5M Tris-HCl (pH 8.8), 0.1% SDS, 25% acrylamide, 0.5% ammonium persulphate and 0.1% v/v TEMED) using 1x Tris-glycine migration buffer (25mM Tris based, 190mM glycine and 0.1% SDS at 8.3 pH) at 100 volts and transferred to Hybond ECL nitrocellulose membrane (GE Healthcare Life Sciences, New Jersey) by applying a constant current at 100 volts for one hour (Transfer buffer: 25mM Tris base, 190mM glycine and 20% methanol at 8.3 pH). The membrane was incubated with napthol blue stain (1% napthol blue black, 45% methanol and 10% glacial acetic acid) for protein visualization and determination of protein loading. The membrane was blocked for one hour in blotting buffer (5% skimmed milk powder, 3% BSA, 0.1% Tween 20 in PBS (Sigma-Aldrich, Oakville, Ontario) followed by a one hour primary antibody, and a one hour secondary antibody incubation period. Primary antibodies used in this study include antibodies purchased from Santa Cruz Biotechnology, California: AChE (sc-11409), an antibody raised to the unique C-terminus of human AChE-R ([21], a generous gift from Prof. Hermona Soreq, The Institute of Life Sciences, The Hebrew university of Jerusalem, Jerusalem, Israel), α-tubulin (sc-8035),

CBF-A (sc-13045) and GAPDH (sc-25778). Secondary antibodies include: goat-anti-rabbit (Bio-Rad, Mississauga, Ontario, Catalogue #172-1019) and goat-anti-mouse (Bio-Rad, Mississauga, Ontario, Catalogue #170-6516) antibodies conjugated to horseradish peroxidase. Antibody dilutions were as follows: primary antibody 1:200 (AChE) and 1:400 (remaining), secondary goat-anti-rabbit antibody was 1:200 and secondary goat-anti-mouse was 1:1000. Protein bands were detected by the ECL Plus Western Blotting Detection System via the chemiluminescence method according to manufacturer's instruction (GE Healthcare Life Sciences, New Jersey).

2.5 Band Densitometry for Protein Quantification

Developed western blot films were scanned and imported into Image J (http://rsbweb.nih.gov/ij/) software to be analyzed via band densitometry. Given that α-tubulin, CBFA and GAPDH protein levels were unchanged throughout development; these protein levels were used to normalize any variation in sample protein loads. After normalization, experimental band intensity values compared and statistically analyzed for developmental changes. Data are presented as mean ± S.E.M. Between-group comparisons were analyzed by ANOVA multiple comparisons test (Graphpad Prism 5). Significance was assumed at $p < 0.05$.

2.6 Enzymatic Activity Quantification

The DetectX® Acetylcholinesterase Activity kit (Arbor Assays, Ann Arbor, Michigan) was used to quantitatively measure AChE activity in detergent soluble and insoluble protein fractions acquired from CD-1 mice hearts at five developmental stages (E11.5, E14.5, E16.5, Neonatal and Adult) as described in section 2.4. The kit utilizes a proprietary non-fluorescent

molecule, ThioStar®, designed to covalently bind to the thiol product of the reaction between the AChE Substrate and AChE, yielding a detectable fluorescent product. In short, the thiostar assay determines accurately the amount of free thiol content in samples, offering an indirect measurement of AChE enzymatic activity. Prior to measuring unknown samples, it was important to optimize the appropriate gain necessary for measuring AChE activity. This was achieved by reading the fluorescence of a known activity concentration (100 mU/mL) taken from the kit's standard (Denoted as the 'Signal') against the dilution assay buffer (Denoted as the "Noise") to give a mathematical ratio that was plotted against various gains (Figure 2.2a). The second graph describes the fluorescence measured at each experimental gain used (Figure 2.2b). Based on these values, a gain of 650 was deemed appropriate for further testing. Figure 2.3 describes the process used to determine that 15 µg of protein is an appropriate concentration to be used in experimental samples. A series of concentrations was tested, and it was found that 15 µg offered a large enough activity reading to allow for increased or decreased fluctuation. The assay was performed according to the manufacturer's instructions, where 100 µl of samples (15 µg of protein as determine by Figure 2.3) or standards was pipetted into duplicate wells into a black/black bottom 96-well plate (XOO1-2EA, Arbor Assays, Ann Arbor, Michigan). Experimental standards were prepared through a series of serial dilutions of the AChE Standard (CO46-28ML, Arbor Assays, Ann Arbour, Michigan) to achieve five final standard concentrations of 100, 50, 25, 12.5 and 6.25 mU/mL. 100 µl of 1x Assay Buffer (XO64-225UL, Arbor Assays, Ann Arbour, Michigan) was also pipetted into duplicate wells as a Zero standard. A reaction mix was prepared using strictly kit contents (10% AChE Substrate Concentrate, 10% ThioStar® Concentrate, 80% DMSO) and added to each of the wells using a multichannel pipet in 50 µl volumes. The plate was gently mixed up

tapping and left to incubate at room temperature for 20 minutes. The fluorescence emission was read at 520 nm with excitation at 355 nm. The duplicate FLU readings were averaged for each standard and sample. Reducing the data using the 4PLC fitting routine on the plate reader, after subtracting the mean FLUs from the zero standard, created a standard curve. Data are presented as mean ± S.E.M. Between-group comparisons were analyzed by ANOVA multiple comparisons test (Graphpad Prism 5). Significance was assumed at $p < 0.001$.

Figure 2.2. Gain optimization. Before samples could be measured, it was important to determine the appropriate gain for experimental testing of the DetectX® Assay. In order to do this, the fluorescent reading of 1x Assay buffer was measured against that of 100 mU/mL of AChE standard over a series of gains between 250-800 dB, where excitation was measured at 350 nm and emission at 520 nm. **a)** The value of the AChE standard ("signal") was divided by the value of the 1x Assay Buffer ("noise") to give a ratio that was plotted against the gain used. **b)** The obtained fluorescence values were plotted against the gain to reveal that a gain of 640-650 gives an FLU of ~75 000 between 0 and 100 mU/mL as indicated by the highlighted regions. The data revealed that a gain of 650 dB was appropriate for further experiments.

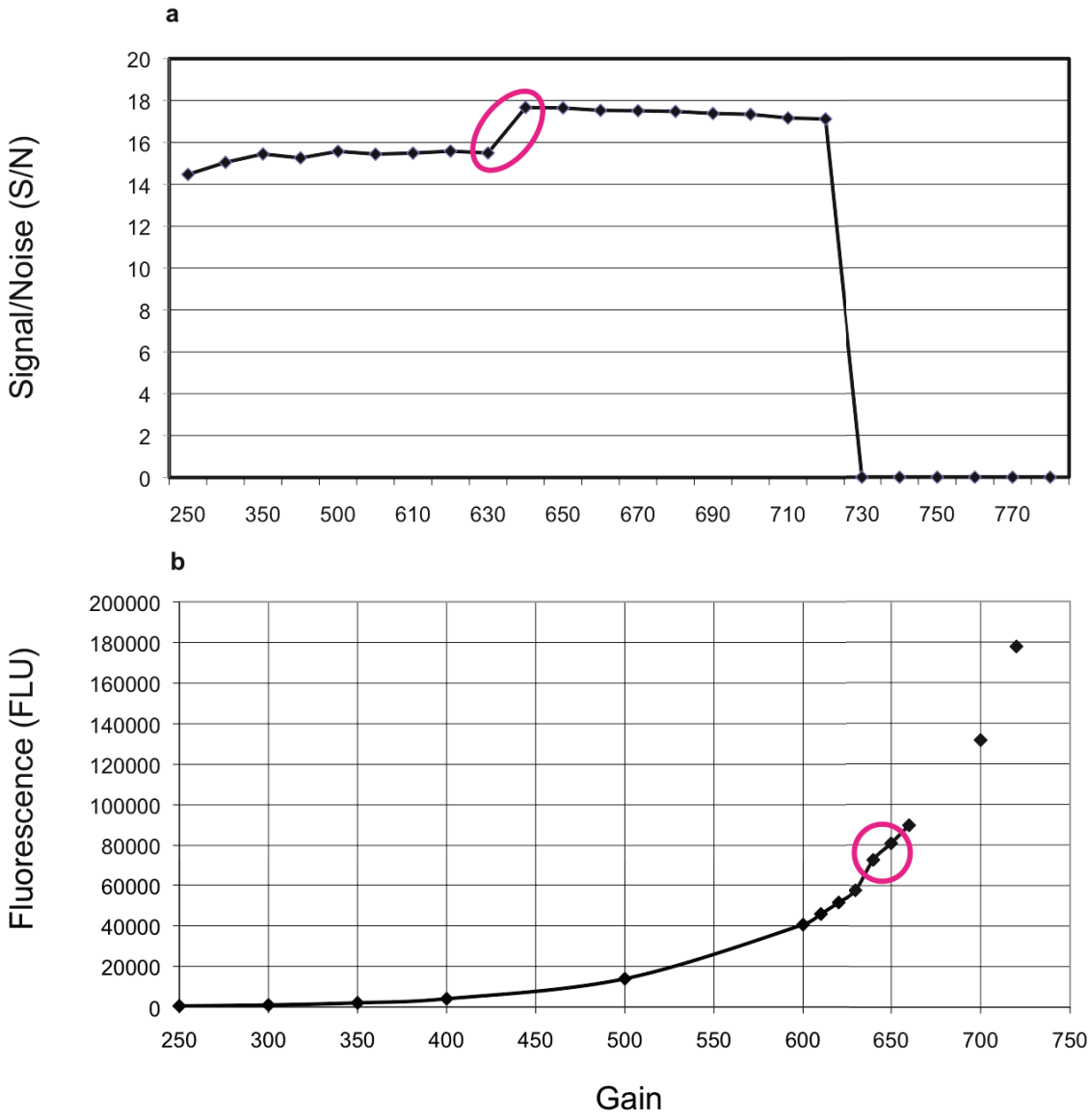
a
Signal/Noise (S/N)
20
18
16
14
12
10
8
6
4
2
0
250
350
500
610
630
650
670
690
710
730
750
770
b
Fluorescence (FLU)
200000
180000
160000
140000
120000
100000
80000
60000
40000
20000
0
250
300
350
400
450
500
550
600
650
700
750
Gain

Figure 2.3. The amount of protein determined to be appropriate for further testing was 15 µg per well. A series of protein concentrations was tested for AChE activity to determine which would be appropriate for further testing. **a)** First, an AChE activity standard was created using five samples of known concentration. **b)** Experimental values were then extrapolated from the standard plot to determine the AChE activity in each sample based on the fluorescence value recorded in each well. The results suggested that 15 µg of protein would be appropriate for further testing, as it gives an AChE activity large enough to allow for either positive or negative experimental fluctuation.

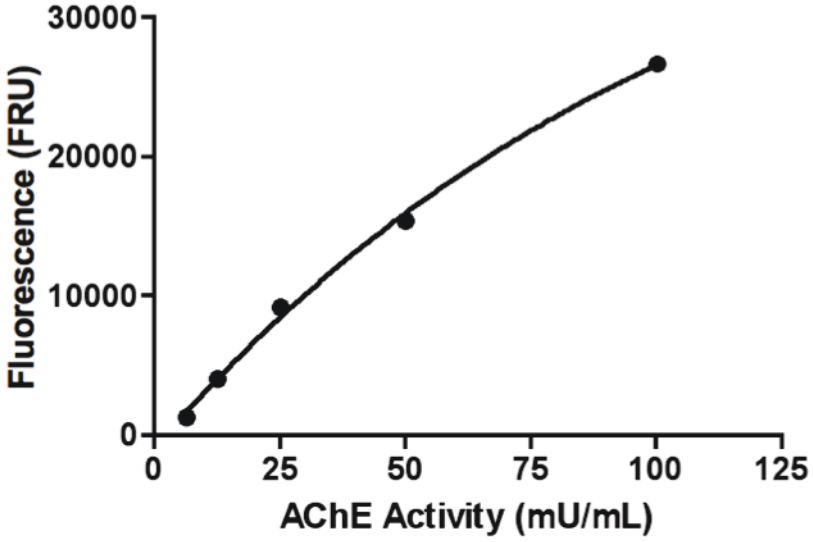
30000
20000
10000
0
Fluorescence (FRU)
0
25
50
75
100
125
AChE Activity (mU/mL)

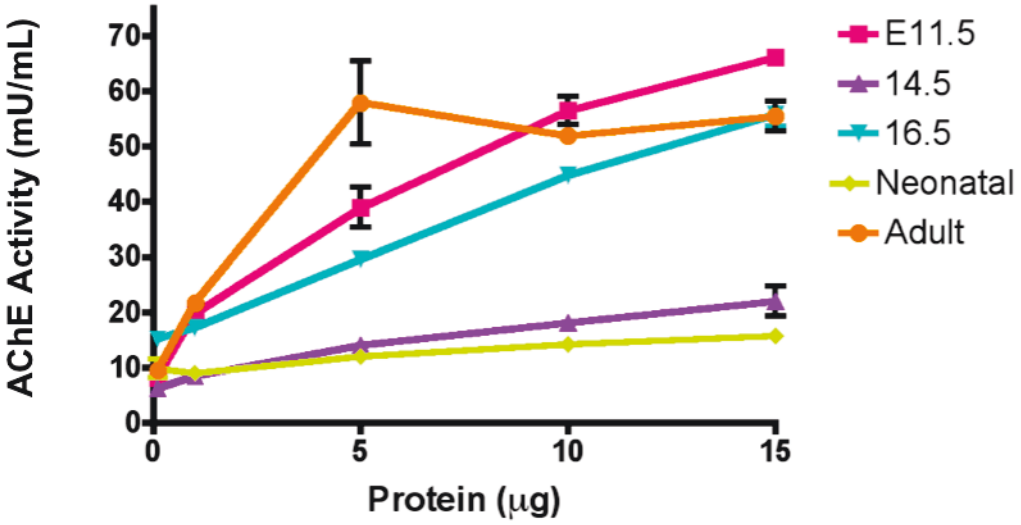
70
60
50
40
30
20
10
0
AChE Activity (mU/mL)
0
5
10
15
Protein (μg)
E11.5
14.5
16.5
Neonatal
Adult

2.7 Cryosectioning

Hearts were removed from embryonic day 11.5 and 14.5 old CD-1 mice and left to rock in 30% sucrose overnight at 4°C. The hearts were then removed from the sucrose and embedded into Tissue-Tek® Optimal Cutting Medium (O.C.T), a water soluble glycol and resins compound that provides a support medium for cryostat sectioning at temperatures of -10°C and below, and leaves no residue during staining procedures. The samples were then stored at -80°C until further use. The samples were sectioned on a Leica CM3050 S Crystat, set to a standard operating chamber temperature of -25°C and an object temperature of -20°C. A fresh blade was adjusted between 0 and 5° for the least compression and left to cool. When the cryostat was ready, the embedded heart samples were removed from -80°C and adhered to a clean cryostat chuck using a small amount of O.C.T. medium. The whole heart samples were sliced to achieve sections ~6-8 microns thick and transferred to a microscope slide (25 X 75 X 0.1 mm; **Fisher**brand®; Stores, Dalhousie University, Halifax). All slides containing cryosections were stored at -20°C until further use.

2.8 Immunofluorescence

Cryosections (described in section 2.7) were removed from -20°C and prepared for immunofluorescence. First, slides were fixed in cold methanol for 15 minutes at 4°C, washed in cold phosphate buffered saline (PBS: 0.138 M NaCl, 0.0027 M KCl, pH 7.4), permeabilized in 0.1% Triton –X 100 (Sigma-Aldrich, Oakville, Ontario) for 5 minutes, and blocked with blocking buffer (1% v/v bovine serum albumin (BSA), 10% v/v goat serum in PBS) for one hour. Following a 5 minute PBS wash (x3), sections were probed with primary antibodies raised against AChE (rabbit polyclonal; 1:200; Santa Cruz Biotechnology, Inc., Dallas, Texas,

U.S.) or AChE-R (rabbit polyclonal; 1:100; a generous gift from Dr. Hermona Soreq, University of Israel) and sarcomeric myosin (MF20, mouse monoclonal; 1:50; Developmental Studies Hybridoma Band, Iowa City, Iowa, U.S.) for one hour at 25°C, followed by a one hour incubation with secondary goat anti-mouse antibodies, conjugated to Alexa Fluor 488 (1:200; Invitrogen, Burlington, Ontario) or goat anti-rabbit antibodies conjugated to Alexa Fluor 555 dye (1:200; Invitrogen, Burlington, Ontario) for one hour. The slides were then washed for 5 minutes with PBS (x3) and incubated with 10 mg/ml bisBenzimide H 33342 trihydrochloride (Hoechst 33342) nuclear stain (Sigma-Aldrich, Oakville, Ontario) for five minutes, washed extensively in cold PBS and mounted under glass coverslips (22x22 mm 0.08-0.13mm thickness, VWR, Mississauga, Ontario) using 1% w/v propyl 3,4,5-trihydroxybenzoate (propyl gallate) in a 1:1 PBS/glycerol solution. All primary and secondary antibodies were diluted in blocking buffer and purchased from Santa Cruz Biotechnology Inc. as denoted by the "sc" present in the catalogue numbers. Images were captured using a Leica DMF2500 fluorescence microscope, fitted with a DFC500 digital acquisition system (Leica Microsystems, Concord, Ontario).

2.9 Transgenic Cell Culture and Drug Treatment

The early transcription factor *Nkx2.5* is the first marker expressed in cardiac progenitor cells (CPCs), which develop in both heart fields during the E7.5 stage, namely the primary heart field (PHF) and the anterior heart field (AHF). Sarcomeric myosin, a protein of the contractile apparatus of cardiomyocytes, is typically expressed at a later stage of development. A combination of Cre/*loxP* based cell labeling for the early cardiac transcription factor *Nkx2.5*, and immunostaining for sarcomeric myosin were used to determine the differentiation

status of the cultured myocardial cells; where those expressing *Nkx 2.5* and not MF20 were considered undifferentiated (and represent the putative CPC population). Cells expressing *Nkx2.5* and MF20 were considered differentiated (mature). The percentage of cells with a mature/immature phenotype was defined as the number of cells with a particular phenotype out of the total number of cells counted.

A double transgenic mouse model was required for the success of this system (Figure 2.4). One strain of transgenic mice has an internal ribosomal entry sequence (IRES) and the Cre- recombinase (Cre) coding sequence which has been inserted into its genome at the 3' untranslated region of the *Nkx2.5* gene (these mice were referred to as the *Nkx2.5*-Cre line). The other line of transgenic mice was engineered to have a transcriptional terminator stop cassette flanked by *loxP* sites upstream from the *Lac Z* gene (the stop cassette is said to be "floxed"; and these mice were referred to as the ROSA- *Lac Z* line). Cre, a recombinase protein from the bacteriophage P1, mediates site-specific recombination between *loxP* sites. Double stranded DNA is cleaved upon detection of a pair of *loxP* sites, resulting in the removal of any DNA situated between them, and followed by the ligation of these newly freed DNA ends to achieve a modification of the original structure. Upon translation of *Nkx2.5* in the initial heart cell population of the double transgenic mice, the Cre- recombinase gene is co-translated. The resulting Cre-protein excises the floxed stop cassette from ROSA-*Lac Z* transgenes, allowing the expression of the *Lac Z* reporter thereafter, and detection of *Nkx2.5*+ cell lineages with β-galactosidase antibodies.

Cells were recovered from E11.5 double transgenic mice hearts (*Nkx2.5*-Cre X ROSA-*lacZ*) as described in section 2.1 and were disaggregated by treatment with 0.2% collagenase. Cells were cultured on two-well chamber slides in Dulbecco's modified Eagle's medium

(DMEM, Wisent, Saint-Bruno, Quebec) supplemented with 10% fetal bovine serum (10% FBS-DMEM), 1x antimycotic-antibiotic (AB/AM, 1000 units penicillin G sodium, 1000 µg streptomycin sulfate, and 2.5 µg amphotericin B as Fungizone® in 0.85% saline) and 1 mM sodium pyruvate at 37°C in a humidified incubator set at 6% CO_2 (Thermo Fisher Scientific, Nepean, Ontario). Cells were seeded at ~500 000 cells per well, in Lab-Tek® II *CC*^{2TM} Chamber Slides™ two-well chambered slides (4cm^2/well; Thermo Fisher Scientific Inc., Rochester, New York). After twenty hours, fresh medium was added to the wells along with 10 μM of galantamine or no galantamine (control) and left to incubate for 22 hours at 37° under $C0_2$.

Figure 2.4. *Nkx2.5* reporter gene system. Mouse 1: Cre- recombinase (Cre) coding sequence inserted into its genome at the 3' untranslated region of the *Nkx2.5* gene. Mouse 2: Engineered to have a transcriptional terminator stop cassette (Stop) flanked by *loxP* sites upstream from the *Lac Z* gene. Cre mediates site-specific recombination between *loxP* sites. Upon translation of *Nkx2.5* the Cre- recombinase gene is co-translated. The resulting Cre-protein excises the floxed stop cassette from ROSA- *Lac Z* transgenes, allowing the expression of the *Lac Z* reporter thereafter, and detection of *Nkx2.5*+ cell lineages with β-galactosidase antibodies.

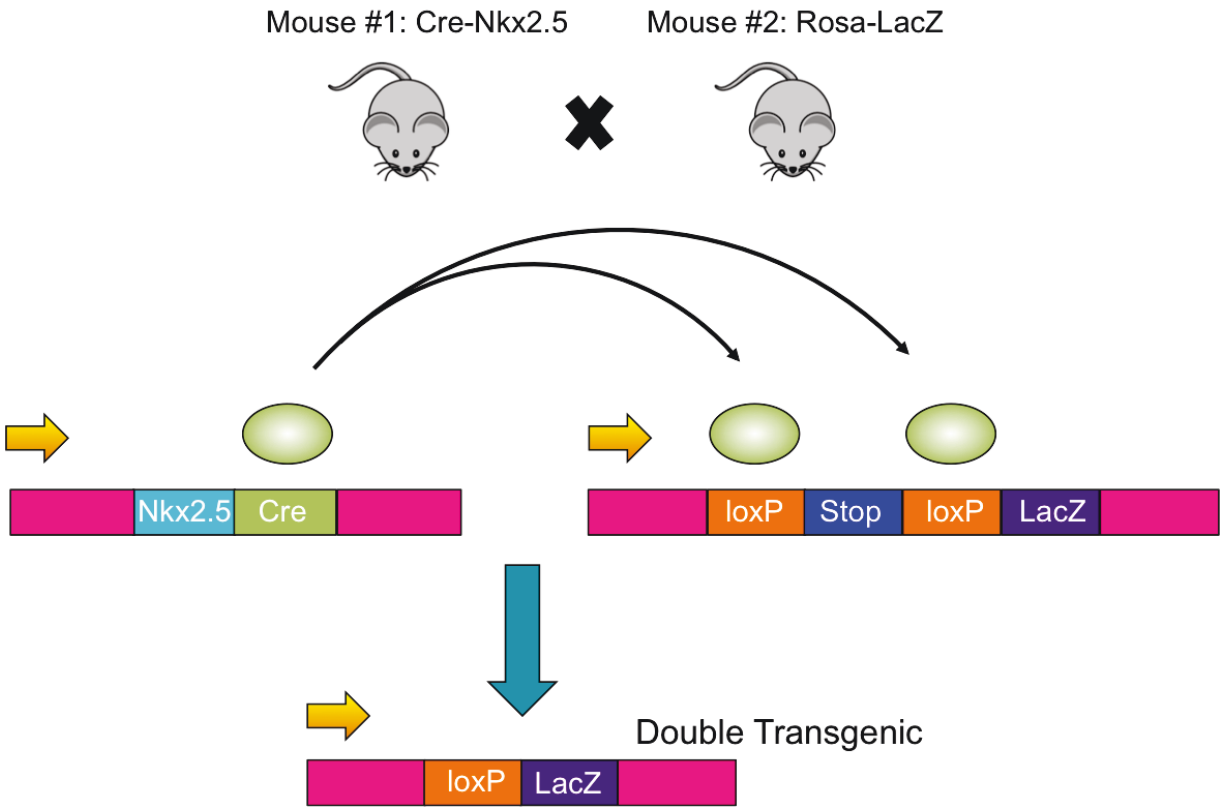
Mouse #1: Cre-Nkx2.5
Mouse #2: Rosa-LacZ
Nkx2.5
Cre
loxP
Stop
loxP
LacZ
Double Transgenic
loxP
LacZ

2.10 [^{3}H]-Thymidine Labeling and Autoradiography

Medium from treated and untreated transgenic cells was removed and replaced with medium containing ^{3}H-thymidine (GE Healthcare Life Sciences, New Jersey) at a concentration of 1.0 μCi per 1 ml of medium. Cells were pulsed with radioactive thymidine for six hours while incubating at 37° C under CO_2. Cells were fixed in cold methanol for 15 minutes and process for immunofluorescence as described in section 2.8. Chamber slides were air dried, coated with Kodak autoradiography emulsion type NTP (MarketLINK Scientific, Burlington, Ontario) and placed in a light-tight box at 4°C for three days. The slides were developed in a Kodak-D19 developer (Sigma-Aldrich, Oakville, Ontario) for four minutes, washed in double distilled water (ddH_2O), fixed with Ilford Rapid Fixer (Polysciences, Pennsylvania) for four minutes, and mounted under glass coverslips (22x22 mm 0.08-0.13mm thickness, VWR, Mississauga, Ontario) using 1% w/v propyl 3,4,5-trihydroxybenzoate (propyl gallate) in a 1:1 PBS/glycerol solution. Cellular morphology was examined under bright field, and nuclei were identified with epi-fluorescence microscopy. Cells containing more than fifteen nuclear silver grains were identified as cells undergoing DNA synthesis. Cells expressing *Nkx 2.5* and not MF20 were considered undifferentiated (and represent the putative CPC population); cells expressing *Nkx2.5* and MF20 were considered differentiated (mature). Labeling index was defined as the number of cells positive for silver grains in the nucleus out of the total number of cells counted. The percentage of cells with a mature/immature phenotype was defined as the number of cells with a particular phenotype out of the total number of cells counted. To determine if galantamine affected the rate of cellular proliferation in the cultured populations, cells were counted in fifty random fields for individual replicates from each treatment group and tested for between group significance.

Data are presented as mean ± S.E.M. Between-group comparisons were analyzed by ANOVA multiple comparisons test (Graphpad Prism 5). Significance was assumed at $p < 0.001$.

Chapter 3.0: Results

3.1 The Three Mammalian Splice Variants of Acetylcholinesterase mRNA are Expressed in the Developing Hearts of CD-1 mice

Mammalian acetylcholinesterase (AChE) has been found to exist in three molecular forms, depending on alternative splicing of its transcripts (Perrier et al 2005). Alternative use of distinct 3' splice acceptor sites in the primary RNA transcript or pre-mRNA yields three different variants (Figure 1.1). The AChE-R variant results from the absence of splicing after the last catalytic exon 4 and inclusion of a 'readthrough' intron 4' which has a short in-frame open reading frame (R domain) followed by a stop codon. The AChE-H variant results from splicing of the exon 4 directly to exon 5 by excluding the 4' intronic sequence. This event leads to the addition of a GPI linkable C-terminus to AChE-H allowing it to be anchored as dimers in the membrane of red blood cells. The AChE-T variant results from the splicing of exon 4 to the alternative exon 6 (also called tailed or synaptic variant encoding region) and lacks sequences corresponding to R and H regions.

To determine if these AChE forms were expressed in CD-1 heart tissue throughout development, the mRNA transcripts of each variant were amplified using reverse-transcription polymerase chain reaction (Figure 3.1). It is important to mention that any primer pair used to amplify the H variant mRNA would also amplify coding sequences of the R form as both splice variants share identical sequences with the exception of 4' readthrough intron (Figure 1.1). In light of this issue, the primer pair used to identify H form was designed to span 4' intron in order to separate the variants via differences in band sizes. It appears that each of these splice variants is indeed present, and expression was indicated to be fairly constant at each stage of heart development by the conventional RT-PCR approach (Figure 3.1). Fidelity

of all RT-PCR reactions were routinely confirmed by the positive amplification of primer pairs specific for glyceraldehyde dehydrogenase (GAPDH) and also confirmed by the absence of any amplification product in control reactions where the RNA was eliminated in the cDNA synthesis step. Notably, the sizes of amplification products for each splice variant PCR were consistent with the predicted sizes derived from bioinformatics analysis (R: 192 bp; H+R: 137 bp + 253 bp AChE-H and T: 168 bp; Figure 3.1). Since the RT-PCR reactions were carried out for 40 cycles, some of these reactions may be subjected to the plateau effect due to attenuation of normally exponential rate of PCR product accumulation in late cycles. In contrast to the semi-quantitative RT-PCR approach, modulations in gene expression can be accurately measured using quantitative RT-PCR (QPCR). Nevertheless, results from semi quantitative RT-PCR indicate that primer pairs specific for R and T forms but not H form can generate single amplification products and as such may be useful for further QPCR analysis.

Figure 3.1. AChE mRNA exists in three splice variants in CD-1 mice hearts. a) Three mammalian AChE isoforms are expressed in the mouse ventricles throughout development as determined by Reverse Transcription Polymerase Chain Reaction (RT-PCR) analysis. Total RNA isolated from the ventricles of embryonic (E11.5, E14.5 and E16.5), neonatal (neo; 2 days after birth) and adult (2 months old) hearts was subjected to RT-PCR using splice variant specific primer pairs. RT-PCR amplification product for the enzyme glyceraldehyde-3-phosphate dehydrogenase (GAPDH) was used as an internal control. Amplicon sizes were determined by comparison with the DNA marker ΦX174DNA-HaeIII Digest following gel electrophoresis in a 2.5% agarose gel. The control lane represents a PCR reaction where the RNA template for the corresponding cDNA synthesis was omitted. N= 5 independent experiments.

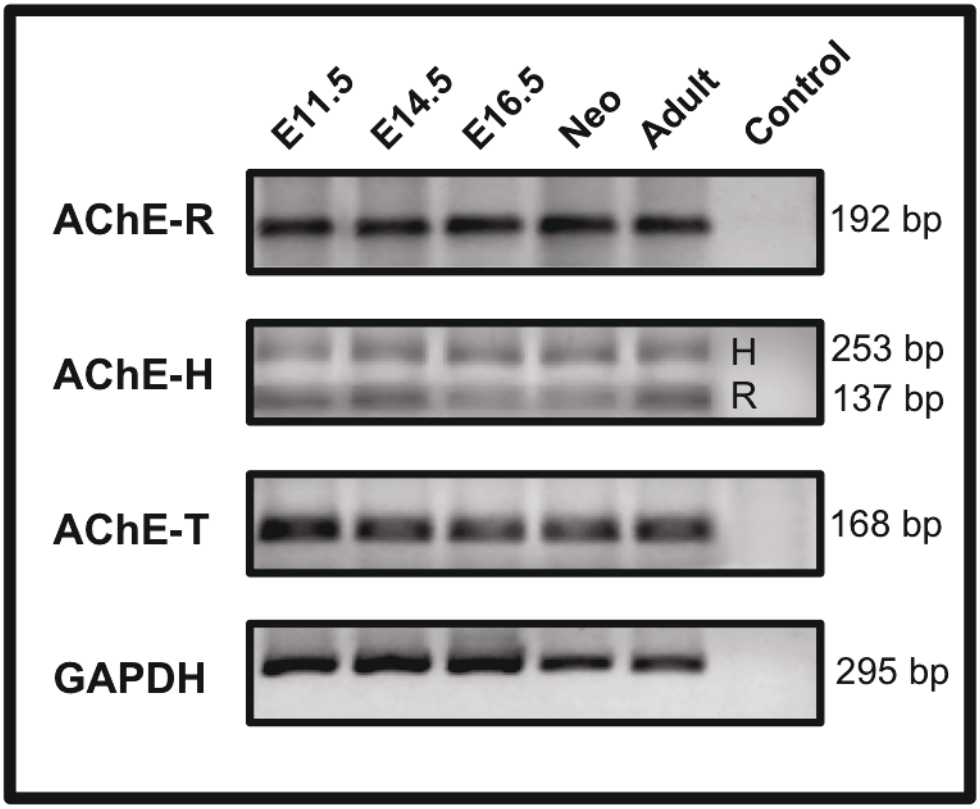
E11.5
E14.5
E16.5
Neo
Adult
Control
AChE-R
192 bp
AChE-H
H
R
253 bp
137 bp
AChE-T
168 bp
GAPDH
295 bp

3.2 Validation of Real-Time Polymerase Chain Reaction Assay for AChE Splice Variants

To rule out whether the plateau effect in RT-PCR masked any possible differences in the developmental expression pattern of different AChE splice variants, we next performed real-time QPCR analysis experiments. The specifity of primer pairs for AChE-R and T variants was confirmed by obtaining a single amplicon during melt curve analysis in QPCR reactions (Figure 3.2a and b). In addition, primer pairs used for internal control GAPDH also revealed a single amplicon (Figure 3. 2c). The melt curve resulting from the AChE-R amplification of no template control (NTC) reaction yielded a small hump indicative of nonspecific primer dimer products, however, these amplicon products were not recorded until 37 of 40 cycles and were therefore considered nonspecific products in NTC. In contrast, the metling curves resulting from the AChE-T and GAPDH amplification of NTC reactions did not yield any amplification product. The efficiency of each primer set was tested over a series of 1:10 serial dilutions of positive control templates, where only efficiency values between 90-100% were considered acceptable. Table 3.1a gives a summary of PCR conditions and efficiency of reactions for each primer pair used in QPCR analysis. Table 3.1b displays the CT values recorded during GAPDH amplification over each of these developmental stages, confirming mRNA expression is unchanged. These results indicate that GAPDH can be used as a suitable internal control to compare AChE expression throughout ontogeny and thus was used a normalization control for further relative gene expression analysis using $\Delta\Delta C_T$ method (Livak & Schmittgen 2001).

Figure 3.2. Primers designed to target AChE-R, AChE-T and GAPDH mRNA sequences are highly specific. Primer specificity is indicated by the single peaks exhibited in the melt curve analysis. These curves were derived from each amplification reaction of all developmental stages tested (E11.5, E14.5, E16.5, Neonatal and Adult). The NTC is highlighted in each panel, revealing problematic primer dimers are not a factor in each of these reactions. N=5 Experiments.

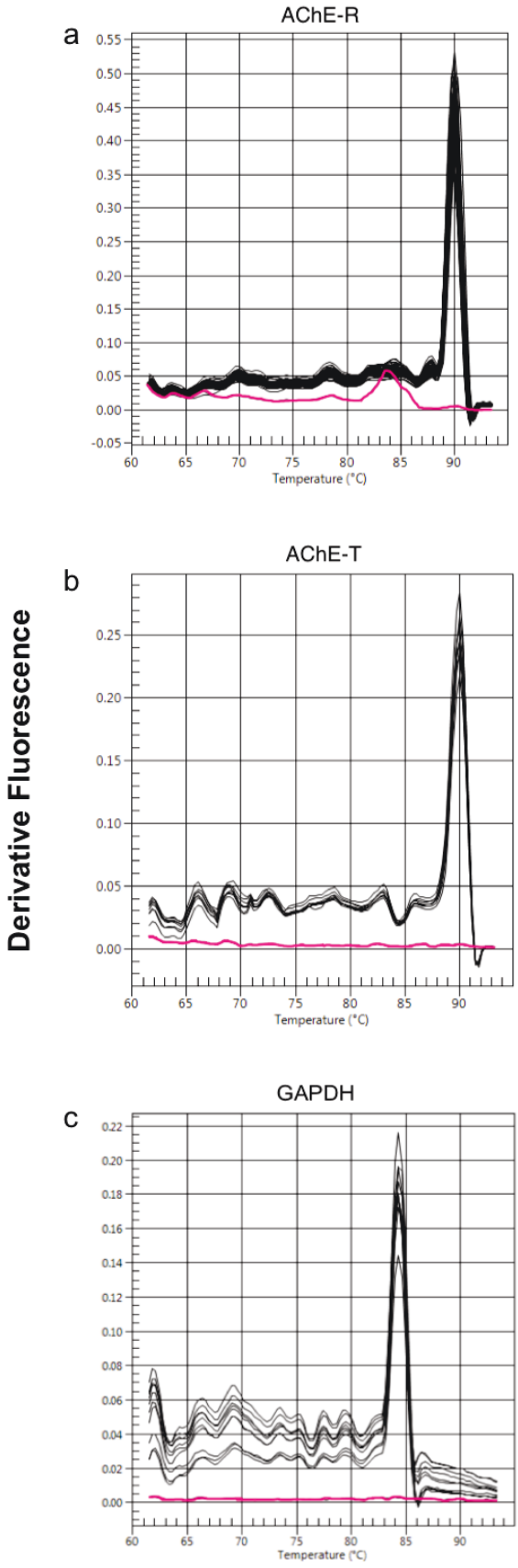
a
AChE-R
0.55
0.50
0.45
0.40
0.35
0.30
0.25
0.20
0.15
0.10
0.05
0.00
-0.05
60
65
70
75
80
85
90
Temperature (°C)
b
AChE-T
0.25
0.20
0.15
0.10
0.05
0.00
60
65
70
75
80
85
90
Temperature (°C)
Derivative Fluorescence
c
GAPDH
0.22
0.20
0.18
0.16
0.14
0.12
0.10
0.08
0.06
0.04
0.02
0.00
60
65
70
75
80
85
90
Temperature (°C)

Table 3.1. Summary of the conditions used for semi-quantitative and Real-Time Quantitative Polymerase Chain Reaction for the mammalian AChE isoforms (R, H and T) and glyceraldehyde-3-phosphate dehydrogenase (GAPDH). a) The mRNA amplification products were resolved on a 1.5% agarose gel for further confirmation. Each of the three AChE isoforms is expressed in E11.5 ventricular myocytes and subsequent developmental stages. b) The CT values at each developmental stage confirm GAPDH mRNA expression is unchanged and can thus be used as a suitable internal control. N=5 experiments.

a.

AChE Variant	Sequence 5'-3'	Product Length	Amplification Cycles	QPCR Efficiency
AChE-R	F: CAGGGGACCCCAATGACCCTCG R: CCCACTCCATGCGCCTACCGGT	192 bp	95°C for 15 s, 60°C for 1 min, 95°C for 15 s, 40 cycles	95.8%
AChE-H*	F: CCGCGCAGCAATATGTGAGCCT R: GCAGGTGCAAGGAGCCTCCGT	253 bp (H) 137 bp (R)	95°C for 15 s, 60°C for 1 min, 95°C for 15 s, 40 cycles	…
AChE-T	F: TAGAGGTGCGGCGGGGACTG R: TGAGCAGCGCTCCTGCTTGC	168 bp	95°C for 15 s, 62°C for 1 min, 95°C for 15 s, 40 cycles	96.3%
GAPDH	F: TTTCCCGTTCTTCAGCATTT R: CTGACCGGCCTGTATGCTAT	150 bp	95°C for 15 s, 60°C for 1 min, 95°C for 15 s, 40 cycles	92.4%

*F = forward primer; R = reverse primer;
*This transcript does not contain any additional introns or exons that might distinguish it from the R transcript (see Figure 1.1), and as such, this primer pair could not be included in our QPCR analysis. Rather, RT-PCR was used to confirm the presence of AChE-H mRNA where amplification products were resolved strictly via band sizes.

b.

Developmental Stage	Average CT value (±SE)
E11.5	15.33 ± 0.057
E14.5	15.42 ± 0.028
E16.5	15.33 ± 0.028
Neonatal	15.32 ± 0.105
Adult	15.32 ± 0.086

3.3 AChE-R and AChE-T mRNA Expression Decreases with Age

To assess whether ACHE expression fluctuated throughout ventricular development, AChE-R and AChE-T mRNA expression was analyzed. Total RNA extracted from CD-1 ventricles was harvested at five developmental stages (E11.5, E14.5, E16.5, neonatal and adult) and evaluated using the quantitative polymerase chain reaction technique (Figure 3.3). $\Delta\Delta C_T$-method was used to calculate fold changes and samples were adjusted for load variations using GAPDH, a housekeeping gene whose transcription levels were shown not to fluctuate with age. The normalized gene expression values for each developmental stage were plotted on a graph and statistically compared to the amplification levels in E11.5 by one-way ANOVA. Compared to the normalized expression levels of AChE-R at E11.5 stage, it appears that AChE-R mRNA expression decreases significantly by E14.5 (1.6 fold; $p<0.01$) and subsequently varies only slightly with age (Figure 3.3a). Compared to the normalized expression levels of AChE-T at E11.5 stage, a more dramatic decrease (2.1 fold; $p<0.001$) was measured at the E14.5 stage for AChE-T expression and this decrease in expression of AChE-T mRNA appears to continue with development (Figure 3.3b). The higher mRNA expression levels of AChE-R and AChE-T at E11.5 suggest that these variants may play a more crucial role at this stage versus later stages of ventricular development.

The relative expression of T to R splice variants is significantly greater ($p<0.01$) at E11.5 and E14.5 stages of ventricular myocytes (Figure 3.3c). By embryonic day 16.5, AChE-T levels are found to be more similar to AChE-R mRNA epression, with no apparent significant differences in expression.

Figure 3.3. mRNA expression of AChE splice variants (R and T) is developmentally regulated. Total RNA isolated from the ventricles of embryonic (E11.5, E14.5 and E16.5), neonatal (neo; 2 days after birth) and adult (2 months old) CD-1 mouse hearts was subjected to Real-Time Quantitative Polymerase Chain Reaction (QPCR) analysis using splice variant specific primer pairs. **a)** AChE-R expression is significantly lower ($p<0.01$) at E14.5 and later stages compared to E11.5. **b)** Similarly, AChE-T expression is significantly decreased ($p<0.001$) in later stages of development compared to the mRNA expression of AChE-T at E11.5 stage. Normalized to GAPDH; One-way ANOVA; n=5 experiments. **c)** The mRNAs coding for AChE-R and AChE-T mRNA are expressed at relatively different amounts in E11.5 and E14.5 mouse ventricles, where the T variant is significantly greater ($p<0.05$). In contrast, the expression patterns become more similar between each splice variant in the later stages of development. All values have been normalized to glyceraldehyde-3-phosphate dehydrogenase (GAPDH) expression. Between group comparisons were analysed by one-way ANOVA with Bonferroni posthoc test. Data are presented as mean ± the standard error of the mean (SEM); N=5 experiments; *$p<0.05$, **$p<0.01$, ***$p<0.001$

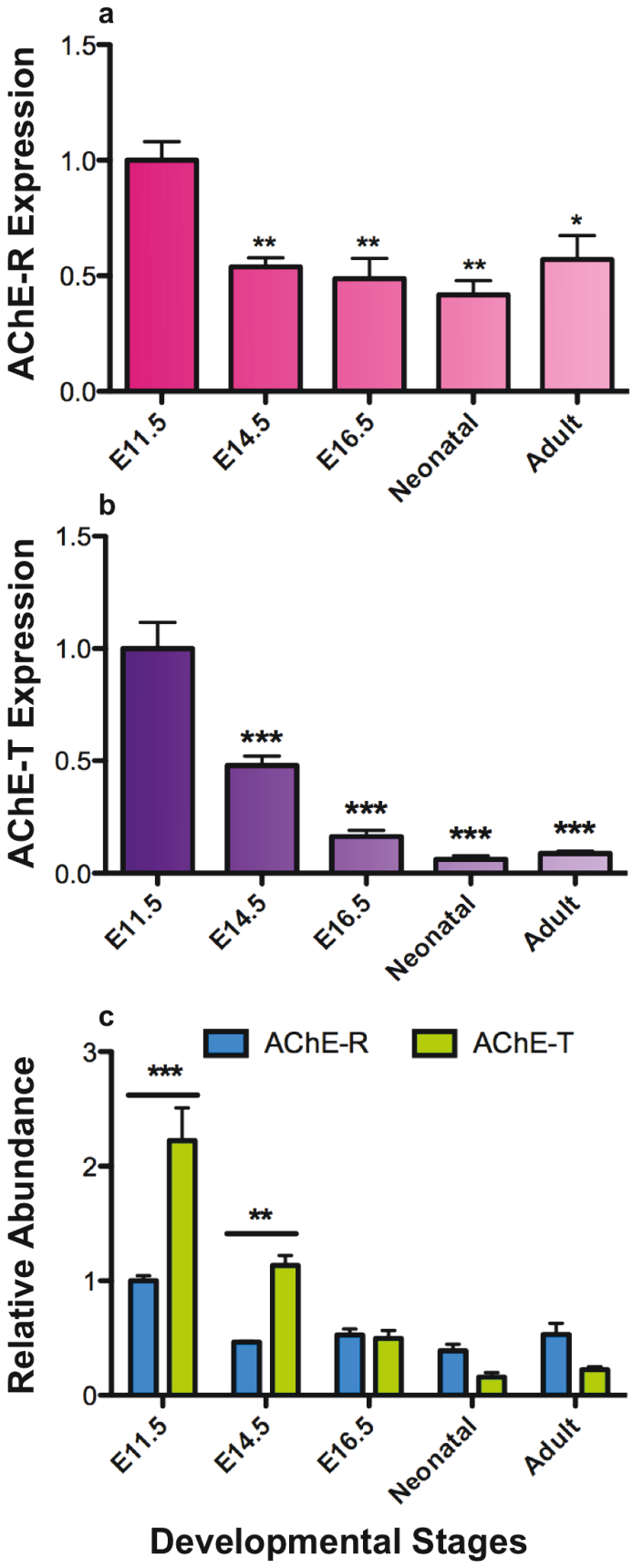
a
AChE-R Expression
1.5
1.0
0.5
0.0
**
**
**
*
E11.5
E14.5
E16.5
Neonatal
Adult
b
AChE-T Expression
1.5
1.0
0.5
0.0
***
***
***
***
E11.5
E14.5
E16.5
Neonatal
Adult
c
AChE-R
AChE-T
Relative Abundance
3
2
1
0
***
**
E11.5
E14.5
E16.5
Neonatal
Adult
Developmental Stages

3.4 Expression profiles of the AChE protein and its biological activity during cardiac development

As we have previously shown, expression of AChE mRNA splice variants are developmentally regulated in cardiac ventricles; however, it is not known whether the transcripts encoding R and T splice variants are translated into functional proteins and whether the protein expression profile resembles that of the mRNA expression pattern. We next investigated the AChE protein expression profiles in detergent soluble protein lysates of CD-1 mouse ventricles at five developmental stages using Western Blot analysis (Figure 3.4a) with a rabbit polyclonal antibody raised against amino acids 481-614 mapped at the C-terminus of the AChE gene (common to all splice variants) and a rabbit polyclonal antibody raised against the unique C-terminus of the AChE-R subunit. Resolved protein bands appeared as 70 kDa molecules under both conditions at all five developmental stages (E11.5, E14.5, E16.5, neonatal, adult) and were corrected for any variation in protein loading using GAPDH; theoretical sizes predicted the T-variant to resolve at 78, 66 and 55 kDa and the R-variant to resolve at 55 kDa (Garcia-Ayllon et al 2012). Due to a time constraint and the lack of sufficient quantities of the R-specific antibody, we were unable to quantify the expression profile of the C-terminus specific fragments nor was the analysis of the detergent insoluble protein lysate fraction completed. Despite these restrictions, the 70 kDa bands resolved using the antibody common to all three isoforms were quantified (Figure 3.4b), revealing no significant changes in AChE enzyme over the developmental period between E11.5 and adulthood.

Protein expression does not, however, always predict enzyme activity. The developmental activity pattern of AChE is unknown in cardiac tissue, giving way for investigation. We quantitatively measured AChE activity in both detergent soluble (cytosolic)

and insoluble (membrane) protein lysates isolated from CD-1 mouse cardiac tissue at each developmental stage using the DetectX fluorescence assay. This assay utilizes a proprietary non-fluorescent molecule, which covalently binds to the thiol product of the reaction between AChE and its substrate ACh, yielding a fluorescent product read at 510 nm. Initially, an AChE dose-response standard curve was generated by plotting the fluorescence values against the known concentrations of the AChE enzyme. Using this assay, as low as 0.01 mU/well (0.1 mU/ml) AChE can be detected with a 20 minute incubation period. Subsequently, the enzyme activities in tissue lysates were extrapolated from the standard curve using the same fluorescence assay (Figure 3.5a). A significant decrease in AChE activity in the detergent soluble fraction (cytosolic lysate) was measured at E14.5 (3.2 fold; $p<0.001$) and neonatal stage (4.2 fold; $p<0.001$) relative to E11.5; however, the E16.5 and adult stages revealed little variation (Figure 3.5b). Interestingly, the membrane fraction (Figure 3.5c) revealed a steady decrease in AChE activity with age. All changes were significant ($p<0.001$) when compared to E11.5, where E14.5 showed a 1.4 fold decrease, E16.5 a 1.6 fold decrease, neonatal a 2-fold decrease and the adult stage a 4.1 fold decrease. Furthermore, differences between absolute protein activities in each fraction were only found to be significant at the E11.5, E16.5 and adult stages, where the cytosolic fraction is significantly greater in each instance (Figure 3.5d). The E11.5 stage revealed a 3.7 fold decrease ($p>0.001$) in the activity of membrane fraction when compared with that of the cytosolic lysates. Similarly, the enzyme activity of membrane fraction decreased by a 6.2 and 10.2 fold, respectively ($p<0.001$) compared to the respective cytosolic values at E16.5 and adult stages.

Figure 3.4. AChE enzyme expression is unchanged with embryonic, fetal and natal development in CD-1 mouse hearts. a) Immunodetection of AChE using denaturing conditions was performed with an antibody raised against the N-terminus of AChE (common to all AChE subunits) and to the unique C-terminus of the AChE-R subunit. Detergent soluble Protein lysates collected from CD-1 mouse ventricles at five developmental stages were resolved by SDS-PAGE on a 7.5% gel and investigated by Western Blot analysis. Samples were probed with AChE/R (MW = 70 kDa) and GAPDH (MW = 37 kDa) antibodies on nitrocellulose . **b)** Relative protein expression of the N-terminus specific antibody AChE was quantified using band densitometry and values were expressed as mean ± SEM. AChE: N=6 experiments; AChE-R: N=1 experiment.

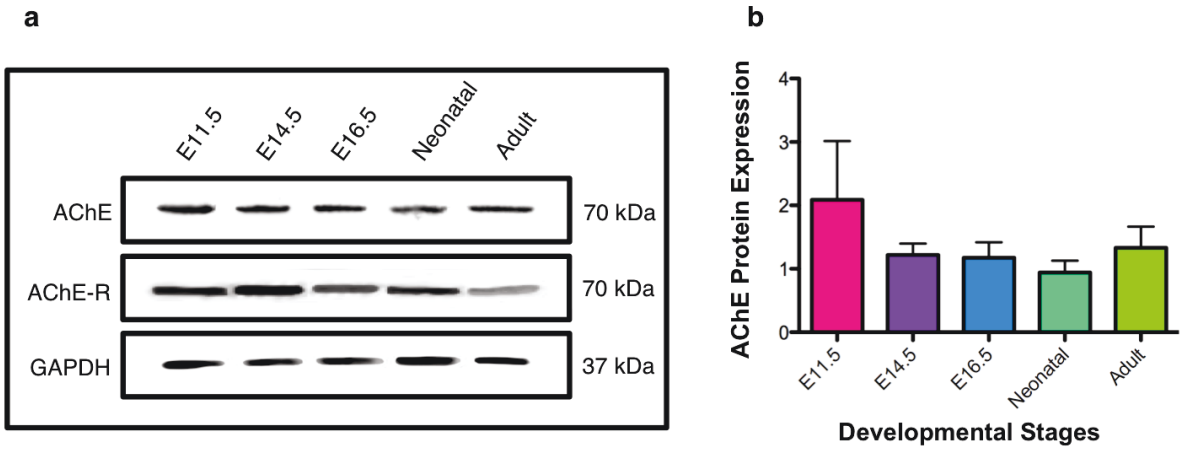
a
E11.5
E14.5
E16.5
Neonatal
Adult
AChE
AChE-R
GAPDH
70 kDa
70 kDa
37 kDa
b
AChE Protein Expression
0
1
2
3
4
E11.5
E14.5
E16.5
Neonatal
Adult
Developmental Stages

Figure 3.5. AChE enzyme activity is higher in E11.5 ventricles compared with E14.5 mouse ventricles. a) AChE standards with known enzymatic activity were incubated with Thiostar® Detection Reagent and the resulting fluorescence values were used to plot a dose response standard curve. **b)** The enzyme activity of AChE was measured in detergent soluble protein lysates and **c)** detergent insoluble membrane lysates isolated from CD-1 ventricular cells. These values were extrapolated from the standard curve shown in panel **a**. The enzyme activity in cytosolic fraction significantly decreased in E14.5 and neonatal stages in comparison with the other three stages. Interestingly, a gradual decrease in AChE activity with age is observed in the membrane fraction. The figure in **d)** compares the absolute enzyme activity of AChE in both fractions at each developmental stage. This direct comparison reveals the difference in activity at three stages (E11.5, E16.5 and Adult), where the protein fraction is significantly greater in each instance. ***$p<0.001$ is considered significant. Between group comparisons were analyzed by two-way ANOVA with Tukey posthoc test. Data are presented as mean ± the standard error of the mean (SEM). N=3 experiments.

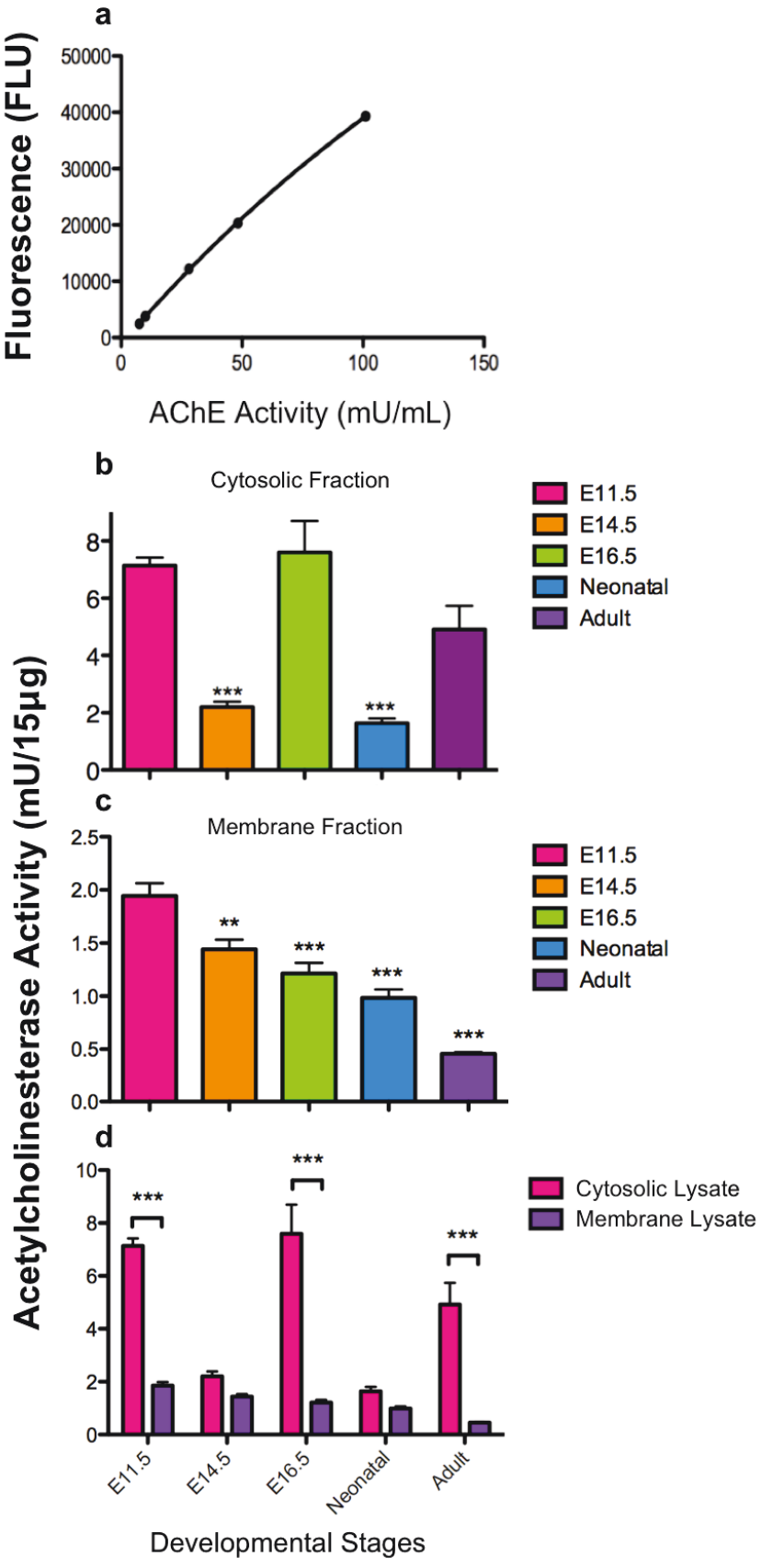
a
Fluorescence (FLU)
50000
40000
30000
20000
10000
0
0
50
100
150
AChE Activity (mU/mL)
b
Cytosolic Fraction
E11.5
E14.5
E16.5
Neonatal
Adult
***
***
c
Membrane Fraction
**
***
***
***
Acetylcholinesterase Activity (mU/15µg)
d
***
***
***
Cytosolic Lysate
Membrane Lysate
E11.5
E14.5
E16.5
Neonatal
Adult
Developmental Stages

3.5 AChE is expressed in cardiac progenitor cells and mature myocytes, localized in both the intracellular compartment and the membrane.

Although AChE expression was detected in cardiac tissue lysates, the cell source was not known, as it may have come from adjacent neurons or erythrocytes rather than resident myocytes. In order to localize protein expression, we utilized fluorescently labeled antibodies and evaluated E11.5 (Figure 3.6) and E14.5 (Figure 3.7) heart sections using epifluorescence microscopy. Co-immunostaining of cardiac sections with the antibodies specific for the sarcomeric myosin (MF20; green) and C-terminus specific AChE (red; common to all AChE subunits) revealed the presence of AChE enzyme in both MF20 positive and negative cell populations at both the E11.5 (Figure 3.6) and E14.5 (Figure 3.7) stages; however the abundance of AChE+/MF20- cells was greatly reduced by E14.5. It appears that most of the red fluorescence is mainly co-localized with the green fluorescing MF20, indicating substantial co-localization and confirming AChE+ cells are indeed of myocyte lineage (20X magnification). A substantial number of AChE positive cells in E11.5 tissue were fairly evenly distributed throughout the trabeculae and compact myocardial zones; although, distribution was accompanied by clusters of increased fluorescence most likely representing secretory vesicles (Gratzl et al 1981; Schweitzer 1993). Furthermore, expression was not limited to the cytoplasm or the membrane, as the confocal imaging of z-stacks clearly illustrates positive staining in both regions.

It has been shown that cells negative for the MF20 antibody, but positive for the early cardiac marker Nkx2.5 gene in E11.5 cells retain their capacity to differentiate into myocytes in culture overtime; however, this is not true of similar cells by E14.5 (McMullen et al 2009a; McMullen et al 2009b). According to this work, we consider MF20 a late myocyte marker, used to indicate cardiomyocyte maturity from the progenitor stage.

AChE seems to be more highly expressed in the trabeculae of the E14.5 ventricle chamber (Figure 3.7) than that of the compact myocardium forming the exterior tissue wall. Rather, distinct puncta (indicated by arrowhead) can be identified in the compact tissue indicating neuronal synapsing, as opposed to the more diffuse signal found in the interior layers (indicated by arrow). The 'merged' frames highlight cell nuclei of both cardiomyocytes and non-cardiomyocyte cells. Tissue sections were also incubated with fluorescently labeled, secondary antibodies to be used as a comparison for non-specific staining. We observed little-to-no stain in these sections; indicating fluorescent patterns revealed in primary incubations can be attributed to the specific binding with MF20 and AChE only. This is a very interesting result in that AChE staining is seen mainly in the trabecular region (finger-like structures) but not the compact zone (outer thick cell zone) of E14.5 ventricular myocardium. This pattern is in contrast to the uniform staining found in the E11.5 stage.

Figure 3.6. AChE is expressed in E11.5 mouse ventricular trabeculae.

AChE was detected using a polyclonal anti-AChE antibody and appeared red under the Leica epifluorescence microscope. Sarcomeric myosin was detected using the anti-myosin antibody MF20, and appeared green under the Leica epifluorescence microscope. Nuclei were stained by incubation with Hoechst's nuclear stain, and appeared blue under the Leica epifluorescence microscope. Sections were taken from E11.5 mouse hearts and analyzed for co-localization of these three markers to determine whether the AChE+ cells are cardiac derived (40X and 100X magnification). It appears that most of the red fluorescence is mainly co-localized with the green fluorescing MF20; indicating substantial co-localization and confirming AChE+ cells are indeed of cardiac lineage. The merged frames highlight cell nuclei of both cardiac and non-cardiac cells. Tissue sections were also incubated with fluorescently labeled, secondary antibodies to be used as a comparison for non-specific staining. We observed little-to-no stain in these sections; indicating fluorescent patterns revealed in primary incubations can be attributed to the specific binding with MF20 and AChE only. Arrowheads indicate membrane bound AChE, whereas arrows indicate intracellular AChE in a z-stack of the E11.5 section.

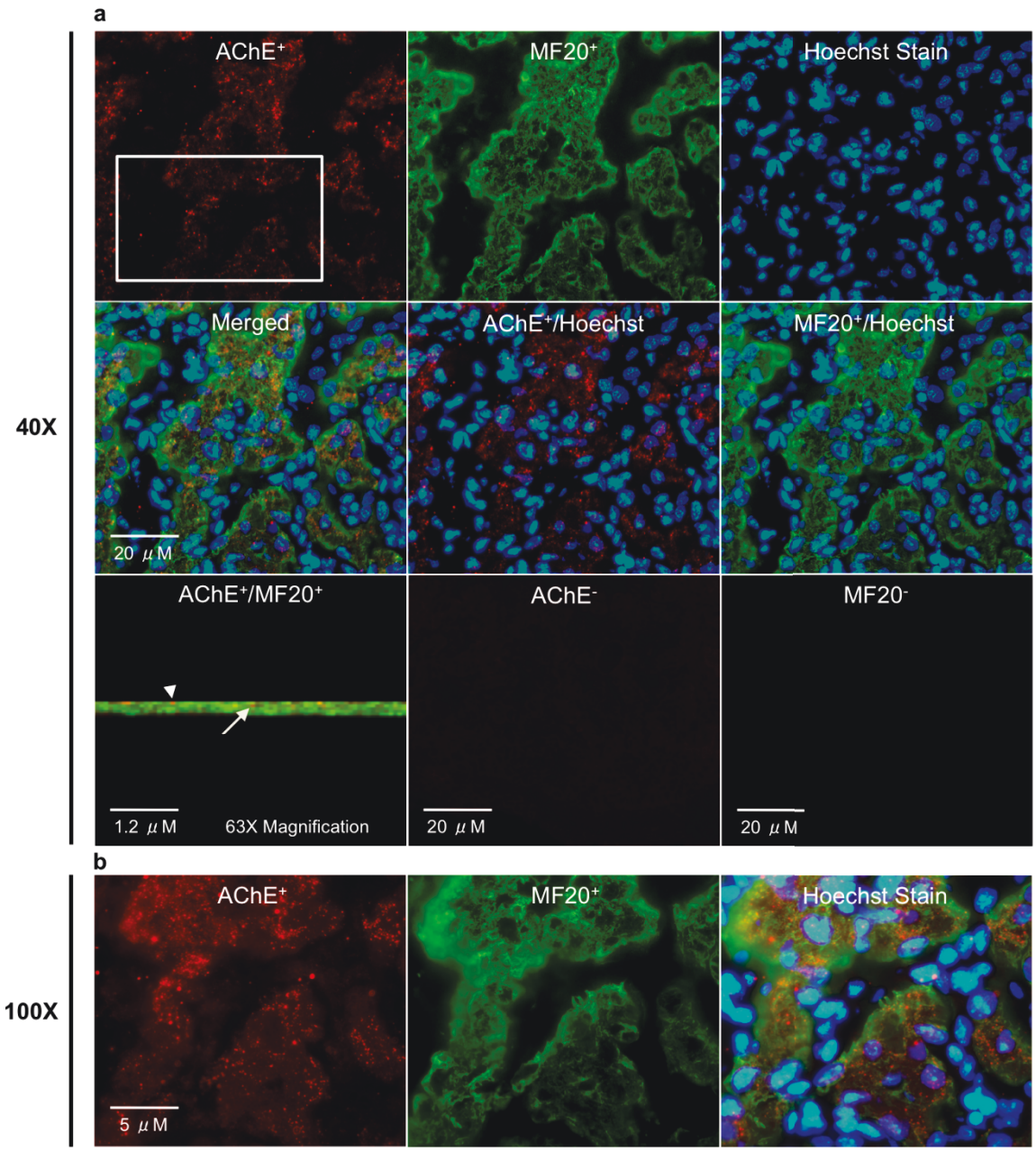
a
AChE+
MF20+
Hoechst Stain
Merged
AChE+/Hoechst
MF20+/Hoechst
40X
20 μM
AChE+/MF20+
AChE-
MF20-
1.2 μM
63X Magnification
20 μM
20 μM
b
AChE+
MF20+
Hoechst Stain
100X
5 μM

Figure 3.7. AChE is expressed in E14.5 mouse ventricular trabeculae. AChE was detected using the anti-AChE antibody and appeared red under the Leica epifluorescence microscope. Sarcomeric myosin was detected using the anti-myosin antibody MF20, and appeared green. Nuclei were stained by incubation with Hoechst's nuclear stain, and appeared blue. Tissue sections were also incubated with fluorescently labeled, secondary antibodies to be used as a comparison for non-specific staining. As no fluorescent signal was resolved, any staining patterns are attributed to the specific binding with MF20 and AChE only. It appears that most of the red fluorescence is mainly co-localized with the green fluorescing MF20, indicating substantial co-localization and confirming AChE+ cells are indeed of myocyte lineage (20X magnification). AChE also seems to be more highly expressed in the trabeculated region of the ventricle chamber (arrow), and distinct puncta can by identified in the outer layer compact tissue (arrowheads).

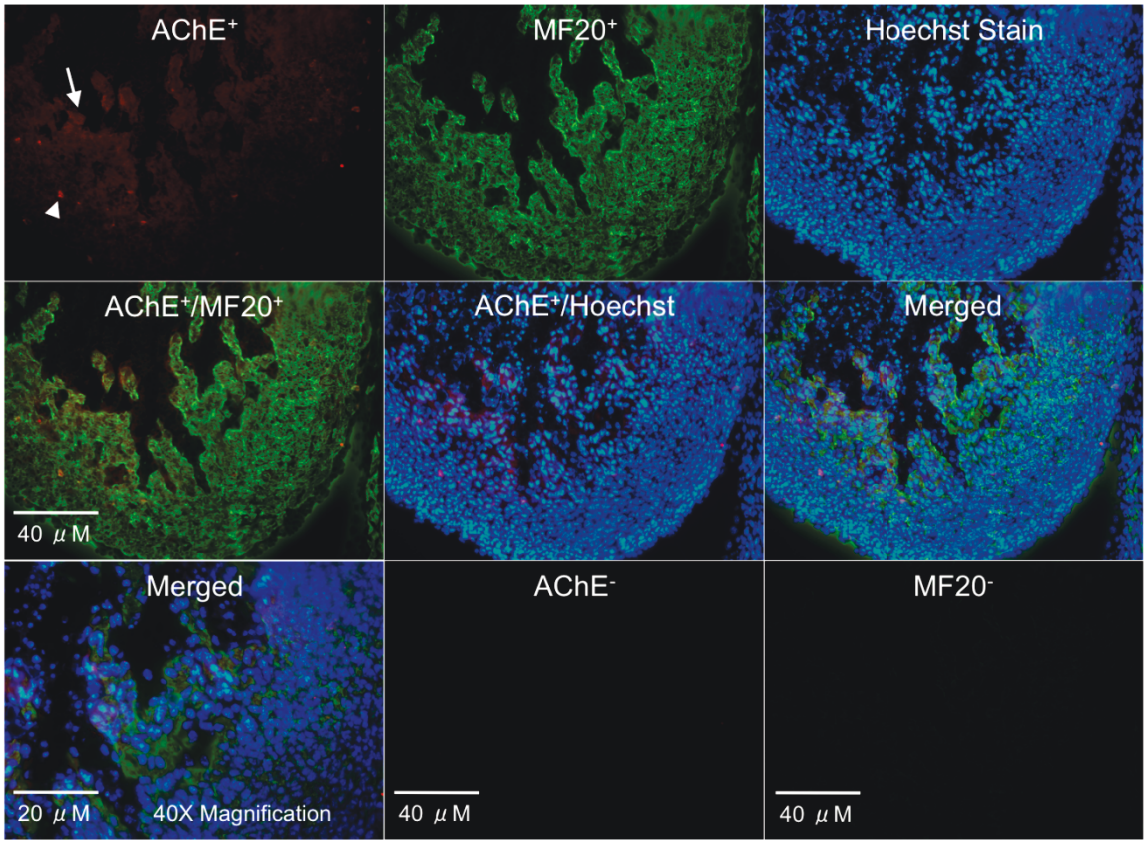
AChE+
MF20+
Hoechst Stain
AChE+/MF20+
AChE+/Hoechst
Merged
40 μM
Merged
AChE-
MF20-
20 μM
40X Magnification
40 μM
40 μM

3.6 AChE Inhibition Differentially Affects Cardiac Cell Development and Differentiation

Now that the presence and activation of AChE in E11.5 cells has been confirmed, we next investigated its importance as a functional player in CPC development and differentiation. To address this, we generated primary cultures of E11.5 ventricles derived from double transgenic crosses between *Nkx2.5*-Cre and ROSA-*lacZ* mouse lines. In these cultures, CPCs and mature cells were readily distinguished by co-immunostaining with antibodies specific for beta-galactosidase and sarcomeric myosin (Figure 3.8). To examine the effects of enzyme inhibition, a competitive AChE inhibitor galantamine was added to transgenic cell cultures and effects on cell cycle and differentiation status were assessed using immunofluorescence (Figure 3.8) and autoradiography (Figure 3.9). Figure 3.8 describes the technique used to distinguish CPCs from mature myocytes, The first panel pictures five individual cells, all positive for *Nkx2.5* (red; cardiac derived), however, only 2 of these cells (indicated by the long arrows) are positive for MF20 (green), indicating a differentiated status. The three labeled with short arrows are considered immature, cardiac progenitor cells (undifferentiated), as they are MF20- but positive for *Nkx2.5*. The lower panel shows a cell positive for both cardiac markers to better illustrate the clear staining patterns observed using these antibodies.

To assess cell cycle activity, we used a radiolabeled thymidine incorporation assay (Figure 3.9). The presence of silver indicates cells undergoing DNA synthesis. Transgenic cell cultures were treated with 10μM of the competitive AChE enzyme inhibitor galantamine and evaluated using the methods described in Figures 3.8 and 3.9. Interestingly, the number of *Nkx2.5*+/MF20- cells (putative CPC population) was ~30% lower than that of

untreated cultures (Figure 3.10a). In contrast, the mature cell population (*Nkx2.5*+/MF20+ cells) more than doubled following drug treatment (Figure 3.10b). The trend is repeated in cells undergoing DNA synthesis, where *Nkx2.5*+/MF20- cells show a >50% reduction in cell cycle activity following galantamine treatment (Figure 3.10c), In contrast, the number of *Nkx2.5*+/MF20+ cells undergoing S-phase increased significantly by two fold in cultures treated with galantamine compared to control cultures in (Figure 3.10d). However, comparison of the total number of cells counted in each group revealed no significant difference, indicating cell survival was unaffected by drug treatment (Figure 3.11).

Figure 3.8. Summary of immunofluorescent staining techniques used to determine the differentiation status of myocardial cells. a) Cells derived from the initial population of *Nkx2.5* expressing myocardial cell lineages were detected using β-galactosidase antibodies and appeared red under the Leica epifluorescence microscope. **b)** Sarcomeric myosin was detected using the anti-myosin antibody MF20, and appeared green. **c)** Nuclei were stained by incubation with Hoechst's nuclear stain, and appeared blue. Displayed in the top panel, cells expressing *Nkx 2.5* and not MF20 are indicated by short arrows; these cells were considered undifferentiated (and represent the putative CPC population). Cells expressing *Nkx2.5* and MF20, indicated by long arrows, were considered mature. The bottom panel displays another example of a mature cell expressing both *Nkx2.5* and MF20.

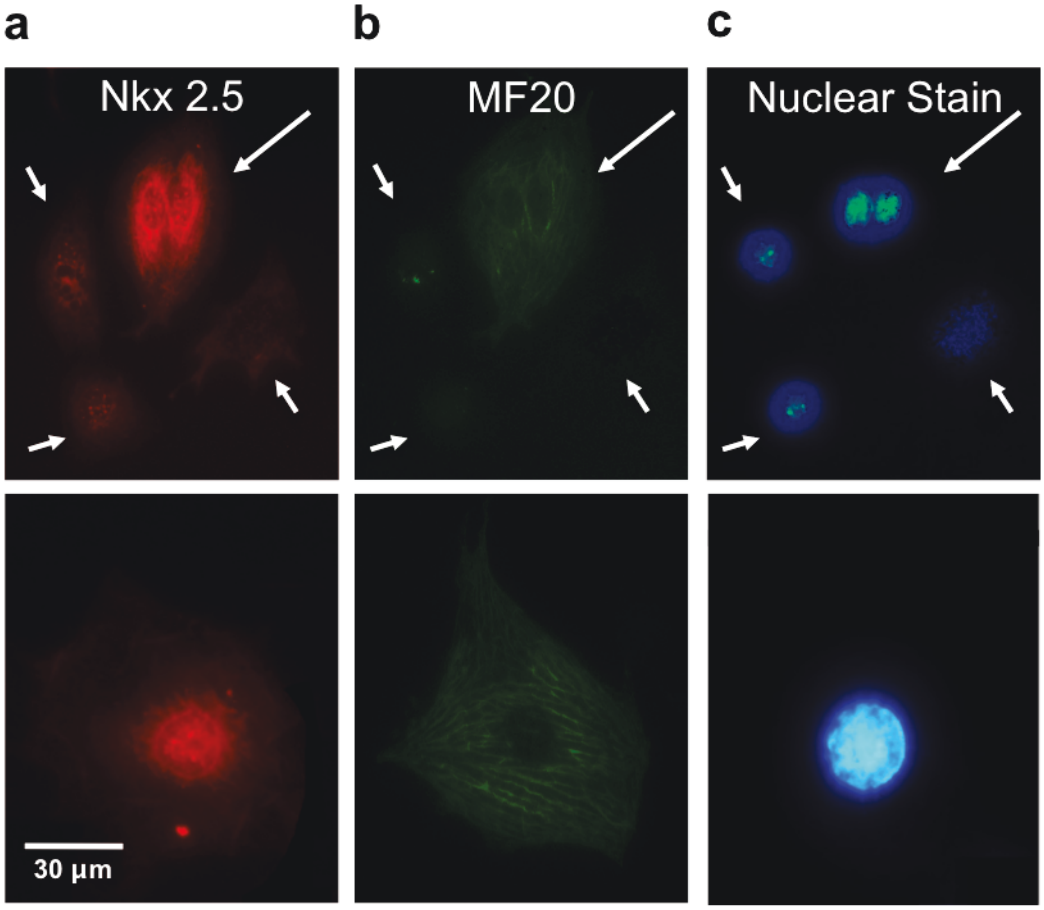
a
b
c
Nkx 2.5
MF20
Nuclear Stain
30 µm

Figure 3.9. Summary of DNA synthesis assessment using autoradiography. DNA synthesis was determined by the co-localization of Hoechst activity (blue nuclear stain) and silver grains. a) The nuclei of three myocardial cells. b) Presence of silver grains indicates that only one of the three cells is undergoing DNA synthesis. Long arrows indicate cells undergoing DNA synthesis; short arrows indicate nuclei not undergoing DNA synthesis.

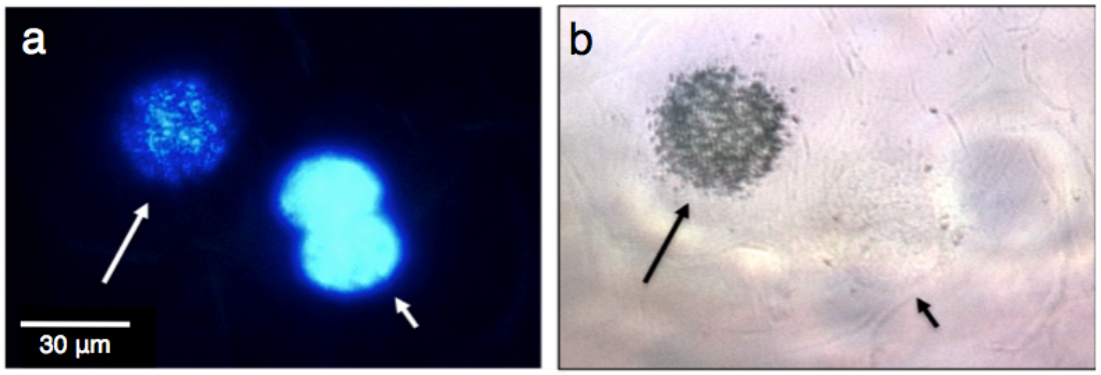
a
30 µm
b

Figure 3.10. Inhibition of AChE differentially affects CPC and mature population proliferation and differentiation. a) The proportion of CPCs (*Nkx2.5*$^{+}$/MF20^{-}) decreased significantly in E11.5 myocardial cell populations treated with 10 μM of galantamine when compared to the control populations. **b)** The proportion of mature cells (*Nkx2.5*$^{+}$/MF20^{+}) increased significantly following treatment with 10 μM galantamine when compared with the control group. **c and d)** Galantamine appears to reduce the levels of cell cycle activity in CPC (*Nkx2.5*$^{+}$/MF20^{-}) populations indicated by a significant decrease in the CPC populations following treatment, in contrast to significantly increasing cell cycle activity in mature cardiac cells (*Nkx2.5*$^{+}$/MF20^{+}). All differences exhibited a p-value < 0.001 indicated by *** and were considered extremely significant. Between group comparisons were analysed by the Student's Unpaired T-Test. Data are presented as mean ± the standard error of the mean (SEM). N=3 experiments, two replicates for each treatment group, and the number of cells counted for each replicate was approximately 450.

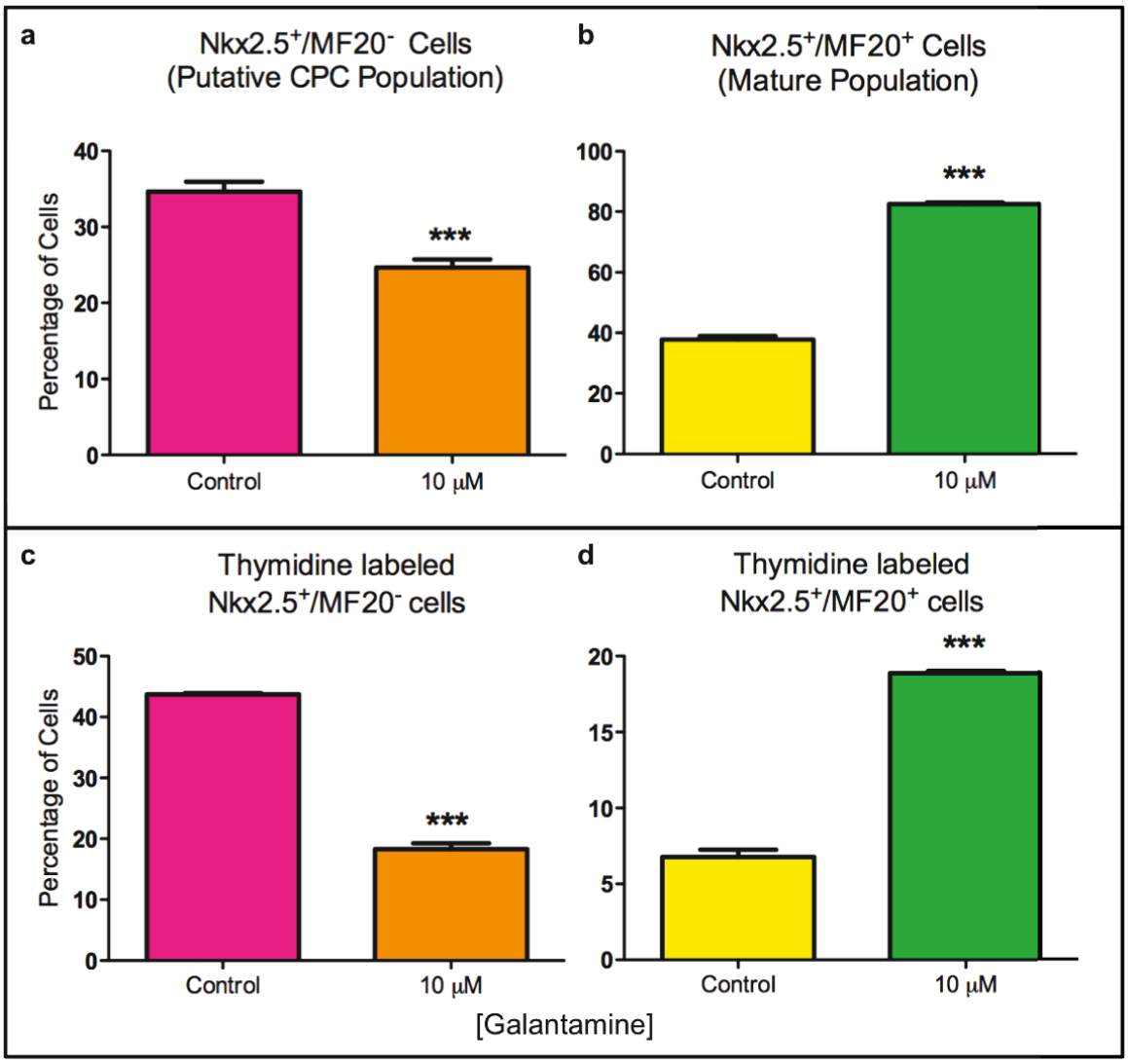
a
Nkx2.5+/MF20- Cells
(Putative CPC Population)
Percentage of Cells
40
30
20
10
0
***
Control
10 μM
b
Nkx2.5+/MF20+ Cells
(Mature Population)
100
80
60
40
20
0
***
Control
10 μM
c
Thymidine labeled
Nkx2.5+/MF20- cells
Percentage of Cells
50
40
30
20
10
0
***
Control
10 μM
d
Thymidine labeled
Nkx2.5+/MF20+ cells
20
15
10
5
0
***
Control
10 μM
[Galantamine]

Figure 3.11. Galantamine did not cause significant cell death in the cultured cell populations. Cells were counted in fifty random fields for individual replicates from both the control and the treatment group. Student Unpaired T-Test (p-value = 0.5481), N=3 experiments, two replicates for each treatment group, and the number of cells counted for each replicate was approximately 1000.

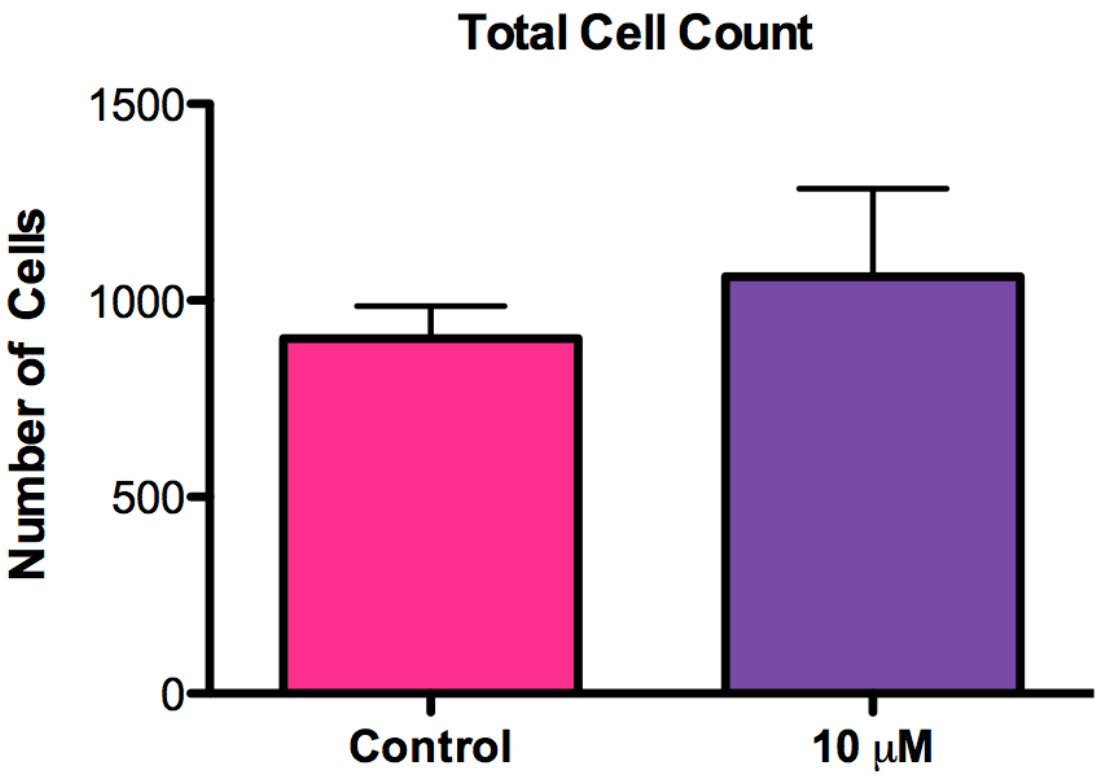
Total Cell Count
Number of Cells
1500
1000
500
0
Control
10 μM

Chapter 4.0: Discussion

Currently, there is little known about the fate of cardiac progenitor cells (CPCs) in the embryonic heart following chamber specification, however, it has been shown that common progenitor cells present in embryonic ventricular myocardium give rise to functional cardiomyocytes and conduction system cells (Laugwitz et al 2005; McMullen et al 2009a). Numerous reports suggest that AChE may have other roles apart from its 'classical' function in terminating impulse transmission at cholinergic synapses. Such functions might involve the hydrolysis of ACh in a non-synaptic context or interactions with transcription factors or proteins important for cell maturation.

It has been suggested that AChE may participate directly in the regulation of bone marrow cell development (Lev-Lehman et al 1994; Soreq et al 1994) and that the readthrough form of human AChE (AChE-R) has been reported to modulate hematopoietic differentiation (Deutsch et al 2002). Furthermore, several groups have provided evidence for the involvement of AChE in neurite growth (Bataille et al 1998; Layer et al 1993; Sharma et al 2001).

Although several mechanisms have been proposed, AChE involvement in cellular proliferation and differentiation has been clearly identified, which leads us to believe that it may be involved in cell fate determination of CPCs; therefore, it is important to characterize the effects of AChE on proliferation and differentiation at the cellular level to better understand CPC development.

Functional heterogeneity in AChE activity is regulated at the transcriptional, post-transcriptional and post-translational levels, leading to complex expression patterns that reflect tissue and cell-type specificity, differentiation state, physiological condition and response to external stimuli (Soreq & Seidman 2001). The concentration of AChE in a tissue, distribution

of its alternative isoforms, its mode of oligomeric assembly, its cellular and subcellular disposition, glycosylation (Velan et al 1993) and proteolytic processing, are all subject to modulation through mechanisms that are not fully understood; however, changes in most of these processes have indeed been shown to regulate the functional heterogeneity of AChE variants (Chan et al 1998; Grisaru et al 2001). Transcriptional control of AChE production depends on a principal and an alternative proximal promoter (Atanasova et al 1999; Li et al 1993), on a distal enhancer domain (Shapira et al 2000), and on an internal enhancer positioned within the first intron (Chan et al 1999). Sequential splicing of AChE pre-mRNA and regulation at the 5' (Atanasova et al 1999; Luo et al 1998); and 3' ends (Li et al 1991) yields tissue-, cell-type- and developmental-state-specific regulation that provide rapid responses to physiological stimuli. Physiological cues that induce ACHE transcription include cell differentiation (Rotundo 1990), reduced AChE levels (Galyam et al 2001) and acetylcholine-mediated excitation elicited by exposure to anti-AChE agents and various traumatic insults (Almkvist et al 2001; Kaufer et al 1998).

In order to assess AChE transcriptional regulation throughout cardiac development, we amplified mRNA isolated from the ventricular myocardium of five developmental stages (E11.5, E14.5, E16.5, Post-natal day 2/Neonatal and Adult). We found that R, H and T splice variants were expressed at each stage of heart development by the conventional RT-PCR approach, and all sizes of amplification products for each splice variant PCR were consistent with the predicted sizes derived from bioinformatics analysis (R: 192 bp; H+R: 137 bp + 253 bp AChE-H and T: 168 bp; Figure 3.1). It should be noted that all primer pairs used to amplify the H variant mRNA also amplified coding sequences of the R form as both splice variants share identical sequences with the exception of 4' readthrough introns; therefore,

quantification was not possible with these primers. In light of this issue, the primer pair used to identify H form was designed to span the 4' intron in order to separate the H and R variants via differences in band sizes during RT-PCR. Quantification by QPCR analysis indicated that AChE-R and AChE-T mRNA levels fluctuate with age, where the highest mRNA levels were found at the E11.5 stage for both variants (Figure 3.3.a and Figure 3.3b). Interestingly, the total expression of the T splice variant was significantly greater at E11.5 and E14.5 when compared with the R variant mRNA (Figure 3.3.c), which may indicate a difference in E11.5 myocardial cell to neuron cell volume ratio, where T mRNA may be higher in content.

At E16.5 to the adult stage, the myocardial cell to neuron cell ratio continues to become much higher, where T mRNA content is lower, resulting in the increased ratio of R:T shown in Figure 3.3. These results instead might suggest that the R transcript may be transcribed more efficiently than the T mRNA. It is also possible that AChE-T mRNA, unlike intraceullular AChE-R mRNA, is not subjected to degredation by the normal protein turnover machinery operating inside the cells. This also raises the question whether the transcripts encoding R and T splice variants are translated into functional proteins and whether the protein expression profile resembles that of the mRNA expression pattern.

Utilizing the Western Blot analysis method, we next investigated the AChE protein expression profiles in detergent soluble protein lysates at each developmental stage using an antibody raised against the C-terminus of AChE (common to all AChE subunits) and to the unique C-terminus of the AChE-R subunit. The theoretical size of AChE is 82 kDa and the AChE-R is 55 kDa (Garcia-Ayllon et al 2012), however, we resolved a 70 kDa band using both antibodies (Figure 3.4). Quantification of the 70 kDa band was completed only on samples flagged with the AChE antibody common to all splice variants and revealed that

translation remains constant throughout development, as no changes with age were detected. Unfortunately due to the lack of sufficient quantities of an R-specific antibody, we were unable to quantify its developmental expression pattern. Although we were able to calculate expected MW values for each protein variant, *in vivo* they may be quite different as a result of posttranslational modifications. Considering our AChE antibody did not differentiate between each isoform, it was impossible to identify the contents of the 70 kDa band; however, because the AChE-R specific antibody revealed a similar band at 70 kDa, we might assume our quantified samples are a mixture of both R and T variants. The R isoform is a soluble monomer found mainly in the cytosolic region, and as a result, we would expect it to be present in higher concentrations than that of the synaptic, membrane-bound T-form and the erythrocytic-specific H-form. Moreover, due to its soluble nature, we would also expect to find the highest levels of R in our protein soluble fraction than in our protein insoluble fractions. Lastly, due to a time constraint, analysis of the detergent insoluble protein lysate fraction was not completed, however, such analysis would provide very useful insight into the prospect of differential translational regulation via compartmentalization. We would expect that the R-form would be diminished in this fraction, as it is a soluble monomer thought to be stored intracellularly and secreted during/to mediate physiological changes (Soreq & Seidman 2001); however, as the T-form is normally anchored to the plasma membrane, higher expression levels would be expected in this fraction.

Protein expression does not, however, always predict enzyme activity as confirmed by the quantitative measurement of AChE activity in both detergent soluble (cytosolic) and insoluble (membrane) protein lysates (Figure 3.5). In contrast to the minimal changes observed in protein expression of the cytosolic lysates, a significant decrease in AChE activity

was measured at E14.5 and neonatal stages relative to E11.5, where the E16.5 and adult stages revealed little variation (Figure 3.5b). The apparent changes in expression observed in Figure 3.5b coincide with specific landmarks in the development of the embryonic heart. High AChE activity recorded at Day E11.5 and Day 16.5 correspond with: 1) day 12, which marks progressive septal formation to construct the four chambers of the heart and 2) day 15 when the alteration of the heart axis occurs (Kaufman 1994). Similarly, this fluctuating pattern of expression is also consistent with that of the cardiac lineage specific markers ANP/BNP in the formation of the developing heart (Cameron 2003), further evidence supporting a potential role for AChE in regulating cardiac growth.

The membrane fraction (Figure 3.5c) revealed the highest activity at E11.5, followed by a steady decrease in AChE activity with age. The higher levels of enzyme activity measured at E11.5 further suggest AChE may be more important in CPCs, as there is a much larger proportion of undifferentiated CPCs at this stage than at E14.5, when the majority of these cells have matured (McMullen et al 2009a). Similarly, previous literature reveals an increase in AChE production during nervous system development in avian (Betz et al 1980) and mammalian systems (Grisaru et al 1999a). Furthermore, transient AChE activation has been recorded in thalamic neurons during mammalian development (Robertson et al 2000), paralleling the developmental changes in activity observed in our cytosolic fraction. Lastly, we found a significant decrease in the absolute protein activity in the membrane fraction when compared with the cytosolic fraction at E11.5 (Figure 3.5d; 3.7 fold decrease; $p<0.001$) indicating the soluble form (R) may play a more significant role than the membrane bound form (T) at this stage.

Localization of AChE splice variants in the neuromuscular junction (NMJ) revealed AChE-T accumulated in the NMJ, whereas AChE-R was found in epidermal cells (Seidman et al 1995). AChE-T, but not AChE-R, would adhere to the active zone at the NMJ. However, the secretory/soluble AChE-R also changed acetylcholine balance in the synaptic cleft (Lev-Lehman et al 2000) and/or competed with AChE-homologous proteins (i.e. neuroligin) for interaction with their binding partners. These studies support a non-classical function for AChE (specifically the R-form), and imply a functional role for AChE-R during differentiation in both CPCs and cardiomyocytes; however, the results related to AChE protein levels or biological activity in this study do not discern between cell types of any kind.

In order to address this issue, we stained E11.5 and E14.5 hearts using fluorescently labeled antibodies. It has been shown that embryonic CPCs are negative for sarcomeric myosin (MF20) staining, but positive for the early cardiac marker *Nkx2.5* expression in E11.5 cells and fully retain their capacity to differentiate into myocytes in culture overtime. However, the abundance of CPCs decreases significantly by E14.5 stage (McMullen et al 2009a; McMullen et al 2009b). We found the presence of AChE enzyme in both MF20 positive and negative cell populations at both the E11.5 (Figure 3.6) and E14.5 (Figure 3.7) stages; however the abundance of AChE+/MF20- cells was greatly reduced by E14.5, lending reason to a greater importance of AChE in E11.5 tissue than in E14.5. As most of the AChE signal was co-localized with the green fluorescing MF20, we concluded that AChE+ cells were indeed of the myocyte lineage. This may provide the first evidence to suggest a role for AChE in cardiac tissue apart from that widely accepted in neuronal tissues. Furthermore, a substantial number of AChE positive cells in E11.5 tissue was fairly evenly distributed

throughout the trabeculae and compact myocardial zones. The trabecular zone houses the fast conduction cells at later stages of heart development.

Interestingly, by E14.5, fast conduction cells have formed (Purkinje fibers), however, the E11.5 trabecular zone does not contain any fast conduction system cells (Christoffels & Moorman 2009). As this system is formed from E11.5-E14.5, and AChE activity is found to be highest in E11.5, then the wide dispersion of AChE+ cells in the trabeculated region may imply that AChE is involved in conduction cell formation. Furthermore, intracellular distribution of AChE+ positive cells were accompanied by clusters of increased fluorescence, most likely representing secretory vesicles (Gratzl et al 1981; Schweitzer 1993) and indicating a presence of the soluble AChE-R splice variant. Lastly, a cross sectional view of the stained section generated by confocal stacks clearly reveals the presence of both intracellular and membrane-bound positive signals, revealing the majority are co-localized with MF20. Of course, immunofluorescent staining using an R-specific antibody is crucial in discerning between the R and T variants and future studies are needed to confirm this postulate. More interestingly, the AChE+ distribution pattern is limited mainly to the trabecular region by E14.5 (Figure 3.7), where distinct puncta (most likely representing neuronal synapsing) can be identified in the compact tissue, as opposed to the more diffuse signal found in the interior layers. It has been shown that following the initiation of neurogenesis in the neocortex, AChE was detectable in clusters of proliferating cells (Dori et al 2005). This resembled previously shown cell clusters, thought to dynamically couple by gap junctions (Bittman et al 1997). Cell clustering during cortical development reflected assembled clonally related dividing cells (Cai et al 1997) and included cell clusters expressing choline acetyltransferase (ChAT), the rate-limiting enzyme in ACh synthesis (Schambra et al 1989). The suggestion that ACh inhibits

precursor cell proliferation *in vivo* through G_i-PCR muscarinic receptor activation (Ma et al 2000) may suggest that AChE, expressed in such clusters, functions by hydrolyzing ACh and terminating its activity as a morphogenic cue. In addition, AChE-T incorporation into progenitor cell membranes might limit the incorporation of enzymatically active AChE to these sites, creating a cholinergic imbalance.

The developmental change related to changes in AChE localization expression between E11.5 and E14.5 offers further evidence for a functional role of AChE in cardiac conduction cell differentiation. A study by Rotundo 1990, revealed skeletal muscle differentiation is associated with transcriptional activation of the AChE gene in subsynaptic nuclei, offering evidence to support an unconventional function with respect to cell lineage commitment.

In order to test this notion, we investigated the importance of AChE as a functional player in CPC development and differentiation using a double transgenic *Nkx2.5*-Cre x ROSA-*lacZ* mouse model. Transgenic cell cultures were treated with 10μM (determined by preliminary experiments) of the competitive AChE enzyme inhibitor galantamine and the results indicate that inhibition of AChE activity can differentially affect the proliferation of CPCs and differentiated myocytes in E11.5 ventricular cell cultures. We found that inhibition of AChE decreased the prevalence of putative CPCs (Figure 3.10a) and simultaneously increased the number of mature cells in the population (Figure 3.10b). Additionally, the proportion of CPCs undergoing cell synthesis was also decreased (Figure 3.10c) in contrast to the increase reported in mature cardiomyocytes (Figure 3.10d). As previously discussed, studies have shown that AChE regulates proliferation and differentiation of neural progenitor cells and hematopoietic stem cells (Dori et al 2005; Dori & Soreq 2006; Pick et al 2004).

Similarly, it is possible that M_1 receptor expression may be higher in differentiated cardiomyocytes compared to CPCs; therefore, upon stimulation of M1 receptors by cholinergic signals, G_q/PLC-pathway is activated and cell cycle activity is increased (Figure 1.4). In contrast, should M_2 levels be higher in CPCs, ACh-ligand activation of G_i receptors would result in inhibition of adenylate cyclase and subsequent reduction of CREB-induced transcription. In the future, we intend to co-treat cells with galantamine and the non-specific muscarinic antagonist atropine in hopes of restoring cAMP levels back to normal. Should the same proportion of mature and immature cells (and those undergoing cellular division) be obtained, when compared with the control population, it would indicate AChE indirectly affects CPC division and differentiation via muscarinic signaling. Further treatment with a receptor-specific muscarinic antagonist such as M_2-selective TD6301 (McNamara et al 2009) would be needed to resolve this discrepancy. However, considering cellular responses were evoked following AChE inhibition, we might assume this enzyme elicits its regulatory affect via cholinergic signals, rather than in a non-classical way. At present, affects of galantamine on embryonic development are unknown. Galantamine is an alkaloid that binds at the base of the AChE active site gorge, interacting with both the choline-binding site (Trp84) and the acyl-binding pocket (Phe288, Phe290) (Greenblatt et al 1999). The tertiary amine appears to make a non-conventional hydrogen bond, via its N-methyl group, to Asp72 and the hydroxyl group forms a strong hydrogen bond with Glu199. Galantamine displays 53-fold selectivity for erythrocyte acetylcholinesterase (AChE-H) over butyrylcholinesterase (BChE). It also displays a 10-fold lower potency towards brain AChE (AChE-T) than towards AChE-H (Thomsen et al 1991). In addition to serving as a cholinesterase inhibitor, galantamine is also a nicotinic activator, acting both on ganglionic and muscle receptors (Schrattenholz et al 1995;

Storch et al 1995) and on nicotinic receptors in the brain (Pereira et al 1993). However, myocardial cells do not typically express nicotinic receptors, and as our *Nkx2.5* reporter assay allowed us to delineate between cardiac and non-cardiac cells, we can confidently conclude that any changes could not have been due to nicotinic activation. Regardless, it might still be important to repeat our assay using other competitive AChE inhibitors such as Donepezil or the non-competitive Sarasin to confirm our observations. Additionally, the use of AChE siRNA might be useful in manipulating ACh gradients in order to promote ACh signaling.

This study has shown for the first time that AChE present in ventricular myocardial cells may regulate embryonic myocardial cell cycle dynamics and subsequent proliferation rates by directly modulating cholinergic signals. Furthermore, AChE may regulate proliferation of CPCs and mature cells in a differential manner. Collectively, our results imply that AChE may play a role in the molecular mechanisms underlying the functional diversification of developing ventricular cells into cardiomyocytes or conduction system cells. Additional research is required to determine M_1 and M_2 muscarinic receptor expression levels in these two cell types, if galantamine effects are mediated through increased stability of ACh by measuring the units of ligand available in E11.5 ventricular cultures, and if galantamine cell cycle inhibition is mediated via M_1 and M_2 receptors using receptor-specific antagonists. The quantification of all the three AChE mRNA splice variants AChE (R, H and T) (Pick et al 2004) has confirmed previous findings, suggesting inclusive presence of a soluble AChE isoform (McMullen et al 2009a; Nyquist-Battie et al 1993; Perrier et al 2005; Pick et al 2004) during cardiac development. Furthermore, the higher enzyme activity measured at E11.5 and a transient dispersion pattern of AChE+ cells from E11.5 to E14.5, suggests a critical importance for AChE during cardiac differentiation. This proposition is further emphasized by

the observation of potential secretory vesicles in E11.5 tissue, implying the AChE-R variant mediates any functional changes exhibited by AChE. However, confirming these observations with an R-specific antibody would be of critical importance. Furthermore, analyzing sections using a double staining method with a cardiomyocyte membrane specific marker, such as EMILIN2 (Van Hoof et al 2010) or wheat germ agglutinin (binds to the N-acetyl-D-glucosamine and sialic acid residues found on the surface of cell membranes) might help to identify the proportion of AChE-R staining that is localized intracellularly versus that which is membrane-bound. Furthermore, it would also be useful to co-label tissue with a conduction cell marker such as connexin 40 or HCN-4 to determine the fate of AChE+ CPCs. Finally, measuring changes in ACh levels following treatment with receptor specific and/or enzyme specific agonists and antagonists may provide insight into the AChE mediated pathway affecting CPC division and differentiation.

Although progress is being made, our understanding of the functional diversification of developing ventricular cells into cardiomyocytes or conduction system cells remains in the elementary stages. Understanding the molecular mechanisms that direct CPC differentiation is imperative in understanding the developmental process and may contribute to the advancement of more effective cell transplantation therapies for the treatment of heart disease. The ultimate goal is to eventually acquire the ability to modulate the fate of stem cells and CPCs after transplantation, to achieve optimal *in-vivo* repopulation of cells to that of endogenous cell proportions, able to fully regenerate lost tissue while limiting (or fully eliminating) the accumulation of non-conductive, non-contractive scar tissue. Perhaps with time and perseverance we will achieve this goal.

References

Aanhaanen WT, Brons JF, Dominguez JN, Rana MS, Norden J, et al. 2009. The Tbx2+ primary myocardium of the atrioventricular canal forms the atrioventricular node and the base of the left ventricle. *Circ Res* 104:1267-74

Almkvist O, Jelic V, Amberla K, Hellstrom-Lindahl E, Meurling L, Nordberg A. 2001. Responder characteristics to a single oral dose of cholinesterase inhibitor: a double-blind placebo-controlled study with tacrine in Alzheimer patients. *Dementia and geriatric cognitive disorders* 12:22-32

Alvarez-Dolado M, Pardal R, Garcia-Verdugo JM, Fike JR, Lee HO, et al. 2003. Fusion of bone-marrow-derived cells with Purkinje neurons, cardiomyocytes and hepatocytes. *Nature* 425:968-73

Anderson RH, Ho SY. 2003. The morphology of the cardiac conduction system. *Novartis Foundation symposium* 250:6-17; discussion 8-24, 276-9

Angelini C, Baccetti B, Piomboni P, Trombino S, Aluigi MG, et al. 2004. Acetylcholine synthesis and possible functions during sea urchin development. *European journal of histochemistry : EJH* 48:235-43

Anumonwo JM, Tallini YN, Vetter FJ, Jalife J. 2001. Action potential characteristics and arrhythmogenic properties of the cardiac conduction system of the murine heart. *Circ Res* 89:329-35

Anversa P, Kajstura J. 1998. Ventricular myocytes are not terminally differentiated in the adult mammalian heart. *Circ Res* 83:1-14

Atanasova E, Chiappa S, Wieben E, Brimijoin S. 1999. Novel messenger RNA and alternative promoter for murine acetylcholinesterase. *The Journal of biological chemistry* 274:21078-84

Atkins DL, Marvin WJ, Jr. 1989. Chronotropic responsiveness of developing sinoatrial and ventricular rat myocytes to autonomic agonists following adrenergic and cholinergic innervation in vitro. *Circ Res* 64:1051-62

Baba S, Heike T, Umeda K, Iwasa T, Kaichi S, et al. 2007. Generation of cardiac and endothelial cells from neonatal mouse testis-derived multipotent germline stem cells. *Stem Cells* 25:1375-83

Bakker ML, Boukens BJ, Mommersteeg MT, Brons JF, Wakker V, et al. 2008. Transcription factor Tbx3 is required for the specification of the atrioventricular conduction system. *Circ Res* 102:1340-9

Bartolini M, Bertucci C, Cavrini V, Andrisano V. 2003. beta-Amyloid aggregation induced by human acetylcholinesterase: inhibition studies. *Biochemical pharmacology* 65:407-16

Bataille S, Portalier P, Coulon P, Ternaux JP. 1998. Influence of acetylcholinesterase on embryonic spinal rat motoneurones growth in culture: a quantitative morphometric study. *The European journal of neuroscience* 10:560-72

Bergmann O, Bhardwaj RD, Bernard S, Zdunek S, Barnabe-Heider F, et al. 2009. Evidence for cardiomyocyte renewal in humans. *Science* 324:98-102

Bernard V, Legay C, Massoulie J, Bloch B. 1995. Anatomical analysis of the neurons expressing the acetylcholinesterase gene in the rat brain, with special reference to the striatum. *Neuroscience* 64:995-1005

Betz H, Bourgeois JP, Changeux JP. 1980. Evolution of cholinergic proteins in developing slow and fast skeletal muscles in chick embryo. *The Journal of physiology* 302:197-218

Beyer S, Kelly RG, Miquerol L. 2011. Inducible Cx40-Cre expression in the cardiac conduction system and arterial endothelial cells. *Genesis (New York, N.Y. : 2000)* 49:83-91

Bigbee JW, Sharma KV, Chan EL, Bogler O. 2000. Evidence for the direct role of acetylcholinesterase in neurite outgrowth in primary dorsal root ganglion neurons. *Brain research* 861:354-62

Birikh KR, Sklan EH, Shoham S, Soreq H. 2003. Interaction of "readthrough" acetylcholinesterase with RACK1 and PKCbeta II correlates with intensified fear-induced conflict behavior. *Proceedings of the National Academy of Sciences of the United States of America* 100:283-8

Bittman K, Owens DF, Kriegstein AR, LoTurco JJ. 1997. Cell coupling and uncoupling in the ventricular zone of developing neocortex. *The Journal of neuroscience : the official journal of the Society for Neuroscience* 17:7037-44

Bourne Y, Taylor P, Bougis PE, Marchot P. 1999. Crystal structure of mouse acetylcholinesterase. A peripheral site-occluding loop in a tetrameric assembly. *The Journal of biological chemistry* 274:2963-70

Brenner T, Hamra-Amitay Y, Evron T, Boneva N, Seidman S, Soreq H. 2003. The role of readthrough acetylcholinesterase in the pathophysiology of myasthenia gravis. *FASEB journal : official publication of the Federation of American Societies for Experimental Biology* 17:214-22

Cai L, Hayes NL, Nowakowski RS. 1997. Synchrony of clonal cell proliferation and contiguity of clonally related cells: production of mosaicism in the ventricular zone of developing mouse neocortex. *The Journal of neuroscience : the official journal of the Society for Neuroscience* 17:2088-100

Cameron VA. 2003. Minireview: Natriuretic Peptides during Development of the Fetal Heart and Circulation. *Endocrinology* 144:2191-4

Caulfield MP. 1993. Muscarinic receptors--characterization, coupling and function. *Pharmacology & therapeutics* 58:319-79

Caulfield MP, Birdsall NJ. 1998. International Union of Pharmacology. XVII. Classification of muscarinic acetylcholine receptors. *Pharmacological reviews* 50:279-90

Chan RY, Adatia FA, Krupa AM, Jasmin BJ. 1998. Increased expression of acetylcholinesterase T and R transcripts during hematopoietic differentiation is accompanied by parallel elevations in the levels of their respective molecular forms. *The Journal of biological chemistry* 273:9727-33

Chan RY, Boudreau-Lariviere C, Angus LM, Mankal FA, Jasmin BJ. 1999. An intronic enhancer containing an N-box motif is required for synapse- and tissue-specific expression of the acetylcholinesterase gene in skeletal muscle fibers. *Proceedings of the National Academy of Sciences of the United States of America* 96:4627-32

Chan RY, Jasmin BJ. 1999. What does acetylcholinesterase do in hematopoietic cells? *Gene Therapy and Molecular Biology* 3:347-54

Cheng G, Litchenberg WH, Cole GJ, Mikawa T, Thompson RP, Gourdie RG. 1999. Development of the cardiac conduction system involves recruitment within a multipotent cardiomyogenic lineage. *Development (Cambridge, England)* 126:5041-9

Chiavegato A, Bollini S, Pozzobon M, Callegari A, Gasparotto L, et al. 2007. Human amniotic fluid-derived stem cells are rejected after transplantation in the myocardium of normal, ischemic, immuno-suppressed or immuno-deficient rat. *J Mol Cell Cardiol* 42:746-59

Christoffels VM, Burch JB, Moorman AF. 2004. Architectural plan for the heart: early patterning and delineation of the chambers and the nodes. *Trends in cardiovascular medicine* 14:301-7

Christoffels VM, Moorman AF. 2009. Development of the cardiac conduction system: why are some regions of the heart more arrhythmogenic than others? *Circulation. Arrhythmia and electrophysiology* 2:195-207

De Coppi P, Bartsch G, Jr., Siddiqui MM, Xu T, Santos CC, et al. 2007. Isolation of amniotic stem cell lines with potential for therapy. *Nat Biotechnol* 25:100-6

de Jong F, Opthof T, Wilde AA, Janse MJ, Charles R, et al. 1992. Persisting zones of slow impulse conduction in developing chicken hearts. *Circ Res* 71:240-50

Delorme B, Dahl E, Jarry-Guichard T, Briand JP, Willecke K, et al. 1997. Expression pattern of connexin gene products at the early developmental stages of the mouse cardiovascular system. *Circ Res* 81:423-37

Deskin R, Slotkin TA. 1981. Central catecholaminergic lesions in the developing rat: effects of cardiac noradrenaline levels, turnover and release. *Journal of autonomic pharmacology* 1:205-10

Deutsch VR, Pick M, Perry C, Grisaru D, Hemo Y, et al. 2002. The stress-associated acetylcholinesterase variant AChE-R is expressed in human CD34(+) hematopoietic progenitors and its C-terminal peptide ARP promotes their proliferation. *Experimental hematology* 30:1153-61

Dhein S, van Koppen CJ, Brodde OE. 2001. Muscarinic receptors in the mammalian heart. *Pharmacological research : the official journal of the Italian Pharmacological Society* 44:161-82

Dori A, Cohen J, Silverman WF, Pollack Y, Soreq H. 2005. Functional manipulations of acetylcholinesterase splice variants highlight alternative splicing contributions to murine neocortical development. *Cereb Cortex* 15:419-30

Dori A, Soreq H. 2006. ARP, the cleavable C-terminal peptide of "readthrough" acetylcholinesterase, promotes neuronal development and plasticity. *Journal of molecular neuroscience : MN* 28:247-55

Dvir H, Silman I, Harel M, Rosenberry TL, Sussman JL. 2010. Acetylcholinesterase: from 3D structure to function. *Chem Biol Interact* 187:10-22

Eralp I, Lie-Venema H, Bax NA, Wijffels MC, Van Der Laarse A, et al. 2006. Epicardium-derived cells are important for correct development of the Purkinje fibers in the avian heart. *The anatomical record. Part A, Discoveries in molecular, cellular, and evolutionary biology* 288:1272-80

Fabrichny IP, Leone P, Sulzenbacher G, Comoletti D, Miller MT, et al. 2007. Structural Analysis of the Synaptic Protein Neuroligin and Its β-Neurexin Complex: Determinants for Folding and Cell Adhesion. *Neuron* 56:979-91

Falugi C. 1993. Localization and possible role of molecules associated with the cholinergic system during "non-nervous" developmental events. *European journal of histochemistry : EJH* 37:287-94

Falugi C, Aluigi MG. 2012. Early appearance and possible functions of non-neuromuscular cholinesterase activities. *Frontiers in molecular neuroscience* 5:54

Falugi C, Lammerding-Koppel M, Aluigi MG. 2008. Sea urchin development: an alternative model for mechanistic understanding of neurodevelopment and neurotoxicity. *Birth defects research. Part C, Embryo today : reviews* 84:188-203

Felder CC. 1995. Muscarinic acetylcholine receptors: signal transduction through multiple effectors. *FASEB journal : official publication of the Federation of American Societies for Experimental Biology* 9:619-25

Flores-Flores C, Martinez-Martinez A, Munoz-Delgado E, Vidal CJ. 1996. Conversion of acetylcholinesterase hydrophilic tetramers into amphiphilic dimers and monomers. *Biochem Biophys Res Commun* 219:53-8

Fluck RA, Wynshaw-Boris AJ, Schneider LM. 1980. Cholinergic molecules modify the in vitro behavior of cells from early embryos of the medaka Oryzias latipes, a teleost fish. *Comparative biochemistry and physiology. C: Comparative pharmacology* 67C:29-34

Fremion F, Darboux I, Diano M, Hipeau-Jacquotte, Seeger MA, Piovant M. 2000. Amalgam is a ligand for the transmembrane receptor neurotactin and is required for neurotactin-mediated cell adhesion and axon fasciculation in *Drosophila*. *The EMBO Journal* 19:4463-72

Galyam N, Grisaru D, Grifman M, Melamed-Book N, Eckstein F, et al. 2001. Complex host cell responses to antisense suppression of ACHE gene expression. *Antisense & nucleic acid drug development* 11:51-7

Garcia-Ayllon MS, Millan C, Serra-Basante C, Bataller R, Saez-Valero J. 2012. Readthrough acetylcholinesterase is increased in human liver cirrhosis. *PloS one* 7:e44598

Gaustad KG, Boquest AC, Anderson BE, Gerdes AM, Collas P. 2004. Differentiation of human adipose tissue stem cells using extracts of rat cardiomyocytes. *Biochem Biophys Res Commun* 314:420-7

Go AS, Mozaffarian D, Roger VL, Benjamin EJ, Berry JD, et al. 2013. Heart disease and stroke statistics--2013 update: a report from the American Heart Association. *Circulation* 127:e6-e245

Gomez H. 1958. The development of the innervation of the heart in the rat embryo. *The Anatomical record* 130:53-71

Gourdie RG, Harris BS, Bond J, Justus C, Hewett KW, et al. 2003. Development of the cardiac pacemaking and conduction system. *Birth defects research. Part C, Embryo today : reviews* 69:46-57

Gourdie RG, Mima T, Thompson RP, Mikawa T. 1995. Terminal diversification of the myocyte lineage generates Purkinje fibers of the cardiac conduction system. *Development (Cambridge, England)* 121:1423-31

Gratzl M, Krieger-Brauer H, Ekerdt R. 1981. Latent acetylcholinesterase in secretory vesicles isolated from adrenal medulla. *Biochimica et biophysica acta* 649:355-66

Greenblatt HM, Kryger G, Lewis T, Silman I, Sussman JL. 1999. Structure of acetylcholinesterase complexed with (–)-galanthamine at 2.3 Å resolution. *FEBS letters* 463:321-6

Greenfield S, Vaux DJ. 2002. Parkinson's disease, Alzheimer's disease and motor neurone disease: identifying a common mechanism. *Neuroscience* 113:485-92

Grifman M, Galyam N, Seidman S, Soreq H. 1998. Functional redundancy of acetylcholinesterase and neuroligin in mammalian neuritogenesis. *Proceedings of the National Academy of Sciences of the United States of America* 95:13935-40

Grisaru D, Deutsch V, Shapira M, Pick M, Sternfeld M, et al. 2001. ARP, a peptide derived from the stress-associated acetylcholinesterase variant, has hematopoietic growth promoting activities. *Molecular medicine (Cambridge, Mass.)* 7:93-105

Grisaru D, Lev-Lehman E, Shapira M, Chaikin E, Lessing JB, et al. 1999a. Human osteogenesis involves differentiation-dependent increases in the morphogenically active 3' alternative splicing variant of acetylcholinesterase. *Molecular and cellular biology* 19:788-95

Grisaru D, Sternfeld M, Eldor A, Glick D, Soreq H. 1999b. Structural roles of acetylcholinesterase variants in biology and pathology. *European journal of biochemistry / FEBS* 264:672-86

Gros D, Dupays L, Alcolea S, Meysen S, Miquerol L, Theveniau-Ruissy M. 2004. Genetically modified mice: tools to decode the functions of connexins in the heart-new models for cardiovascular research. *Cardiovascular research* 62:299-308

Guan K, Nayernia K, Maier LS, Wagner S, Dressel R, et al. 2006. Pluripotency of spermatogonial stem cells from adult mouse testis. *Nature* 440:1199-203

Guizzetti M, Costa LG. 2002. Effect of ethanol on protein kinase Czeta and p70S6 kinase activation by carbachol: a possible mechanism for ethanol-induced inhibition of glial cell proliferation. *Journal of neurochemistry* 82:38-46

Gurjarpadhye A, Hewett KW, Justus C, Wen X, Stadt H, et al. 2007. Cardiac neural crest ablation inhibits compaction and electrical function of conduction system bundles. *American journal of physiology. Heart and circulatory physiology* 292:H1291-300

Gurwitz D, Razon N, Sokolovsky M, Soreq H. 1984. Expression of muscarinic binding sites in primary human brain tumors. *Brain research* 316:61-70

Haissaguerre M, Shah DC, Jais P, Shoda M, Kautzner J, et al. 2002. Role of Purkinje conducting system in triggering of idiopathic ventricular fibrillation. *Lancet* 359:677-8

Hammond P, Rao R, Koenigsberger C, Brimijoin S. 1994. Regional variation in expression of acetylcholinesterase mRNA in adult rat brain analyzed by in situ hybridization. *Proceedings of the National Academy of Sciences of the United States of America* 91:10933-7

Hildreth V, Webb S, Bradshaw L, Brown NA, Anderson RH, Henderson DJ. 2008. Cells migrating from the neural crest contribute to the innervation of the venous pole of the heart. *Journal of anatomy* 212:1-11

Holmes C, Jones SA, Budd TC, Greenfield SA. 1997. Non-cholinergic, trophic action of recombinant acetylcholinesterase on mid-brain dopaminergic neurons. *Journal of neuroscience research* 49:207-18

Hoogaars WM, Tessari A, Moorman AF, de Boer PA, Hagoort J, et al. 2004. The transcriptional repressor Tbx3 delineates the developing central conduction system of the heart. *Cardiovascular research* 62:489-99

Hosea NA, Radic Z, Tsigelny I, Berman HA, Quinn DM, Taylor P. 1996. Aspartate 74 as a primary determinant in acetylcholinesterase governing specificity to cationic organophosphonates. *Biochemistry* 35:10995-1004

Hsieh PC, Segers VF, Davis ME, MacGillivray C, Gannon J, et al. 2007. Evidence from a genetic fate-mapping study that stem cells refresh adult mammalian cardiomyocytes after injury. *Nature medicine* 13:970-4

Inestrosa NC, Alarcon R. 1998. Molecular interactions of acetylcholinesterase with senile plaques. *Journal of physiology, Paris* 92:341-4

Inestrosa NC, Alvarez A, Perez CA, Moreno RD, Vicente M, et al. 1996. Acetylcholinesterase accelerates assembly of amyloid-beta-peptides into Alzheimer's fibrils: possible role of the peripheral site of the enzyme. *Neuron* 16:881-91

Jackson KA, Majka SM, Wang H, Pocius J, Hartley CJ, et al. 2001. Regeneration of ischemic cardiac muscle and vascular endothelium by adult stem cells. *J Clin Invest* 107:1395-402

Johnson G, Moore SW. 1999. The adhesion function on acetylcholinesterase is located at the peripheral anionic site. *Biochem Biophys Res Commun* 258:758-62

Johnson G, Moore SW. 2000. Cholinesterases modulate cell adhesion in human neuroblastoma cells in vitro. *International journal of developmental neuroscience : the official journal of the International Society for Developmental Neuroscience* 18:781-90

Jongbloed MR, Mahtab EA, Blom NA, Schalij MJ, Gittenberger-de Groot AC. 2008. Development of the cardiac conduction system and the possible relation to predilection sites of arrhythmogenesis. *TheScientificWorldJournal* 8:239-69

Jongbloed MR, Wijffels MC, Schalij MJ, Blom NA, Poelmann RE, et al. 2005. Development of the right ventricular inflow tract and moderator band: a possible morphological and functional explanation for Mahaim tachycardia. *Circ Res* 96:776-83

Karpel R, Ben Aziz-Aloya R, Sternfeld M, Ehrlich G, Ginzberg D, et al. 1994. Expression of three alternative acetylcholinesterase messenger RNAs in human tumor cell lines of different tissue origins. *Experimental cell research* 210:268-77

Karpel R, Sternfeld M, Ginzberg D, Guhl E, Graessmann A, Soreq H. 1996. Overexpression of alternative human acetylcholinesterase forms modulates process extensions in cultured glioma cells. *Journal of neurochemistry* 66:114-23

Kaufer D, Friedman A, Seidman S, Soreq H. 1998. Acute stress facilitates long-lasting changes in cholinergic gene expression. *Nature* 393:373-7

Kaufman MH. 1994. *The Atlas of Mouse Development*. San Diego: Academic Press

Kawashima K, Fujii T. 2000. Extraneuronal cholinergic system in lymphocytes. *Pharmacology & therapeutics* 86:29-48

Kitajima S, Miyagawa-Tomita S, Inoue T, Kanno J, Saga Y. 2006. Mesp1-nonexpressing cells contribute to the ventricular cardiac conduction system. *Developmental dynamics : an official publication of the American Association of Anatomists* 235:395-402

Ko J, Zhang C, Arac D, Boucard AA, Brunger AT, Südhof TC. 2009. Neuroligin-1 performs neurexin-dependent and neurexin-independent functions in synapse validation. *The EMBO Journal* 28:3244-55

Koenigsberger C, Chiappa S, Brimijoin S. 1997. Neurite differentiation is modulated in neuroblastoma cells engineered for altered acetylcholinesterase expression. *Journal of neurochemistry* 69:1389-97

Kupershmidt S, Yang T, Anderson ME, Wessels A, Niswender KD, et al. 1999. Replacement by homologous recombination of the minK gene with lacZ reveals restriction of minK expression to the mouse cardiac conduction system. *Circ Res* 84:146-52

Lamers WH, te Kortschot A, Los JA, Moorman AF. 1987. Acetylcholinesterase in prenatal rat heart: a marker for the early development of the cardiac conductive tissue? *The Anatomical record* 217:361-70

Landwehrmeyer B, Probst A, Palacios JM, Mengod G. 1993. Expression of acetylcholinesterase messenger RNA in human brain: an in situ hybridization study. *Neuroscience* 57:615-34

Lapidot-Lifson Y, Patinkin D, Prody CA, Ehrlich G, Seidman S, et al. 1992. Cloning and antisense oligodeoxynucleotide inhibition of a human homolog of cdc2 required in hematopoiesis. *Proceedings of the National Academy of Sciences of the United States of America* 89:579-83

Laugwitz KL, Moretti A, Lam J, Gruber P, Chen Y, et al. 2005. Postnatal isl1+ cardioblasts enter fully differentiated cardiomyocyte lineages. *Nature* 433:647-53

Layer PG. 1990. Cholinesterases preceding major tracts in vertebrate neurogenesis. *BioEssays : news and reviews in molecular, cellular and developmental biology* 12:415-20

Layer PG, Weikert T, Alber R. 1993. Cholinesterases regulate neurite growth of chick nerve cells in vitro by means of a non-enzymatic mechanism. *Cell and tissue research* 273:219-26

Layer PG, Willbold E. 1995. Novel functions of cholinesterases in development, physiology and disease. *Progress in histochemistry and cytochemistry* 29:1-94

Lev M, Thaemert JC. 1973. The conduction system of the mouse heart. *Acta anatomica* 85:342-52

Lev-Lehman E, Deutsch V, Eldor A, Soreq H. 1997. Immature human megakaryocytes produce nuclear-associated acetylcholinesterase. *Blood* 89:3644-53

Lev-Lehman E, Evron T, Broide RS, Meshorer E, Ariel I, et al. 2000. Synaptogenesis and myopathy under acetylcholinesterase overexpression. *Journal of molecular neuroscience : MN* 14:93-105

Lev-Lehman E, Ginzberg D, Hornreich G, Ehrlich G, Meshorer A, et al. 1994. Antisense inhibition of acetylcholinesterase gene expression causes transient hematopoietic alterations in vivo. *Gene therapy* 1:127-35

Li Y, Camp S, Rachinsky TL, Bongiorno C, Taylor P. 1993. Promoter elements and transcriptional control of the mouse acetylcholinesterase gene. *The Journal of biological chemistry* 268:3563-72

Li Y, Camp S, Rachinsky TL, Getman D, Taylor P. 1991. Gene structure of mammalian acetylcholinesterase. Alternative exons dictate tissue-specific expression. *The Journal of biological chemistry* 266:23083-90

Liao J, Norgaard-Pedersen B, Brodbeck U. 1993. Subunit association and glycosylation of acetylcholinesterase from monkey brain. *Journal of neurochemistry* 61:1127-34

Lipp JA, Rudolph AM. 1972. Sympathetic nerve development in the rat and guinea-pig heart. *Biology of the neonate* 21:76-82

Livak KJ, Schmittgen TD. 2001. Analysis of relative gene expression data using real-time quantitative PCR and the 2(-Delta Delta C(T)) Method. *Methods (San Diego, Calif.)* 25:402-8

Lopez AJ. 1998. Alternative splicing of pre-mRNA: developmental consequences and mechanisms of regulation. *Annual review of genetics* 32:279-305

Luo ZD, Camp S, Mutero A, Taylor P. 1998. Splicing of 5' introns dictates alternative splice selection of acetylcholinesterase pre-mRNA and specific expression during myogenesis. *The Journal of biological chemistry* 273:28486-95

Ma W, Maric D, Li BS, Hu Q, Andreadis JD, et al. 2000. Acetylcholine stimulates cortical precursor cell proliferation in vitro via muscarinic receptor activation and MAP kinase phosphorylation. *The European journal of neuroscience* 12:1227-40

Majumdar MK, Thiede MA, Mosca JD, Moorman M, Gerson SL. 1998. Phenotypic and functional comparison of cultures of marrow-derived mesenchymal stem cells (MSCs) and stromal cells. *Journal of cellular physiology* 176:57-66

Makino S, Fukuda K, Miyoshi S, Konishi F, Kodama H, et al. 1999. Cardiomyocytes can be generated from marrow stromal cells in vitro. *J Clin Invest* 103:697-705

Martin-Puig S, Wang Z, Chien KR. 2008. Lives of a heart cell: tracing the origins of cardiac progenitors. *Cell Stem Cell* 2:320-31

Massoulie J, Anselmet A, Bon S, Krejci E, Legay C, et al. 1998. Acetylcholinesterase: C-terminal domains, molecular forms and functional localization. *Journal of physiology, Paris* 92:183-90

Massoulie J, Pezzementi L, Bon S, Krejci E, Vallette FM. 1993. Molecular and cellular biology of cholinesterases. *Progress in neurobiology* 41:31-91

McMullen NM, Zhang F, Hotchkiss A, Bretzner F, Wilson JM, et al. 2009a. Functional characterization of cardiac progenitor cells and their derivatives in the embryonic heart post-chamber formation. *Developmental dynamics : an official publication of the American Association of Anatomists* 238:2787-99

McMullen NM, Zhang F, Pasumarthi KB. 2009b. Assessment of embryonic myocardial cell differentiation using a dual fluorescent reporter system. *Journal of cellular and molecular medicine* 13:2834-42

McNamara A, Pulido-Rios MT, Sweazey S, Obedencio GP, Thibodeaux H, et al. 2009. Pharmacological properties of TD-6301, a novel bladder selective muscarinic receptor antagonist. *European journal of pharmacology* 605:145-52

Meilhac SM, Kelly RG, Rocancourt D, Eloy-Trinquet S, Nicolas JF, Buckingham ME. 2003. A retrospective clonal analysis of the myocardium reveals two phases of clonal growth in the developing mouse heart. *Development (Cambridge, England)* 130:3877-89

Miquerol L, Meysen S, Mangoni M, Bois P, van Rijen HV, et al. 2004. Architectural and functional asymmetry of the His-Purkinje system of the murine heart. *Cardiovascular research* 63:77-86

Miquerol L, Moreno-Rascon N, Beyer S, Dupays L, Meilhac SM, et al. 2010. Biphasic development of the mammalian ventricular conduction system. *Circ Res* 107:153-61

Moorman AF, Christoffels VM. 2003a. Cardiac chamber formation: development, genes, and evolution. *Physiological reviews* 83:1223-67

Moorman AF, Christoffels VM. 2003b. Development of the cardiac conduction system: a matter of chamber development. *Novartis Foundation symposium* 250:25-34; discussion -43, 276-9

Moskowitz IP, Kim JB, Moore ML, Wolf CM, Peterson MA, et al. 2007. A molecular pathway including Id2, Tbx5, and Nkx2-5 required for cardiac conduction system development. *Cell* 129:1365-76

Munoz FJ, Aldunate R, Inestrosa NC. 1999. Peripheral binding site is involved in the neurotrophic activity of acetylcholinesterase. *Neuroreport* 10:3621-5

Myers DC, Fishman GI. 2004. Toward an understanding of the genetics of murine cardiac pacemaking and conduction system development. *The anatomical record. Part A, Discoveries in molecular, cellular, and evolutionary biology* 280:1018-21

Nakamura T, Colbert MC, Robbins J. 2006. Neural crest cells retain multipotential characteristics in the developing valves and label the cardiac conduction system. *Circ Res* 98:1547-54

Nakamura T, Ikeda T, Shimokawa I, Inoue Y, Suematsu T, et al. 1994. Distribution of acetylcholinesterase activity in the rat embryonic heart with reference to HNK-1 immunoreactivity in the conduction tissue. *Anatomy and embryology* 190:367-73

Nijholt I, Farchi N, Kye M, Sklan EH, Shoham S, et al. 2004. Stress-induced alternative splicing of acetylcholinesterase results in enhanced fear memory and long-term potentiation. *Molecular psychiatry* 9:174-83

Nyquist-Battie C, Hagler KE, Millington WR. 1993. Glycyl-L-glutamine regulates the expression of asymmetric acetylcholinesterase molecular forms in cultured cardiac post-natal myocytes. *J Mol Cell Cardiol* 25:1111-8

Okamoto K, Miyoshi S, Toyoda M, Hida N, Ikegami Y, et al. 2007. 'Working' cardiomyocytes exhibiting plateau action potentials from human placenta-derived extraembryonic mesodermal cells. *Experimental cell research* 313:2550-62

Orlic D, Kajstura J, Chimenti S, Jakoniuk I, Anderson SM, et al. 2001. Bone marrow cells regenerate infarcted myocardium. *Nature* 410:701-5

Ott P, Lustig A, Brodbeck U, Rosenbusch JP. 1982. Acetylcholinesterase from human erythrocytes membranes: dimers as functional units. *FEBS letters* 138:187-9

Pallante BA, Giovannone S, Fang-Yu L, Zhang J, Liu N, et al. 2010. Contactin-2 expression in the cardiac Purkinje fiber network. *Circulation. Arrhythmia and electrophysiology* 3:186-94

Patel R, Kos L. 2005. Endothelin-1 and Neuregulin-1 convert embryonic cardiomyocytes into cells of the conduction system in the mouse. *Developmental dynamics : an official publication of the American Association of Anatomists* 233:20-8

Patinkin D, Lev-Lehman E, Zakut H, Eckstein F, Soreq H. 1994. Antisense inhibition of butyrylcholinesterase gene expression predicts adverse hematopoietic consequences to cholinesterase inhibitors. *Cellular and molecular neurobiology* 14:459-73

Paulus JM, Maigne J, Keyhani E. 1981. Mouse megakaryocytes secrete acetylcholinesterase. *Blood* 58:1100-6

Pazos A, Wiederhold KH, Palacios JM. 1986. Central pressor effects induced by muscarinic receptor agonists: evidence for a predominant role of the M2 receptor subtype. *European journal of pharmacology* 125:63-70

Pennisi DJ, Rentschler S, Gourdie RG, Fishman GI, Mikawa T. 2002. Induction and patterning of the cardiac conduction system. *The International journal of developmental biology* 46:765-75

Pereira EFR, Reinhardt-Maelicke S, Schrattenholz A, Maelicke A, Alburquerque EX. 1993. Identification and Functional Characterization of a New Agonist Site on Nicotinic Acetylcholine Receptors of Cultured Hippocampal Neurons. *The Journal of pharmacology and experimental therapeutics* 265:1474-91

Perrier NA, Kherif S, Perrier AL, Dumas S, Mallet J, Massoulie J. 2003. Expression of PRiMA in the mouse brain: membrane anchoring and accumulation of 'tailed' acetylcholinesterase. *The European journal of neuroscience* 18:1837-47

Perrier NA, Salani M, Falasca C, Bon S, Augusti-Tocco G, Massoulie J. 2005. The readthrough variant of acetylcholinesterase remains very minor after heat shock, organophosphate inhibition and stress, in cell culture and in vivo. *Journal of neurochemistry* 94:629-38

Perry C, Pick M, Podoly E, Gilboa-Geffen A, Zimmerman G, et al. 2007. Acetylcholinesterase/C terminal binding protein interactions modify Ikaros functions, causing T lymphopenia. *Leukemia* 21:1472-80

Perry C, Sklan EH, Soreq H. 2004. CREB regulates AChE-R-induced proliferation of human glioblastoma cells. *Neoplasia (New York, N.Y.)* 6:279-86

Pezzementi L, Chatonnet A. 2010. Evolution of cholinesterases in the animal kingdom. *Chemico-Biological Interactions* 187:27-33

Pick M, Flores-Flores C, Soreq H. 2004. From brain to blood: alternative splicing evidence for the cholinergic basis of Mammalian stress responses. *Annals of the New York Academy of Sciences* 1018:85-98

Piomboni P, Baccetti B, Moretti E, Gambera L, Angelini C, Falugi C. 2001. Localization of molecules related to cholinergic signaling in eggs and zygotes of the sea urchin, Paracentrotus lividus. *Journal of submicroscopic cytology and pathology* 33:187-93

Planat-Benard V, Menard C, Andre M, Puceat M, Perez A, et al. 2004. Spontaneous cardiomyocyte differentiation from adipose tissue stroma cells. *Circ Res* 94:223-9

Poelmann RE, Jongbloed MR, Molin DG, Fekkes ML, Wang Z, et al. 2004. The neural crest is contiguous with the cardiac conduction system in the mouse embryo: a role in induction? *Anatomy and embryology* 208:389-93

Radic Z, Reiner E, Taylor P. 1991. Role of the peripheral anionic site on acetylcholinesterase: inhibition by substrates and coumarin derivatives. *Molecular pharmacology* 39:98-104

Rangappa S, Fen C, Lee EH, Bongso A, Sim EK. 2003. Transformation of adult mesenchymal stem cells isolated from the fatty tissue into cardiomyocytes. *The Annals of thoracic surgery* 75:775-9

Re RN, Cook JL. 2008. The physiological basis of intracrine stem cell regulation. *American journal of physiology. Heart and circulatory physiology* 295:H447-53

Reinecke H, MacDonald GH, Hauschka SD, Murry CE. 2000. Electromechanical coupling between skeletal and cardiac muscle. Implications for infarct repair. *The Journal of cell biology* 149:731-40

Rentschler S, Vaidya DM, Tamaddon H, Degenhardt K, Sassoon D, et al. 2001. Visualization and functional characterization of the developing murine cardiac conduction system. *Development (Cambridge, England)* 128:1785-92

Reyes AE, Perez DR, Alvarez A, Garrido J, Gentry MK, et al. 1997. A monoclonal antibody against acetylcholinesterase inhibits the formation of amyloid fibrils induced by the enzyme. *Biochem Biophys Res Commun* 232:652-5

Robertson RT, Annis CM, Baratta J, Haraldson S, Ingeman J, et al. 2000. Do subplate neurons comprise a transient population of cells in developing neocortex of rats? *The Journal of comparative neurology* 426:632-50

Ross ME, Evinger MJ, Hyman SE, Carroll JM, Mucke L, et al. 1990. Identification of a functional glucocorticoid response element in the phenylethanolamine N-methyltransferase promoter using fusion genes introduced into chromaffin cells in primary culture. *The Journal of neuroscience : the official journal of the Society for Neuroscience* 10:520-30

Rota M, Kajstura J, Hosoda T, Bearzi C, Vitale S, et al. 2007. Bone marrow cells adopt the cardiomyogenic fate in vivo. *Proceedings of the National Academy of Sciences of the United States of America* 104:17783-8

Rotundo RL. 1990. Nucleus-specific translation and assembly of acetylcholinesterase in multinucleated muscle cells. *The Journal of cell biology* 110:715-9

Rubart M, Pasumarthi KB, Nakajima H, Soonpaa MH, Nakajima HO, Field LJ. 2003. Physiological coupling of donor and host cardiomyocytes after cellular transplantation. *Circ Res* 92:1217-24

Schambra UB, Sulik KK, Petrusz P, Lauder JM. 1989. Ontogeny of cholinergic neurons in the mouse forebrain. *The Journal of comparative neurology* 288:101-22

Schrattenholz A, Pereira EFR, Roth U, Weber K-H, Alburquerque EX, Maelicke A. 1995. Agonist Responses of Neuronal Nicotinic Acetyicholine Receptors Are Potentiated by a Novel Class of Allosterically Acting Ligands. *Molecular pharmacology* 49:1-6

Schweitzer ES. 1993. Regulated and constitutive secretion of distinct molecular forms of acetylcholinesterase from PC12 cells. *Journal of cell science* 106 (Pt 3):731-40

Seidman S, Sternfeld M, Ben Aziz-Aloya R, Timberg R, Kaufer-Nachum D, Soreq H. 1995. Synaptic and epidermal accumulations of human acetylcholinesterase are encoded by alternative 3'-terminal exons. *Molecular and cellular biology* 15:2993-3002

Shah BH, Catt KJ. 2004. GPCR-mediated transactivation of RTKs in the CNS: mechanisms and consequences. *Trends in neurosciences* 27:48-53

Shapira M, Tur-Kaspa I, Bosgraaf L, Livni N, Grant AD, et al. 2000. A transcription-activating polymorphism in the ACHE promoter associated with acute sensitivity to anti-acetylcholinesterases. *Human molecular genetics* 9:1273-81

Sharma KV, Koenigsberger C, Brimijoin S, Bigbee JW. 2001. Direct evidence for an adhesive function in the noncholinergic role of acetylcholinesterase in neurite outgrowth. *Journal of neuroscience research* 63:165-75

Sharma VK, Banerjee SP. 1978. Presynaptic muscarinic cholinergic receptors. *Nature* 272:276-8

Shoba T, Tay SS. 2000. Nitrergic and peptidergic innervation in the developing rat heart. *Anatomy and embryology* 201:491-500

Silman I, Sussman JL. 2008. Acetylcholinesterase: how is structure related to function? *Chem Biol Interact* 175:3-10

Simpson PC, Kariya K, Karns LR, Long CS, Karliner JS. 1991. Adrenergic hormones and control of cardiac myocyte growth. *Molecular and cellular biochemistry* 104:35-43

Small DH, Reed G, Whitefield B, Nurcombe V. 1995. Cholinergic regulation of neurite outgrowth from isolated chick sympathetic neurons in culture. *The Journal of neuroscience : the official journal of the Society for Neuroscience* 15:144-51

Soonpaa MH, Field LJ. 1997. Assessment of cardiomyocyte DNA synthesis in normal and injured adult mouse hearts. *The American journal of physiology* 272:H220-6

Soonpaa MH, Field LJ. 1998. Survey of studies examining mammalian cardiomyocyte DNA synthesis. *Circ Res* 83:15-26

Soreq H, Patinkin D, Lev-Lehman E, Grifman M, Ginzberg D, et al. 1994. Antisense oligonucleotide inhibition of acetylcholinesterase gene expression induces progenitor cell expansion and suppresses hematopoietic apoptosis ex vivo. *Proceedings of the National Academy of Sciences of the United States of America* 91:7907-11

Soreq H, Seidman S. 2001. Acetylcholinesterase--new roles for an old actor. *Nature reviews. Neuroscience* 2:294-302

Srivatsan M, Peretz B. 1997. Acetylcholinesterase promotes regeneration of neurites in cultured adult neurons of Aplysia. *Neuroscience* 77:921-31

St Amand TR, Lu JT, Zamora M, Gu Y, Stricker J, et al. 2006. Distinct roles of HF-1b/Sp4 in ventricular and neural crest cells lineages affect cardiac conduction system development. *Developmental biology* 291:208-17

Sternfeld M, Ming G, Song H, Sela K, Timberg R, et al. 1998. Acetylcholinesterase enhances neurite growth and synapse development through alternative contributions of its hydrolytic capacity, core protein, and variable C termini. *The Journal of neuroscience : the official journal of the Society for Neuroscience* 18:1240-9

Storch A, Schrattenholz A, Cooper JC, Ghani EMA, Gutbrod O, et al. 1995. Physostigmine, galanthamine and codeine act as 'noncompetitive nicotinic receptor agonists' on clonal rat pheochromocytoma cells. *European journal of pharmacology* Molecular Pharmacology Section 290

Suma K. 2001. Sunao Tawara: a father of modern cardiology. *Pacing and clinical electrophysiology : PACE* 24:88-96

Sussman JL, Harel M, Frolow F, Oefner C, Goldman A, et al. 1991. Atomic structure of acetylcholinesterase from Torpedo californica: a prototypic acetylcholine-binding protein. *Science* 253:872-9

Szelenyi JG, Bartha E, Hollan SR. 1982. Acetylcholinesterase activity of lymphocytes: an enzyme characteristic of T-cells. *British journal of haematology* 50:241-5

Tarasenko LM, Grebennikova VF, Tarasenko VV, Tsaprika SG, Silenko Iu I, Deviatkina TA. 1992. [The proteinase and alpha 1-antitrypsin activities in the tissues during emotional stress in rabbits]. *Fiziologicheskii zhurnal* 38:115-7

Taylor P, Li Y, Camp S, Rachinsky TL, Ekstrom T, et al. 1993. Structure and regulation of expression of the acetylcholinesterase gene. *Chem Biol Interact* 87:199-207

Taylor P, Radic Z. 1994. The cholinesterases: from genes to proteins. *Annual review of pharmacology and toxicology* 34:281-320

Thomsen T, Kaden B, Fischer JP, Bickel U, Barz H, et al. 1991. Inhibition of Acetylcholinesterase Activity in Human Brain Tissue and Erythrocytes by Galanthamine, Physostigmine and Tacrine. *Eur J Clin Chem Clin Biochem* 29:487-92

Toma C, Pittenger MF, Cahill KS, Byrne BJ, Kessler PD. 2002. Human mesenchymal stem cells differentiate to a cardiomyocyte phenotype in the adult murine heart. *Circulation* 105:93-8

Van Hoof D, Dormeyer W, Braam SR, Passier R, Monshouwer-Kloots J, et al. 2010. Identification of cell surface proteins for antibody-based selection of human embryonic stem cell-derived cardiomyocytes. *Journal of proteome research* 9:1610-8

Velan B, Kronman C, Ordentlich A, Flashner Y, Leitner M, et al. 1993. N-glycosylation of human acetylcholinesterase: effects on activity, stability and biosynthesis. *The Biochemical journal* 296 (Pt 3):649-56

Ventura C, Cantoni S, Bianchi F, Lionetti V, Cavallini C, et al. 2007. Hyaluronan mixed esters of butyric and retinoic Acid drive cardiac and endothelial fate in term placenta human mesenchymal stem cells and enhance cardiac repair in infarcted rat hearts. *The Journal of biological chemistry* 282:14243-52

Vincent SD, Buckingham ME. 2010. How to make a heart: the origin and regulation of cardiac progenitor cells. *Current topics in developmental biology* 90:1-41

Viragh S, Challice CE. 1977. The development of the conduction system in the mouse embryo heart. II. Histogenesis of the atrioventricular node and bundle. *Developmental biology* 56:397-411

Viragh S, Challice CE. 1982. The development of the conduction system in the mouse embryo heart. *Developmental biology* 89:25-40

Winitsky SO, Gopal TV, Hassanzadeh S, Takahashi H, Gryder D, et al. 2005. Adult murine skeletal muscle contains cells that can differentiate into beating cardiomyocytes in vitro. *PLoS biology* 3:e87

Wu SM, Chien KR, Mummery C. 2008. Origins and fates of cardiovascular progenitor cells. *Cell* 132:537-43

Xie J, McCobb DP. 1998. Control of alternative splicing of potassium channels by stress hormones. *Science* 280:443-6

Yang L, He HY, Zhang XJ. 2002. Increased expression of intranuclear AChE involved in apoptosis of SK-N-SH cells. *Neuroscience research* 42:261-8

Zeev-Ben-Mordehai T, Paz A, Peleg Y, Toker L, Wolf SG, et al. 2009. Amalgam, an axon guidance Drosophila adhesion protein belonging to the immunoglobulin superfamily: Over-expression, purification and biophysical characterization. *Protein Expression and Purification* 63:147-57

Zhang XJ, Yang L, Zhao Q, Caen JP, He HY, et al. 2002. Induction of acetylcholinesterase expression during apoptosis in various cell types. *Cell death and differentiation* 9:790-800

Zhou XM, Mizushima A, Uchida S, Watanabe Y, Yoshida H. 1988. The SH-H subgroup of cardiac M2 receptors (M2 alpha) inhibits adenylate cyclase activity. *European journal of pharmacology* 154:229-36